The characterization of 17β-hydroxysteroid dehydrogenase type 2 (17βHSD2) activity towards novel C19 substrates.

by
Monique Barnard

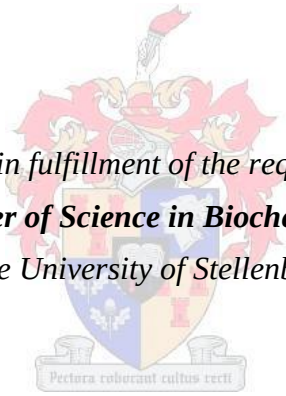

Dissertation presented in fulfillment of the requirements for the degree
Master of Science in Biochemistry
at the University of Stellenbosch.

Supervisor: Dr. K-H. Storbeck

March, 2017

The financial assistance of the National Research Foundation (NRF) towards this research is hereby acknowledged. Opinions expressed and conclusions arrived at, are those of the author and are not necessarily to be attributed to the NRF.

Declaration

By submitting this thesis electronically, I declare that the entirety of the work contained therein is my own, original work, that I am the sole author thereof (save to the extent explicitly otherwise stated), that reproduction and publication thereof by Stellenbosch University will not infringe any third party rights and that I have not previously in its entirety or in part submitted it for obtaining any qualification.

M. Barnard
March 2017

Summary

Castration resistant prostate cancer (CRPC) is an androgen dependent disease driven by the intratumoural metabolism of adrenal androgen precursors to potent androgens. The alternative 5α-dione pathway converts the adrenal steroids DHEA and androstenedione (A4) to the potent androgen DHT, while the recently identified 11β-hydroxyandrostenedione (11OHA4) pathway converts the adrenal steroid 11OHA4 into the potent androgens 11-ketotestosterone (11KT) and 11-ketodihydrotestosterone (11KDHT).

Two 17β-hydroxysteroid dehydrogenase (17βHSD) enzymes catalyse vital reactions in both pathways. 17βHSD2 catalyses the oxidation of androgens to their less active form, while 17βHSD5, which is better known as AKR1C3, catalyses the reduction of weak androgens to more potent androgens. The relative activity and expression levels of these enzymes are therefore vital in regulating the amount of active androgen produced. The aim of this project was to characterise the activity of 17βHSD2 towards 11-oxygenated steroids from the 11OHA4 pathway and to investigate the effect of different ratios of AKR1C3 and 17βHSD2 on the flux through the alternative 5α-dione and 11OHA4 pathways.

17βHSD2 activity towards the 11-oxygenated steroids 11KT and 11KDHT were characterised for the first time using HEK293 cells transiently transfected to express 17βHSD2. The results showed that 17βHSD2 efficiently catalysed the conversion of 11KT and 11KDHT to their respective products. Interestingly the catalytic efficiency tended to be higher for the conversion of testosterone (T) to A4 than the conversion of 11KT to 11KA4, although this difference was not significant.

The effect of increasing ratios of AKR1C3:17βHSD2, which occur during CRPC, were subsequently investigated. HEK293 cells, which do not endogenously express either AKR1C3 or 17βHSD2, were transiently transfected to express each enzyme, and the cells subsequently combined in different ratios. PC3 cells, which endogenously express 17βHSD2, were transfected with increasing amounts of AKR1C3 to obtain different AKR1C3:17βHSD2 ratios.

Collectively the results showed that increased expression of AKR1C3 had a significant influence on the flux through the 11OHA4 pathway, leading to the production of more potent androgens, but had little or no effect on the classical pathways. Increasing AKR1C3:17βHSD2 expression in both HEK293 and PC3 cells lead to increased levels of 11KA4 being converted to 11KT while the conversion of A4 to T remained low. A mathematical model was subsequently constructed and

confirmed the experimental findings. These results were further validated in three prostate cancer cell lines each expressing different AKR1C3:17βHSD2 ratios.

Taken together, the results from this study show that 17βHSD2 likely plays an important role in regulating intratumoural androgen levels and that increased AKR1C3:17βHSD2 ratios favour the flux through the 11OHA4 pathway.

Opsomming

Kastrasie weerstandige prostaat karsinoom (CRPC) is ‘n sieke wat aangedryf word deur die teenwoordigheid van kragtige androgene afkomstig van swakker adrenal voorlopers. Die alternatiewe 5α-dione padweg skakel die adrenale voorloper steroide DHEA(S) en androsteendioon (A4) om na die meer potente androgen dihidroksitestosteroon (DHT), terwyl die 11β-hidroksiandrosteendione (11OHA4) padweg die adrenal steroïed 11OHA4 omskakel na potente androgene soos 11-keto-testosteroon (11KT) and 11-keto-5α-dihidroksitestosteroon (11KDHT).

Twee 17β-hidroksisteroïed dehidrogenase ensieme kataliseer belangrike reaksies in beide van bogenoemde padwee. Die ensiem 17βHSD2 kataliseer die oksidasie van potente androgene na swakker steroïede terwyl 17βHSD5, beter bekend as AKR1C3, die reduksie van potente androgene omskakel na swakker steroiede. Dus is die uitdrukkings vlakke van hierdie twee ensieme belangrik vir die regulering van potente androgene in die ligaam. Die doelwit van hierdie studie was dus om die aktiwiteit van die ensim 17βHSD2 te karakteriseer vir nuwe 11-geoksideerde steroiede geproduseer deur die 11OHA4 padweg en die effek van verskillende verhoudings van AKR1C3:17βHSD2 op die vloed deur die alternatiewe 5α-dione en 11OHA4 padweg te ondersoek.

Die aktiwiteit van 17βHSD2 tot die 11-geoksideerde steroiede 11KT and 11KDHT was gekarakteriseer vir die eerste keer deur die uitdrukking van 17βHSD2 in HEK293 selle. Die resultate het getoon dat 17βHSD2 effektief 11KT sowel as 11KDHT omskakel na hul onderskeie produkte. Dis was interressant om waar te neem dat 17βHSD2 T meer effektief omskakel na A4 in vergelyking met die effektiwiteit van die omskakeling van 11KT tot 11KA4, alhoewel die verskil nie statisties relevant is nie.

Die effek van ‘n toename in die verhouding tussen AKR1C3:17βHSD2, soos waargeneem in die geval van CRPC, was ondersoek. HEK293 selle wat geen van die twee bogenoemde ensieme uitdruk nie, was gemanipuleer om die ensiem van belang uit te druk waarna die selle gemeng is volgens die verhouding van AKR1C3:17βHSD2 verlang. PC3 cells wat reeds 17βHSD2 uitdruk was ook gemanipuleer om toenemende vlakke van AKR1C3 uit te druk.

Saamgevat, bewys die resultate dat ‘n toename in die uitdrukking van AKR1C3 ‘n merkwaardige invloed op die vloed deur die 11OHA4 padweg gehad het wat tot gevolg lei tot die produksie van meer potente androgene, terwyl die teenoorgestelde is geldig vir die vloed deur die klassieke

padweg. Toenemende AKR1C3:17βHSD2 uitdrukking in beide die HEK293 en die PC3 selle het gelei tot ‘n toename in die produksie van 11KT vanaf 11KA4 terwyl die produksie van T vanaf A4 konstant laag gebly het. ‘n Wiskundige model afgelei van die resultate wat bekom is, bevestig hierdie eksperimentele bevindinge. Verder was die resultate ook bevestig deur die drie PCa sel lyne wat verskillende verhoudings van AKR1C3:17βHSD2 uitdruk.

Opgesom, bewys die resultate dat 17βHSD2 moontlik ‘n belangrike rol speel in die regulering van intratumorale androgeen vlakke en dat die toeneming in AKR1C3:17βHSD2 verhouding die vloed deur die 11OHA4 padweg bevoordeel.

Dedication

Dedicated to my father, who will always
be my biggest hero and inspiration

Acknowledgements

Dr Storbeck, you are simply the best supervisor any student could ask for. Thank you for taking a chance on me and trusting me in the laboratory for my masters. Your passion for your research is contagious, thank you for making me even more excited about science and shaping me to become a better scientist every day. Thank you for all your help with writing this thesis, without you none of this would be possible. Thank you for always being kind even in difficult situations. I am grateful to you for always being available, replying to emails, making time for meetings, all your advice and sometimes just plain understanding. It's the small things that make the biggest difference.

Prof Snoep, for lending us your expertise in constructing the Mathematical model which so beautifully concluded this project.

Dr Stander from CAF, thank you for sharing you knowledge on all things MS related.

Ralie, thank you for keeping the lab working flawlessly and your willingness to always help when there is a troublesome situation. Thank you for always keeping your cool even when things go wrong.

I would like to thank all the **Swartbeckian group members** for all the laughs, memories and assistants the past two years.

Jonathan and Elzette for always being a message away, being patient and always being willing to help. You both made me feel part of a family in the lab. You are both so special to me.

To my loving parents, thank you for all the unconditional love, patients, motivation, time and money invested in me. I can never express my love and gratitude towards you both. Mom thanks for not only being my mom, but for being my best friend. I always knew you were only a phone call away. Thank you for all the long conversations, for always being interested, supportive and available. Thank you for being the sticky glue that keeps everyone together. You are truly an

inspiration not only to me but to everyone around you. If I could become half the woman you are one day, my life would be a success. Dad, when I think of quitting I remember your words of encouragement. I have never had anyone in the world believe in my potential like you do and that is the biggest gift I could ever ask for. Thanks for being my partner in crime. You taught me to be a tough girl while still loving this fragile world God created with a soft heart. If I could see the world through your eyes, every day would be beautiful.

To my grandmother, thank you for all the caring and encouragement. Thank you for letting me go into this world with all your wisdom and love.

Lise Barnard, we have come a long way. You where my first biochemistry lab-partner four years ago and since then you were stuck with me. Thank you for always helping me out, for all the borrowing, the late night working and motivation. Thank you for always lending me an ear when I needed to talk and always believing in me, sometimes even more than I believe in myself. You are truly my best friend and I was so privileged to have had you by my side the past two years.

Niel, you are the love of my life. We shared the same passion and love for science and realised we shared another type of love for each other. I can honestly say this was the best two years of my life thanks to you. Thank you for being my rock, for always being reliable, always going out of your way to help when I need you. Thank you for always putting me first, for always thinking of me. Thank you for all the late nights working in the lab or writing up, for all the lunches and tea and even just the phone calls asking me how things are going. Thank you for always being interested, for always being by my side. It was such a privilege to have had the opportunity to share the lab with you for the past two years. Although we won't share a lab next year I hope I will share the rest of my life with you. You make me the happiest girl on earth and I love you so much.

All praise and glory to God almighty for giving me the type of strength only found in His name. For all the grace, the unconditional love I felt every day of my life. I am grateful for His blessings in the form of people, who enrich every inch of who I am.

Contents

List of figures

List of tables

Abbreviations

11K-5α-dione	11-keto-5α-androstanedione
11KA4	11-ketoandrostenedione
11KDHT	11-keto-5α-dihydrotestosterone
11KT	11-ketotestosterone
11OHA4	11β-hydroxyandrostenedione
11βHSD	11β-hydroxysteroid dehydrogenase
17OH-allopregnanolone	5α-pregnane-3α,17α-diol-20-one
17OH-dihydroprogesterone	5α-pregnane-17α-ol-3,20-dione
17OH-PREG	17α-hydroxypregnenolone
17OH-PROG	17α-hydroxyprogesterone
17βHSD	17β-hydroxysteroid dehydrogenase
3α-adiol	5α-androstane-3α,17β-diol
3βHSD	3β-hydroxysteroid dehydrogenase/Δ5-Δ4-isomerase
5α-dione	5α-androstanedione
A4	Androstenedione
ADT	Androgen deprivation therapy
AKR	Aldo-keto reductase
AKR1C1	Aldo-keto reductase 1C1 / 3α-hydroxysteroid dehydrogenase type 2
AKR1C2	Aldo-keto reductase 1C2 / 3α-hydroxysteroid dehydrogenase type 3
AKR1C3	Aldo-keto reductase 1C3 / 17β-hydroxysteroid dehydrogenase type 5
AR	Androgen receptor
ARE	Androgen response element
AST	Androsterone
BPH	Benign Prostatic Hyperplasia
BRCA2	Breast cancer type 2
CAH	Congenital adrenal hyperplasia
CRPC	Castration resistant prostate cancer
CYP17A1	Cytochrome P450 17α-hydroxylase/17,20-lyase
CYP21A2	Cytochrome P250 family 21, subfamily A, member 2
DHEA	Dehydroepiandrostenedione

DHEA-S	Dehydroepiandrostenedione sulphate
DHT	5α-dihydrotestosterone
DMEM	Dulbecco's modified eagle's medium
DOC	11-deoxycorticosterone
E_1	Estrone
E_2	17β-Estradiol
FBS	Fetal bovine serum
HEK-293	Human embryonic kidney cell line
HSD	Hydroxysteroid dehydrogenase
HSP	Heat shock protein
KLK3	Kallikrein-3
K_m	Michaelis-Menten constant
LH	Luteinizing hormone
LHRH	Luteinizing hormone-releasing hormone
LNCaP	Lymph node-cancer of the prostate cell line
MAPK	Mitogen-activated protein kinase
MTBE	Methyl tert-butyl ether
NADH/NAD^+	Nicotinamide adenine dinucleotide
NADPH/$NADP^+$	Nicotinamide adenine dinucleotide phosphate
NF-κB	Nuclear factor kappa-light-chain-enhancer of activated B cells
NSAID	Non-steroidal anti-inflammatory drug
PBS	Phosphate buffered saline
PCa	Prostate cancer
PG	Prostaglandin
PI3K	Phosphatidylinositol 3-kinase
POR	Cytochrome P450 reductase
PPARs	Peroxisome proliferator-activated receptors
PREG	Pregnenolone
PROG	Progesterone
PSA	Prostate specific antigen
qPCR	quantitative polymerase chain reaction
SAR	Structure activity relationships
SRD	Short-chain dehydrogenase/reductase
SRD5A	Steroid 5α-reductase
T	Testosterone
TMPRSS2	Transmembrane protease, serine 2

UPC^2-MS/MS	Ultra performance convergence chromatography tandem mass spectrophotometry
VCaP	Vertebral-cancer of the prostate cell line
V_{max}	Maximum velocity of enzymatic reaction

Chapter 1

The role of 17βHSD enzymes in castration resistant prostate cancer

1.1. The prostate

The prostate is a tubuloalveolar exocrine gland which forms part of the male reproductive system. It is situated just under the bladder, in front of the rectum and surrounds part of the urethra (figure 1.1) (1, 2). At birth the prostate has a volume of roughly 0.250 mL, which increases to approximately 10 mL at puberty and continues to increase throughout a male's lifetime. The average size of an adult male prostate is often described as being slightly larger than a walnut and having an average weight of 11 grams with a normal range of between 7-16 grams (3). Changes in prostate size, especially enlargements, are commonly associated with a number of different diseases and are thus an indicator that further diagnostic testing may be required (1).

The prostate is not essential for survival, but plays an important role in male reproduction and fertility as it contributes to the composition of semen, providing sperm with zinc, citrate and fructose (1). The prostate also secretes proteins such as kallikrein-3 (KLK3), also known as prostate specific antigen (PSA), which is a protease responsible for the breakdown of large proteins in the seminal coagulum into smaller polypeptides thus helping to liquefy the semen (4). In a healthy male, PSA is contained within the prostate and very rarely leaks into the bloodstream (5). Disruption of the basement membrane occurs during the development of prostate cancer (PCa) and results in the leakage of PSA into circulation (5, 6). Serum PSA levels are therefore used as a biomarker for the detection of PCa but are not exclusive to PCa as PSA leakage also occurs due to other diseases of the prostate, such as benign prostatic hyperplasia (BPH), as well as during physical damage to the prostate (5).

The prostate was originally divided into four lobes named the anterior lobe, the posterior lobe, the lateral lobe and the median or middle lobe (7). In 1968, John McNeal suggested revised

subdivisions of the prostate which he referred to as “zones” rather than lobes. He named these zones the peripheral zone, central zone, transition zone and the anterior fibro-muscular zone (stroma) (figure 1.1). It has since been observed that the peripheral zone is prone to the development of cancerous tumours (table 1.1), while the transition zone is more prone to the development of BPH (8, 9).

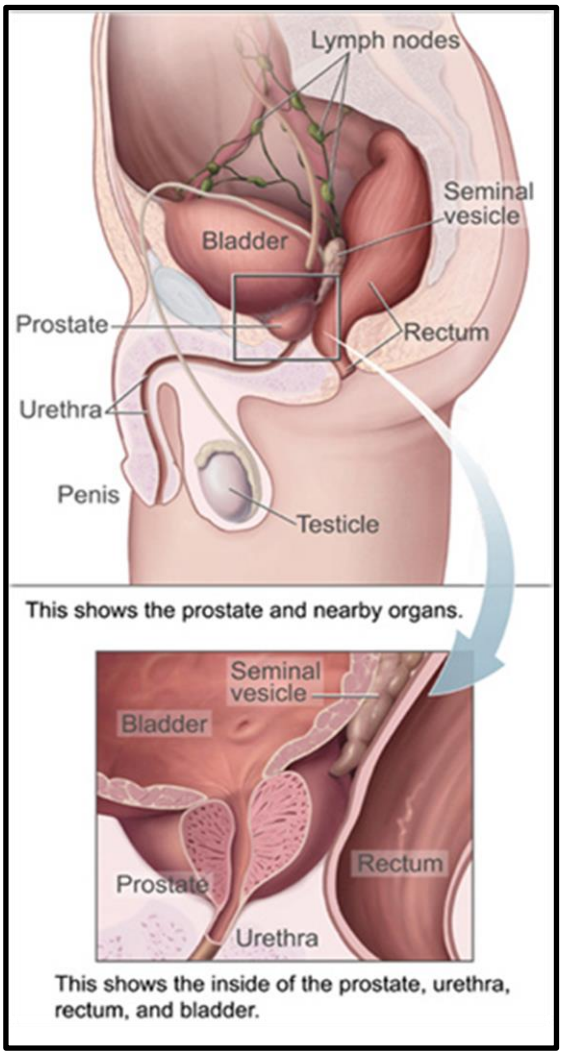

Figure 1.1: Schematic representation of the male reproductive system. The position of the prostate is pointed out by the square. Reproduced from: https://en.wikipedia.org/wiki/Prostate#/media/File:Prostatelead.jpg

The growth and maintenance of the healthy prostate is dependent on male sex hormones, which are known as androgens. Androgen levels in the foetus are high towards the end of gestation, but decrease after birth. Levels rise again during puberty as the testes begin to produce large amounts of the primary androgen, testosterone (T) (2, 10). Androgens are responsible for initiating prostate development, for the continues embryonic and neonatal prostatic growth and the initiation of the secretory activity of the prostate (2). The maintenance of the prostatic tissue and production of

secretory proteins, such as PSA, is controlled and maintained by androgens throughout a male's lifetime. The role of androgens in the development and maintenance of the prostate is especially clear when considering the termination of the secretory activity as well as apoptotic cell death and involution of the prostate gland which is observed following castration (2, 11, 12). The resumption of growth and function is observed following the administration of T (11). It should, however, be noted that while T is the primary androgen in male circulation within the prostate T is reduced to the more potent androgen, 5α-dihydrotestosterone (DHT), by the activity of steroid 5α-reductase (SRD5A). Inhibition of SRD5A reduces the development of the prostate, but does not completely inhibit it, thus demonstrating that there is not an absolute requirement for DHT in prostate maintenance, but that DHT is the more potent androgen (2, 13).

Table 1.1: The four subdivisions of the prostate. The contribution to the mass/volume of the prostate and their susceptibility to prostate cancer (PCa) of each subdivision are also shown. Zones were first divided into lobes, which can now be associated with different zones as indicated below.

Zone	Lobe corresponding to part of zone	Fraction of gland	Origin of PCa
Peripheral zone	Lateral lobe Posterior lobe	70% in young adult	70-80% (8, 9)
Central zone	Lateral lobe Median lobe	25%	2.5% (14)
Transition zone	Lateral lobe Anterior lobe	5% by puberty	10-20% (8, 9)
Anterior fibro-muscular zone (stroma)	Lateral lobe	5%	-

1.2. Androgen signalling

As mentioned above, androgens are essential for sexual development and reproductive function in males. The primary androgen T is produced by the Leydig cells of the testes under the control of the Hypothalamic-pituitary-gonadal (HPG) axis. Electrical pulses from neurons in the arcuate nucleus of the hypothalamus stimulate the release of gonadal releasing hormone (GnRH), which in turn stimulates the release of luteinizing hormone (LH) and follicle stimulating hormone (FSH) from the pituitary. These hormones then stimulate the production of T and low levels of the estrogen, 17β-estradiol (E_2), by the Leydig cells. This process is tightly regulated by negative feedback, where both T and E_2 inhibit the release of LH, FSH and GnRH (figure 1.2A) (15). As mentioned

above, T is reduced the more potent androgen, DHT, in peripheral target tissue such as the prostate which express SRD5A.

The human adrenal cortex produces weakly androgenic androgen precursors such as dehydroepiandrostenedione sulphate (DHEA-S), dehydroepiandrostenedione (DHEA), androstenedione (A4) and 11β-hydroxyandrostenedione (11OHA4), which can all be converted to active androgens in peripheral tissue (16). Similar to GnRH, corticotropin-releasing hormone (CRH) regulates the release of adrenocorticotropin (ACTH) from the pituitary, which in turn, stimulate the production of steroids including cortisol and adrenal androgen precursors from the zona fasciculata and zona reticularis of the adrenal cortex, respectively (15). Cortisol in turn inhibits the release of CRH and ACTH through a negative feedback loop. This axis is referred to as the Hypothalamic-pituitary-adrenal (HPA) axis (figure 1.2B). In humans, the production of adrenal androgen precursors starts at ages between 6 and 8 years old and is not accompanied by increases in cortisol levels (12). These changes in androgen precursor levels as well as a sudden growth spurt and bone maturation forms part of a process known as adrenarche and are due to the development of the zona reticularis in the adrenal cortex. Adrenarche is independent of the HPG axis maturation and function (13).

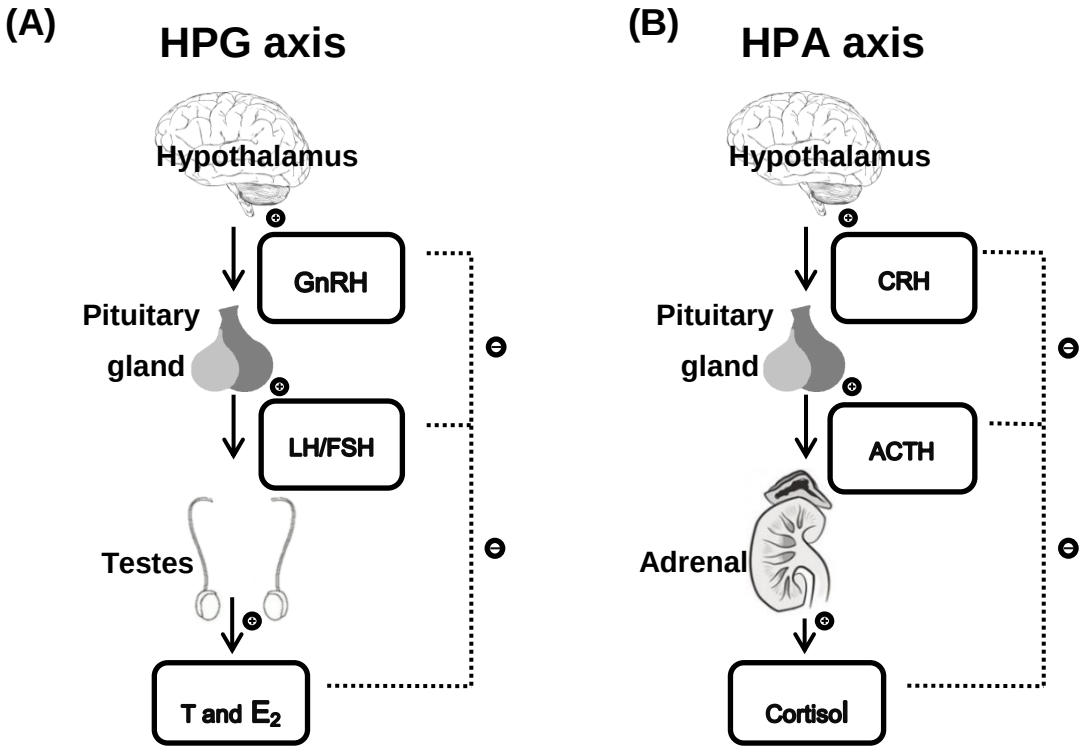

Figure 1.2: Schematic representation of (A) the hypothalamus-pituitary-gonadal (HPG) axis and (B) the hypothalamus-pituitary-adrenal (HPA) axis. The HPG consists of a cascade of steps leading to the production of T and E_2 by the Leydig cells of the testes. T and E_2 inhibit the release of GnRH, LH and FSH through negative feedback loops. Similarly, the HPA consists of a cascade of steps leading to the release cortisol and the weak androgen precursor, DHEA-S from the adrenal cortex. Cortisol inhibits the release of ACTH and CRH through a negative feedback loop.

Androgens act by binding to and activating the androgen receptor (AR). AR agonists include the potent androgens T and DHT. While both of these androgens have the ability to bind and activate the AR, the AR has a 10 times higher affinity for DHT (EC_{50} 0.018 µM) than for T (EC_{50} 0.195 nM) (17). Furthermore, DHT dissociates from the AR at a slower rate when compared to T (18).

The AR is a member of a subfamily of nuclear receptors called NR3C4 (nuclear receptor subfamily 3, group C, member 4) (19). This receptor consist of three function domains: the N-terminal transactivation domain; the DNA binding domain (DBD); and the C-terminal ligand binding domain (LBD) with a hinge region linking the DBD and LBD (18, 20). The functional domains share conserved areas with other steroid receptors such as the estrogen, progesterone (PROG), glucocorticoid, and mineralocorticoid receptors (21, 22). Nuclear receptors can regulate gene expression by activating or suppressing the transcription of specific genes. The AR can activate transcription by binding to *cis*-acting DNA elements or repress gene transcription by binding to a *cis*-negative DNA motifs. The AR can also interact with other trans-acting factors such as the protein complex nuclear factor kappa-light-chain-enhancer of activated B cells (NF-κB) through protein–protein interaction leading to transcriptional interference also known as transrepression (23–26).

During transactivation an agonist binds to the AR and the receptor undergoes a conformational change and dissociates from the heat shock proteins (HSP) with which it is complexed. The activated receptor subsequently forms a homodimer with another activated receptor. The dimerized complex translocates into the nucleus where it binds to a 15 bp DNA element, called the AR-response element (ARE). This transactivates the transcription of androgen-regulated genes, such as PSA, which are essential for the development of male sexual characteristics and male reproductive function (18, 27, 28).

Negative gene regulation can be divided into two types, namely repression and transrepression. During repression, the receptor binds to the DNA response element but instead of eliciting a transcriptional response it inhibits transcription. This includes ligand independent repression in which unliganded receptor homodimers binding to the DNA response element and inhibit transcription (29). During transrepression the ligand-activated AR does not bind to DNA, but instead has a protein-protein interaction with promoter-bound transcription factors. This interferes with the initiation of transcription and the gene is thus repressed (29). An example of this is the inhibition of c-Jun and c-Fos activity, which together form part of the AP-1 early response transcription factor, by direct protein-protein interaction with the AR. This mechanism interferes with the subsequent binding of co-activators (30, 31). Another example is the protein-protein interaction which is seen between the AR and the transcription factor NF-κB. The AR results in the transrepression of genes regulated by NF-κB, which include immunoregulatory proteins, cytokines, rel/lκB protein, cyclins, growth factors and regulators of apoptosis (30).

1.3. Prostate cancer

Global statistics suggest that one in every seven men will be diagnosed with PCa during their lifetime (32). A cancer profile research report by the world health organisation (WHO) estimated that 9957 men were diagnosed with PCa in South Africa in 2014, almost twice as many as men diagnosed with lung cancer for that same year (32). A total of 20 700 male deaths were attributed to cancer in 2014 in South Africa, of which 16% were due to PCa (5).

The development of PCa can be attributed to several different factors. Alterations in the phosphatidylinositol 3-kinase (PI3K) signalling pathway, which is responsible for promoting the growth of cells and preventing apoptosis, have been found in 40% of primary PCa and 70% of metastatic PCa cases (27, 33–35). Increased expression of oncogenes and the down regulation of tumour suppressor genes have also been shown to play an important role in PCa development. For example, the transcription factor, c-myc, which plays a role in cell cycle progression and apoptosis is commonly overexpressed, while the RNA binding protein involved in nuclear processes, p53, and the tumour suppressor protein, Rb, are down regulated or inactivated, though the incidence of these changes were found to be more common in metastatic tumours than in primary tumours (35). Concomitant alterations and mutations in the AR have also been observed in PCa cells, and will be discussed in more detail in section 1.4.1. (27). Recurring chromosomal translocations resulting in the formation of fusion proteins that contribute to PCa development are also common (27). The 5' untranslated region of the transmembrane protease serine 2 (TMPRSS2) was found to fuse to the oncogene ERG in cancers which over expresses erythroblast transformation-specific (ETS) family members (36–39). Fusions include TMPRSS2-ERG, TMPRSS2-ETV1 (37, 40) and TMPRSS2-ETV4 (38, 40). TMPRSS2 is highly specific to prostate tissue and is localized to the prostate luminal epithelial cells (37, 40). Cerveira *et al.* and Tomlins *et al.* have shown that androgen stimulation can cause the over expression of ERG in a TMPRSS2-ERG positive cell line and this deregulation of ERG through the androgen dependent activation of TMPRSS2 has been suggested to alter cell proliferation and apoptosis (37, 40, 41).

1.4. Castration resistant prostate cancer (CRPC)

PCa, like the healthy prostate, is dependent on the activation of AR signalling. In 1966, before the discovery of the AR, Charles Huggins was awarded the Nobel Prize for showing that supplementation with T increased the growth of prostate tumours in rats, while castration led to a delay in the growth of the tumour (18, 44). While PCa can initially be treated with radiation therapy and chemotherapy, metastatic cancers are treated using androgen deprivation therapy (ADT) (27).

The aim of ADT is to prevent the production of T by the testes and is accomplished by chemical or surgical castration. Chemical castration is achieved by the administration of luteinizing hormone-releasing hormone (LHRH) agonists such as leuprolide and is often accompanied by treatment with AR antagonists such as bicalutamide or flutamide (42). ADT treatment results in a decrease in the activation of AR and ultimately leads to tumour regression. While ADT is initially effective, in most cases the cancer re-emerges after 2-3 years in an aggressive and fatal form known as castration resistant prostate cancer (CRPC) (42). Men aged 65 and older are especially prone to developing CRPC (43).

Robinson *et al.* recently conducted a comprehensive study investigating genomic alterations in patients affected by CRPC (figure 1.3). The aim of the study was to identify discrete molecular subtypes of CRPC, considering short insertion/deletions, copy number alterations and fusion transcripts (figure 1.3) (44).

Alterations in the PI3K pathway were found in 49% of individuals affected by CRPC. This pathway consists of enzymes involved in a variety of cellular functions such as cell growth, proliferation, differentiation, motility, survival and intracellular trafficking. Alterations in this pathway include biallelic (pertaining to both alleles, both alternative forms of a gene) loss of phosphatase and tensin homolog (PTEN), hotspot mutations, amplifications and triggering fusions in PIK3CA, and p.E17K activating mutations in the Akt1 gene which encodes for the RAC-alpha serine/threonine-protein kinase and which plays a role in metabolism, growth, proliferation, survival, transcription and protein synthesis through serine and/or threonine phosphorylation of a range of downstream targets (44).

Mutations in the Wnt signalling pathway were found in 18% of cases and including hotspot activated mutations previously found in Catenin beta-1 encoding gene (CTNNB1) (45) and recurrent alterations in Adenomatous polyposis coli (APC) (44). This pathway is involved in cellular processes including cell fate determination, motility, polarity, primary axis formation and organogenesis and has also been implicated in stem cell renewal (46). In the case of CRPC, studies recently identified alterations in Ring Finger Protein 43 (RNF43) and Zinc And Ring Finger 3 (ZNRF3) which were also previously found in colorectal, endometrial and adrenocortical cancers (44, 47, 48). These were conjointly exclusive with APC alterations. Studies also found R-Spondin 2 (RSPO2) fusions in association with RSPO2 overexpression also previously observed in colorectal cancers (44, 49).

A loss in tumour suppressor gene encoding for the production of retinoblastoma protein (RB1) was observed in 21% of CRPC cases (44). Further expanding the scope of CRPC cell cycle gene alterations they found focal amplification involving the cyclin D1 encoding gene (CCND1) in 9% of the cases and less common events involving CDKNZA/B. This results in cell cycle instability and

can lead to enhanced response to CDK4 inhibitors in other tumour types and is predicted to have similar activity in PCa (44, 50).

Twenty-three percent of CRPC cases involve alterations in DNA repair pathways with 12.7% of those including the loss in the tumour suppressor gene, BRCA2 which encodes for breast cancer type 2 susceptibility proteins. Up to 90% of these losses were found to be biallelic and were mostly due to somatic point deletions (44). Further studies revealed that 22.7% cases of CRPC contained alterations in DNA repair and recombination genes such as MLH1 or MLH2 (44, 51).

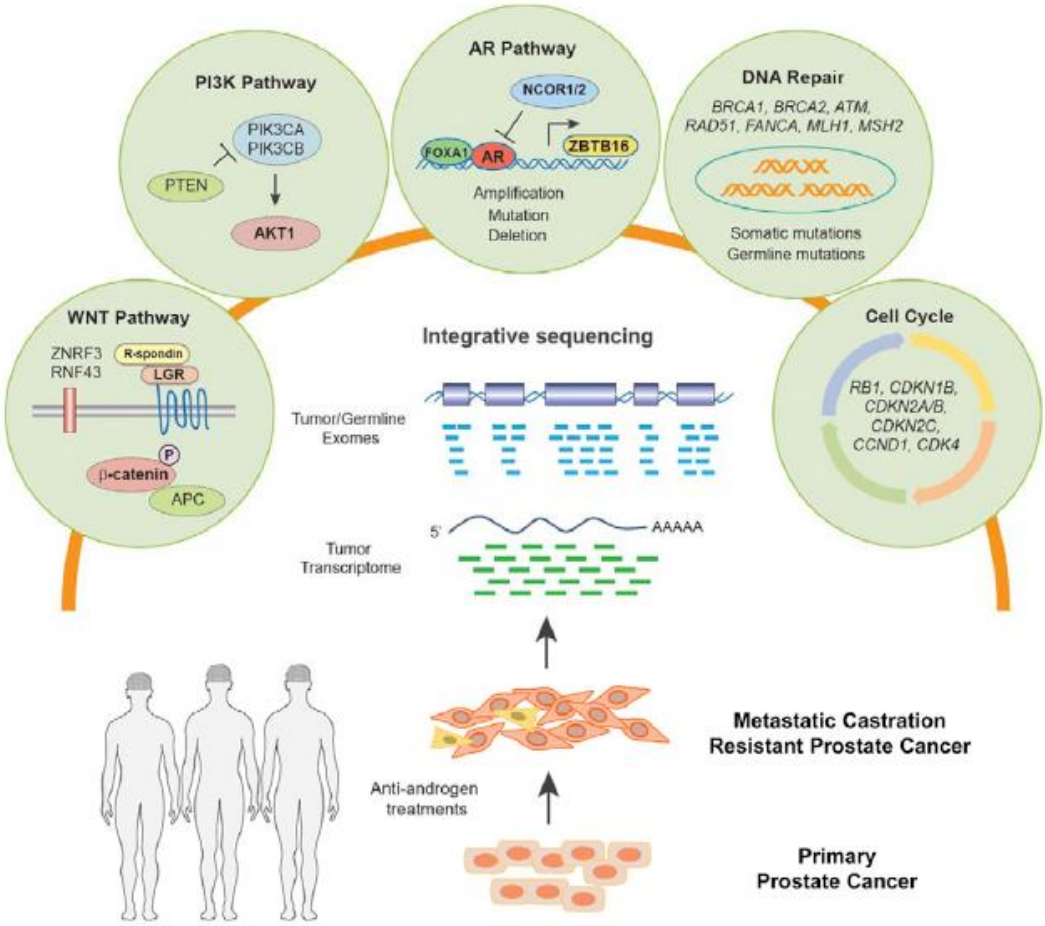

Figure 1.3: Common pathways altered in CRPC. Schematic showing the five most common pathways which are altered in metastatic castration-resistant prostate cancer. Reproduced with permission from: Robinson *et al.* (2016) Integrative Clinical Genomics of Advanced Prostate Cancer. *Cell*. 161, 1215–1228.

Alterations in the AR signalling pathway, mostly amplifications and mutations, were found in 71.3% cases of CRPC (44). These included changes to the AR itself, as well as changes to FOXA1, NCOR1/2, SPOP (52), and ZBTB16 (44). Mutations in the AR were found to occur at residues which were previously found to confer agonism to AR antagonists including flutamide (T878A) and

bicalutamide (W742C) (44). FOXA1, NCOR1 and NCOR2 are responsible for the regulation of the AR, and were found to be altered in both primary cancers and CRPC while ZBTB16 plays and role in cell cycle progression, and interacts with a histone deacetylase (44, 53, 54).

1.4.1. Androgen receptor mutations

Mechanisms proposed as an explanation for the development of CRPC were at first directed towards finding alterations in AR structure, function and ligand binding. This included the over expression of the AR, AR gene mutations, enhanced AR signal transduction through downstream regulatory molecules, co-factor recruitment alterations (increase expression of transcriptional co-activator proteins), cross-talk leading to the activation of the receptor independent of ligand binding and AR splice alternatives (55–58) (figure 1.4). AR mutations where found to occur in up to 40% (57, 59, 60) of primary tumours while up to 50% (57, 61) of recurrent tumours presented AR mutations.

Alterations in the steroid binding specificity of the AR increases the range of ligands which are able to bind and possibly activate the receptor (57, 62–64). Studies have also observed a correlation between the depletion of androgens and mutations in the functional domain of the AR which is essential for interaction with co-activators (65).

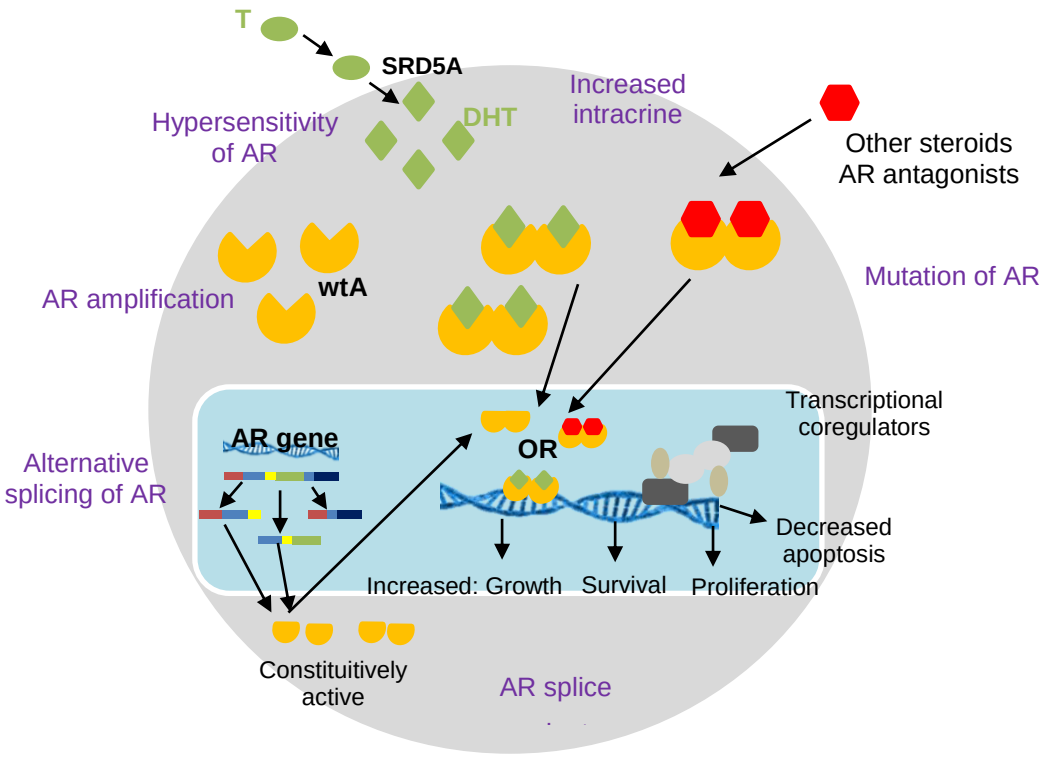

Figure 1.4: Alterations and mutations of the androgen receptor which could contribute to the development of CRPC. Adapted from: Anantharaman, A; Friedlander, T W. (2015) Targeting the androgen receptor in metastatic castrate-resistant prostate cancer: A review. Urologic Oncology: Seminars and Original Investigations. 34, 356–367.

Gregory *et al.* showed both an increase in the expression and stability of the AR as well as an increase in the sensitivity of this receptor for its ligand in recurrent tumours (66, 67). Chen *et al.* suggested that an increase in AR expression is essential for the progression from androgen-dependent to castration-resistant cancer. They observed an increase in AR expression sufficient to be activated in the presence of a 80% reduction in normal intra-prostatic androgen concentrations (55). It is commonly believed that an increase in AR expression and structural stability combined with an increased sensitivity for lower levels of androgens such as DHT will lead to continued proliferation of cells even after ADT. Enhanced sensitivity of AR signalling has also been shown to be due to alterations in other signal transduction pathways including the RAS/Raf/MAP, protein kinase A (PKA) and PI3K pathways (68).

In addition, a number of pathways can crosstalk with AR signalling. During non-genomic AR signalling cytoplasmic ligand bound AR can facilitate the activation of kinase-signalling cascades including Ras-Raf-1, PI3K/Akt and PKA, leading to the activation of mitogen-activated protein kinase (MAPK)/extracellular signal-regulated kinase (ERK) which ultimately leads to cell proliferation (69). Other signalling pathways can also lead to the activation of the AR without the need for androgens. For example, the cyclic adenosine monophosphate activated protein kinase A (cAMP/PKA) pathway can activate the AR, leading to increased PSA expression, in an androgen independent manner (70) thus contributing to PCa progression (71). It should, however, be noted that an increase in PSA gene expression via PKA still requires a functional AR (70, 72). ERK may also phosphorylate the AR as well as its co-activators, leading to enhanced genomic AR activity in the presence of a ligand. This could also occur in an ERK-independent manner by the activation of the rapamycin (mTOR) pathway or intracellular Ca^{+2} level modulations by plasma membrane G protein-coupled receptors (GPCRs) (69). While the mechanisms described above have been shown to play important roles in the development of CRPC, in most cases the activation of the AR is still dependent on the binding of a ligand (66). An AR splice variant, AR-V7, which lacks a functional LBD has however been shown to activate AR reporter genes in the absence of ligand and is therefore believed to play a role in some CRPC cases (73).

1.4.2. CRPC is an androgen dependant disease

CRPC was formerly known as androgen independent hormone refractory PCa, as it was believed to be independent of androgens. Studies have since shown that in most cases CRPC remains androgen-dependent (57, 74). Mohler *et al*. (57) therefore proposed that CRPC should be referred to as a recurrent disease and not an androgen independent disease. Imaging and cytology experiments have revealed that while castration inhibits the activation of AR signalling this activity is reactivated during the development of CRPC and is accompanied by a concomitant increase in

PSA levels (19, 66, 75, 76). Mostaghel *et al*. (77–79) have confirmed that the progression of CRPC correlates with an increase in PSA levels and that PSA remains in the top 1% of all genes expressed in CRPC tumours (77–79). The dependence of CRPC on the presence of androgens have since been confirmed by clinical studies which have shown that the anti-androgens, Abiraterone (CYP17A1 inhibitor) and Enzalutamide (AR antagonist), significantly improve patient outcomes (80).

Abiraterone inhibits the key steroidogenic enzyme Cytochrome P450 17α-hydroxylase/17,20-lyase (CYP17A1), which is essential for the production of all androgens and androgen precursors. Attard *et al.*, (74) treated 21 chemotherapy-naïve patients with 250-2000 mg Abiraterone acetate per day. They found that within 8 days of treatment the T levels of the participating patients dropped from a median of 7ng/dL to an undetectable level and remained at these levels for the duration of the treatment period. DHEA levels were found to decrease by 70.4% within 28 days after treatment. Decreases in DHEA and E_2 levels were also observed. Conversely the inhibition of CYP17A1 resulted in significant increase in up-stream steroid metabolites. For example, a 40-fold increase in corticosterone and a 10-fold increase in 11-deoxycorticosterone (DOC) levels were observed. Additionally, a 6-fold increase in ACTH was observed. Notably, Attard *et al.* (74) found that 66% of the patients receiving treatment showed a 30% or more decrease in PSA levels three months after treatment was initiated.

Table 1.2: Androgen levels in different prostate tissues. Mean tissue androgen levels in castration resistant metastases from anorchid patients versus primary prostate tissues from eugonadal men. Adapted from: R. B. Montgomery *et al.* (2008) Maintenance of Intratumoural Androgens in Metastatic Prostate Cancer: A Mechanism for Castration-Resistant Tumour Growth. *Cancer Res*. 68(11). 4447-54.

Tissue source	Testosterone, ng/g (95% CI)*	DHT, ng/g (95% CI)*
Benign prostate	0.04 (0.00–0.24)	1.92 (1.63–2.21)
Cancer prostate	0.23 (0.03–0.44)	2.75 (2.45–3.04)
Control tissue[ł]	0.10 (0.00–0.26)	0.05 (0.00–0.30)
Metastatic tissue	0.74 (0.59–0.89)	0.25 (0.00–0.50)

Abbreviation: 95% CI, 95% confidence interval.
*P < 0.0001 for comparison among benign prostrate versus cancer prostrate, control tissue versus metastatic tissue, and cancer prostrate versus metastatic tissue for both testosterone and DHT (except P= 0.01 for difference in testosterone between benign prostate and cancer prostrate).
[ł]Nontumour tissues were obtained concurrently with tumour metastases from men with CRPC.

A study by Ryan *et al*. (81) investigated the effect of 1000 mg abiraterone on the life expectancy of 1088 asymptomatic chemotherapy-naïve PCa patients. The group was divided into two sections, one receiving abiraterone treatment and the other receiving a placebo treatment. Results showed that the median overall survival was significantly longer in the abiraterone group (34.7 months) compared to the placebo group (30.3 months) (81).

In contrast to Abiraterone, Enzalutamide is a nonsteriodal antiandrogen which acts as an AR antagonist by binding to the LBD of the AR thereby preventing nuclear translocation of the receptor, DNA binding and the recruitment of co-activators (82). Cabot *et al.* (82) showed that metastatic CRPC patients receiving Enzalutamide had an extended life expectancy compared to the placebo group not receiving the treatment (18.4 months vs 13.6 months). Enzalutamide was shown to lower the risk of fatality by 37% and delayed the growth of the tumour despite the presence of low concentrations of androgens (82). Enzalutamide was also shown to result in the reduction of tumour sizes during xenograph studies (82). Taken together, these results shifted the spotlight to the levels of androgens and their sources following ADT.

A study by Sharifi and Auchus (15) showed that intratumoural levels of DHT were approximately 1 nM (0.5 ng/g - 1.0 ng/g) in patients after castration and that these levels were sufficient for the activation of the AR. In fact these levels of DHT have been suggested to be 50-fold higher than the concentration required for half maximal activation of AR (15, 17). Montgomery *et al*. (66) suggested that there are two ways in which these intratumoural androgen concentrations can be supported during CRPC. First is the uptake and conversion of androgen precursors produced by the adrenal and second the *de novo* synthesis of androgens in peripheral tissue. Studies have since shown that a major contributing factor to intratumoural androgen levels is the intratumoural conversion of adrenal androgen precursors to active androgens (83).

1.5. Steroidogenesis

All steroid hormones are derived from cholesterol and thus share a common cyclopentanophenanthrene-4-ring structure. The first steroid hormones to be discovered were divided into the androgens and estrogens based on their physiological effects. Androgens are broadly considered to be male sex hormones while estrogens are considered female sex steroids. Later the progestogens, mineralocorticoids and glucocorticoids were also placed into their according groups based on their function (9).

Progestogens, such as PROG, are also sex steroids and play an important role in normal reproductive functions, which include ovulation, uterine and mammary gland development as well as neurobehavioral expression associated with sexual responsiveness (84–86). Glucocorticoids,

such as cortisol, are responsible for the regulation of carbohydrate, protein and fat metabolism, as well as the modulation of immune function (18, 87, 88). The mineralocorticoid aldosterone regulates water and salt balance by regulating the reabsorption of sodium from the distal convoluted and cortical collecting tube of the kidney (18, 89–93).

The primary sites of *de novo* steroid biosynthesis (steroidogenesis) in men are the testis (Leydig cells) and the adrenal cortex. Two major groups of enzymes are required for steroid biosynthesis – the cytochrome P450s (CYP) and the hydroxysteroid dehydrogenases (HSD).

1.5.1. Cytochrome P450 enzymes

The majority of mammalian CYP enzymes consist of approximately 500 amino acid residues. All CYPs contain a single heme group which is essential for catalytic function (94, 95). These enzymes are oxidative in nature and catalyse physiologically and mechanically non-reversible reactions. In their reduced state and with carbon monoxide bound as a ligand the CYP enzymes demonstrate a characteristic absorption maximum of 450 nm. CYP enzymes can be divided into two groups, namely type 1 CYPs, which are found in the mitochondria and accept electrons from NADPH, via ferredoxin reductase and ferredoxin, and type 2 enzymes which are located in the endoplasmic reticulum and accept electrons from NADPH via P450 oxidoreductase (POR) (95, 96). CYP enzymes are responsible for the metabolism of a variety of xenobiotics in the liver and the biosynthesis of steroid hormones in the adrenal and gonads. The CYP catalytic cycle is complex and includes the activation and cleavage of molecular oxygen, with one atom of oxygen being included in the substrate and the other released as water (95).

1.5.2. Hydroxysteroid dehydrogenase (HSD)

Hydroxysteroid dehydrogenases (HSDs) are a group of enzymes which are usually 35-45 kDa in size (95). These enzymes make use of either $NADH/NAD^+$ or $NADPH/NADP^+$ as co-factors to catalyse redox reactions such as the conversion of a secondary alcohol to a ketone (94, 97). HSD catalysed reactions are reversible under controlled conditions *in vitro*, but one reaction is usually dominant *in vivo.*

HSD enzymes are classified according to their structure or function. Structurally HSD enzymes are classified as either short-chain dehydrogenases/reductases (SDRs) or Aldo-keto reductases (AKR) (95, 97, 98). The tertiary structure of SDRs consist of a Rossman fold, or β-α-β secondary structure, which is a characteristic of oxidation/reduction enzymes that utilize nicotinamide as cofactor (95, 97, 98). In contrast, the tertiary structure of AKR enzymes consist of either β-barrels

or triosephosphate isomerase (TIM-barrels) motifs (95, 97, 98). Both SDRs and AKRs contain tyrosine and lysine residues in their active site and these residues play an important role in substrate binding and specificity (95, 97, 98).

Functionally the steroid metabolising HSD enzymes, are divided into one of two groups – the dehydrogenases and reductases (95, 97, 98). Enzymes classified as dehydrogenases use NAD^+ as cofactor to oxidise their substrate from a hydroxysteroid to ketosteroid (95, 97, 98). Conversely, reductases use NADPH to reduce ketosteroids to hydroxysteroids (95, 97, 98). Thermodynamic analysis of HSD enzymes indicated that these enzymes prefer the reduction of ketosteroids. Concomitantly, the oxidative enzymes need to overcome an uphill thermodynamic hurdle (97). This is accomplished by the availability of cofactors. For example, *in vivo* the catalytic activity of 11βHSD1 is dependent on the presence of the cofactor NADPH in order to catalyse the reduction of cortisone to cortisol (99). A high NADPH/$NADP^+$ ratio is maintained by the co-expression of hexose-6-phosphate deyhydrogenase (H6PDH) which catalyses the conversion of glucose-6-phosphate to 6-phosphogluconate and is coupled to the reduction of $NADP^+$ to NADPH. In H6PDH knockout mice, the drop in NADPH concentration results in 11βHSD1 acting as a dehydrogenase instead of a reductase (99). H6PDH thus regulates the directionality of 11βHSD1 activity *in vivo* (99–101).

1.5.3. Steroidogenesis in the testis

Steroidogenesis starts with the transfer of cholesterol from the outer to the inner membrane of the mitochondria by the steroidogenic acute regulatory protein (StAR) as can be seen in figure 1.5. Thereafter cholesterol undergoes side-chain cleavage to produce pregnenolone (PREG), a reaction which is catalysed by cytochrome P450 side-chain cleavage (CYP11A1). PREG is subsequently converted to 17α-hydroxypregnenolone (17OHPREG) by the 17α-hydroxylase activity of CYP17A1 (figure 1.5). The 17,20-lyase activity of CYP17A1, which is augmented by cytochrome b5, then results in the cleavage of the 17-20 carbon bond leading to the production of DHEA. 3βHSD2 subsequently converts DHEA to A4, which is then converted to T by 17βHSD3 (94) (figure 1.5). The production of T by the Leydig cells is regulated by the HPG-axis as discussed in section 1.2. This axis regulates the expression of CYP11A1 and CYP17A1 as well as the function of StAR.

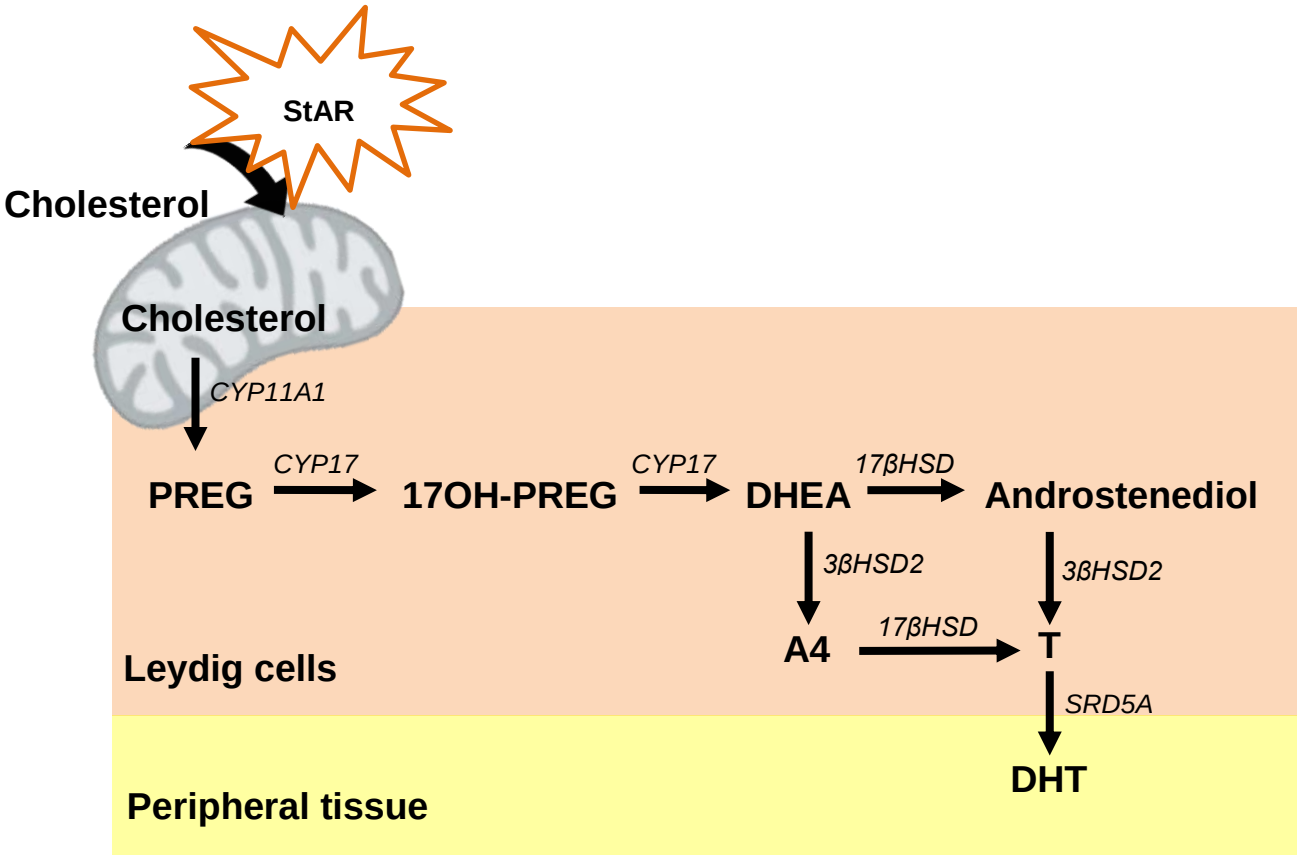

Figure 1.5: Schematic of steroidogenesis in the Leydig cells of the testes.

1.5.4. Steroidogenesis in the adrenal

The adrenal cortex is divided into three zones, which differ in the enzymes they express and as a result their steroid output (95, 102). All three zones express CYP11A1 and StAR. The zona glomerulosa also expresses 3βHSD2, CYP21A2 and cytochrome P450 aldosterone synthase (CYP11B2) thus leading to the production of the mineralocorticoid aldosterone. The zona fasciculata expresses CYP17A1, 3βHSD2, CYP21A2, and CYP11B1 resulting in the production of the glucocorticoid cortisol (figure 1.6) (95, 103). The zona reticularis expresses high levels of CYP17A1 and cytochrome b_5 resulting in the synthesis of high levels of DHEA (figure 1.6). The majority of DHEA is sulphated by the activity of SULTA2 leading to the production of DHEA-S (95, 102, 104, 105). DHEA is also converted to A4 by the activity of 3βHSD2 (figure 1.7). Besides the production of A4 and DHEA, the adrenal also produces the 11-oxygenated C19 steroid precursor 11OHA4. A4 is converted to 11OHA4 in the adrenal by the P450 enzyme, CYP11B1. Interestingly, 11OHA4 has been shown to be more abundant in adrenal vein samples when compared to A4 with low levels of 11KA4, 11OHT and 11KT also being produced (figure 1.6) (106–108).

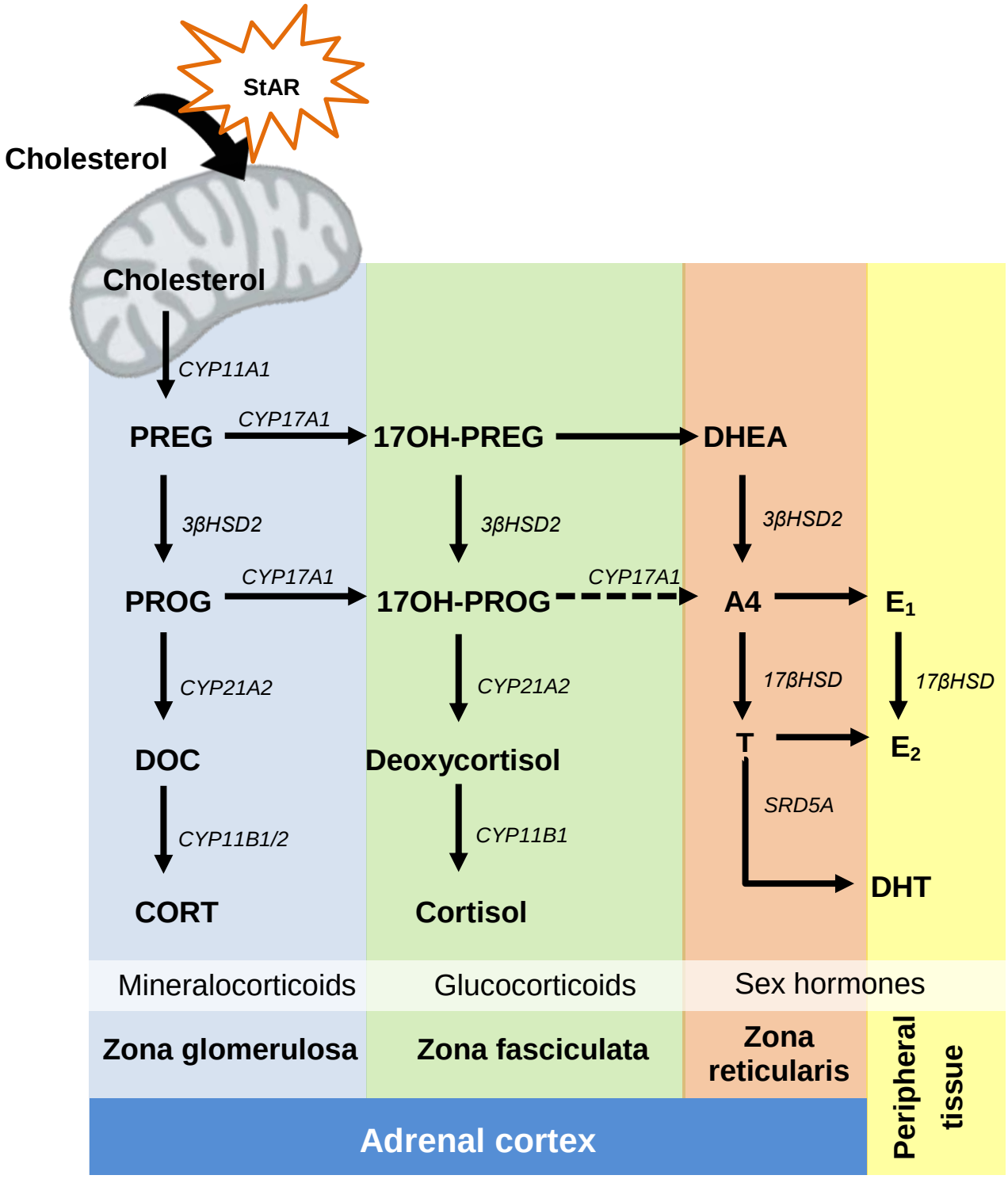

Figure 1.6: Schematic of steroidogenesis in the adrenal gland.

1.5.5. Steroid metabolism in CRPC

1.5.5.1. The Alternative pathway (5α-dione pathway)

Circulating levels of T are reduced significantly following ADT (<50 ng/dL) (109, 110). Studies have shown that this does not however reduce the production of androgens in CRPC tissue. In CRPC,

the adrenal steroid DHEA is converted to A4 by the activity of 3βHSD. It was initially assumed that the resulting A4, together with A4 from circulation, is subsequently converted to T by the reductive 17βHSD enzymes followed by the reduction of T to DHT by SRD5A (classical pathway). A study done by Chang *et al.* however showed that the development and progression of CRPC is driven by an alternative pathway to DHT which bypasses T production. In this pathway A4 is preferentially reduced by 5α-reductase type 1 (SRD5A1) yielding 5α-dione, which is subsequently converted directly to DHT by the activity of reductive 17βHSD enzymes (figure 1.7).

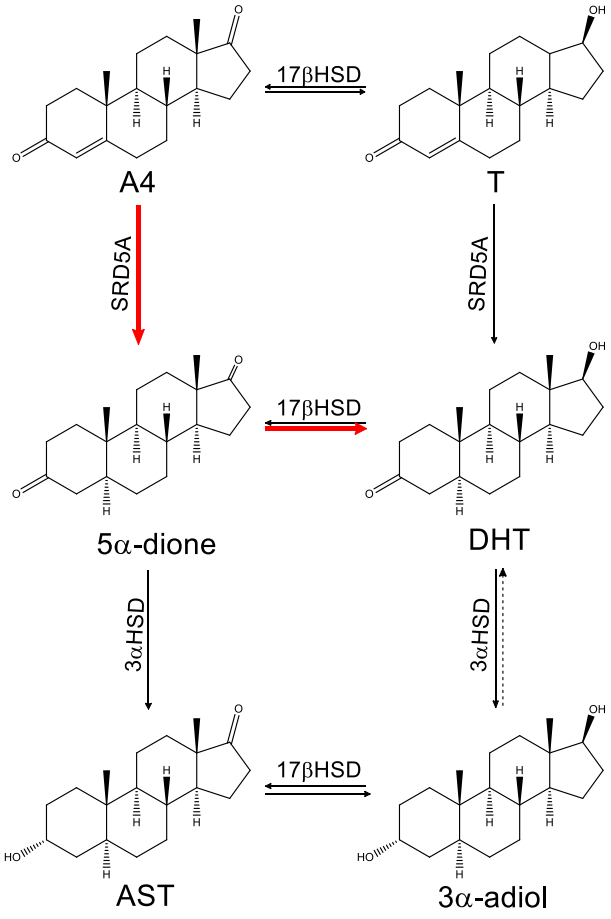

Figure 1.7: The metabolism of A4 to DHT in CRPC. The preferred alternative pathway is shown in red.

Chang *et al.* used six human PCa cell lines, to investigate the metabolism of A4. The cells where supplemented with [^{3}H]-A4 and the levels of the resulting metabolites, including 5α-dione and T, were separated by high pressure liquid chromatography (HPLC) and measured using a radioactive detector. The flux from A4 to 5α-dione was more rapid than the conversion of A4 to T for all six cell lines. These findings were subsequently confirmed using LAPC4 and LNCaP xenograft models in

surgically castrated mice supplemented with T or A4 as well as by quantifying steroid levels in tumour biopsies from patients with CRPC (111).

The flux through the alternative 5α-dione pathway has been shown to be due to the preference of SRD5A1 for A4 as a substrate. While both T and A4 have a ∆4, 3-keto structure and are both thus susceptible to 5α-reduction by SRD5A1, A4 is more efficiently reduced (111). During the development of CRPC the expression of SRD5A2 is decreased by approximately 50%, while the expression of SRD5A1 is significantly upregulated (112). The increased levels of SRD5A1 therefore favour the reduction of A4 to 5α-dione pushing the flux towards the synthesis of DHT, while bypassing T.

1.5.5.2. The 11β-hydroxyandrostenedione pathway

The human adrenal gland produces large quantities of the C19 steroid 11OHA4 in addition to the androgen precursors DHEA-S, DHEA and A4 (106–108). 11OHA4 is in fact approximately two times more abundant than A4 in adrenal vein samples in both in unstimulated and ACTH stimulated conditions (106). For many years the 11β-hydroxylation of A4 to 11OHA4 by CYP11B1 was believed to be a manner of inactivating A4, preventing it from being further metabolised to androgens such as T and DHT (108, 113).

Our group has, however, shown that 11OHA4 is not a dead-end product of adrenal steroidogenesis, but that it is a precursor to active androgens including 11-ketotestosterone (11KT), and 11-ketodihydrotestosterone (11KDHT) (108, 113). In addition to 11OHA4 the adrenal also produces low levels of 11KA4, 11OHT and 11KT (113) (figure 1.8).

Storbeck *et al.* (108) showed that 11OHA4 is metabolised by the activity of 11βHSD, SRD5A and 17βHSD which are all expressed in the prostate. In the preferred route 11OHA4 is converted to 11KA4 by 11βHSD2. AKR1C3 subsequently reduces 11KA4 to produce 11KT, which can further be converted to 11KDHT by SRD5A1 (107, 108) Interestingly, Storbeck *et al.* (106, unpublished data) showed that 11OHA4 cannot be converted to 11OHT by either AKR1C3 or 17βHSD3. 11OHT is however produced by the direct 11β-hydroxylation of T in both the adrenal (106, 107) and possibly the testes (114). 11OHT can be converted to 11KT by 11βHSD2 or to 11OHA4 by 17βHSD2 (16).

Storbeck *et al.* (108) subsequently tested the relative androgenic activity of the metabolites identified in the 11OHA4 pathway using a promoter reporter based transactivation assay. The androgenic activity of 1 nM of the metabolites was calculated relative to that of DHT, which was set at 100% (figure 1.9). While 11OHDHT was found to be only a partial agonist with 47% activity, 11KDHT demonstrated full agonist activity (96%). (108). Interestingly, T and 11KT also exhibited similar agonistic activity of 61% and 62% respectively (108). Only 30% agonist activity was,

however, observed for 11OHT, while no activity was observed for 11OHA4, 11OH-5α-dione or 11KA4 (figure 1.9) (108).

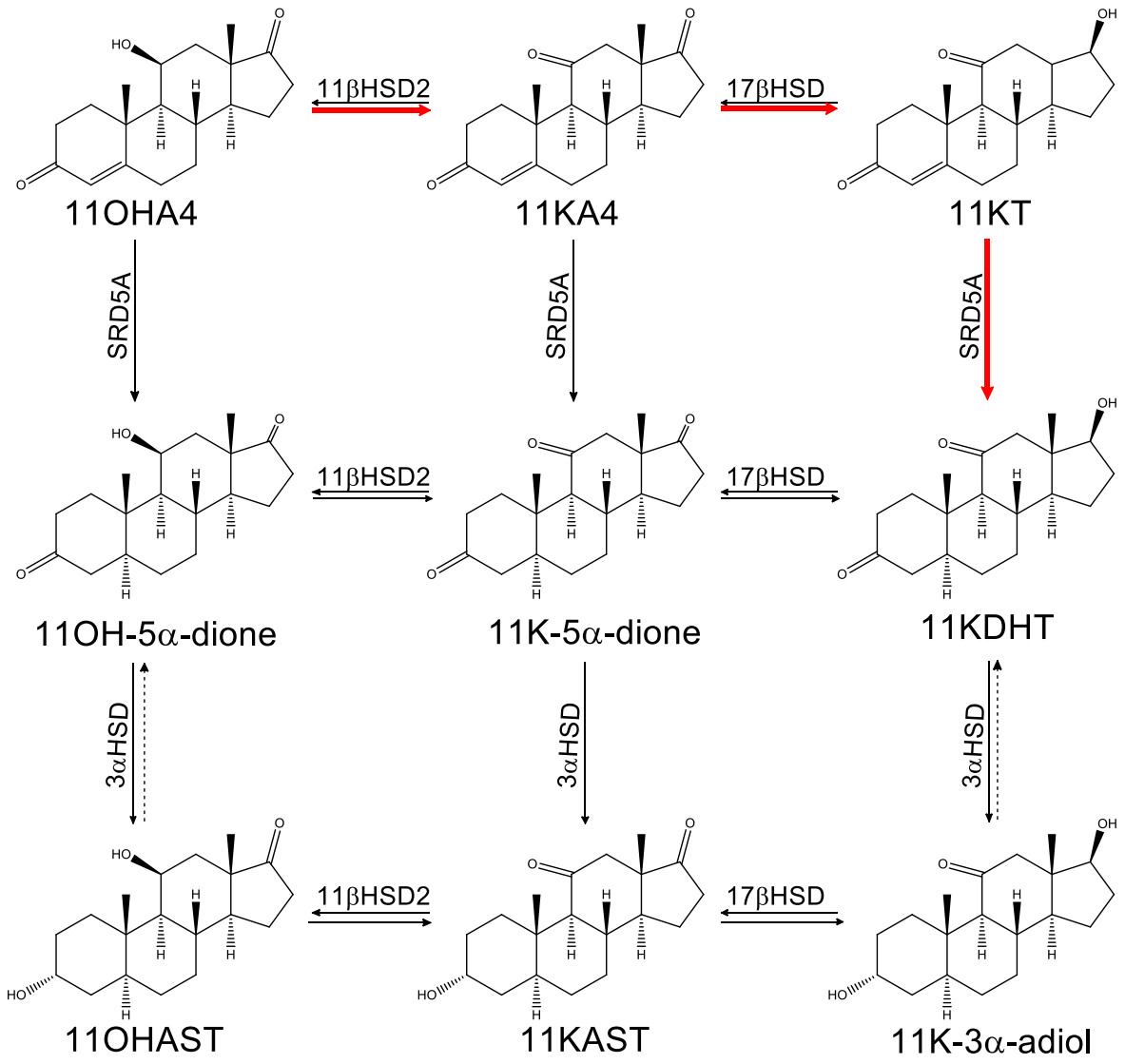

Figure 1.8: The 11OHA4 pathway. The weak precursor 11OHA4 is converted to more potent androgens 11KT and 11KDHT by the enzymes 17βHSD, SRD5A and 11βHSD. The preferred pathway is shown in red.

A study by Pretorius *et al.* (115) subsequently compared the androgenic activity of 11KT and 11KDHT to that of T and DHT, respectively. First using whole cell binding assays they found that the human AR has similar binding affinities for 11KT, 11KDHT, T and DHT (figure 1.10). Next using promoter reporter assays with a selective androgen response element (ARE) they found that 11KT, 11KDHT, T and DHT are all full AR agonists with similar efficiencies and that 11KDHT and DHT are equipotent. Similarly 11KT and T were found to be equipotent (115).

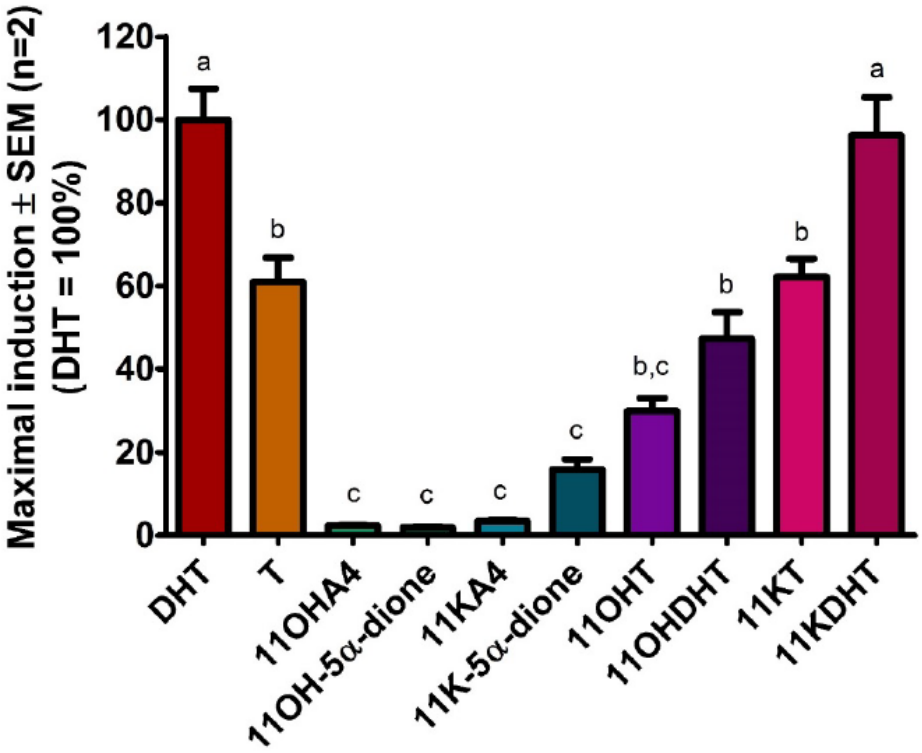

Figure 1.9: Transactivation of the human androgen receptor (AR) by 1 nM C19 steroids. Reproduced with permission from: Storbeck, K.-H., Bloem, L. M., Africander, D., Schloms, L., Swart, P., and Swart, A. C. (2013) 11β-Hydroxydihydrotestosterone and 11-ketodihydrotestosterone, novel C19 steroids with androgenic activity: a putative role in castration resistant prostate cancer. *Mol. Cell. Endocrinol.* 377, 135–46.

Pretorius *et al.* went on to show that the rate of metabolism was significantly higher for T and DHT in both VCaP and LNCaP cell lines when compared to 11KT and 11KDHT (figure 1.12). Thus 11KT and 11KDHT have the potential to remain active longer as they are metabolised at a lower rate (115).

Pretorius *et al*. also investigated the effect of DHT, 11KDHT, T and 11KT on the mRNA expression levels of three AR regulated genes in LNCaP (mutated AR) and VCaP (wild type AR) PCa cell lines as well as the alterations in protein expression in VCaP cells. They also went on to investigate the effect of these 11-oxygenated steroids on the proliferation of the above mentioned PCa cell lines.

Their results showed that 11KDHT and 11KT were able to upregulate all three AR regulated genes investigated (KLK3, TMPRSS2 and FKBP5) in LNCaP and VCaP cells and that both 11KDHT and 11KT induced cell growth in both androgen dependent cell lines (figure 1.11). Interestingly, they observed that 11KT and 11KDHT resulted in higher fold induction of KLK3, FKBPS and TMPRSS2 in LNCaP cells when compared to T and DHT (115). Proteomic analysis of VCaPs treated with DHT, 11KDHT, T and 11KT confirmed that 11KT and 11KDHT could regulate the expression of

known androgen regulated proteins. Taken together their results confirmed that these 11-oxygenated steroids were *bona fide* androgens capable of inducing the expression of endogenous AR regulated genes.

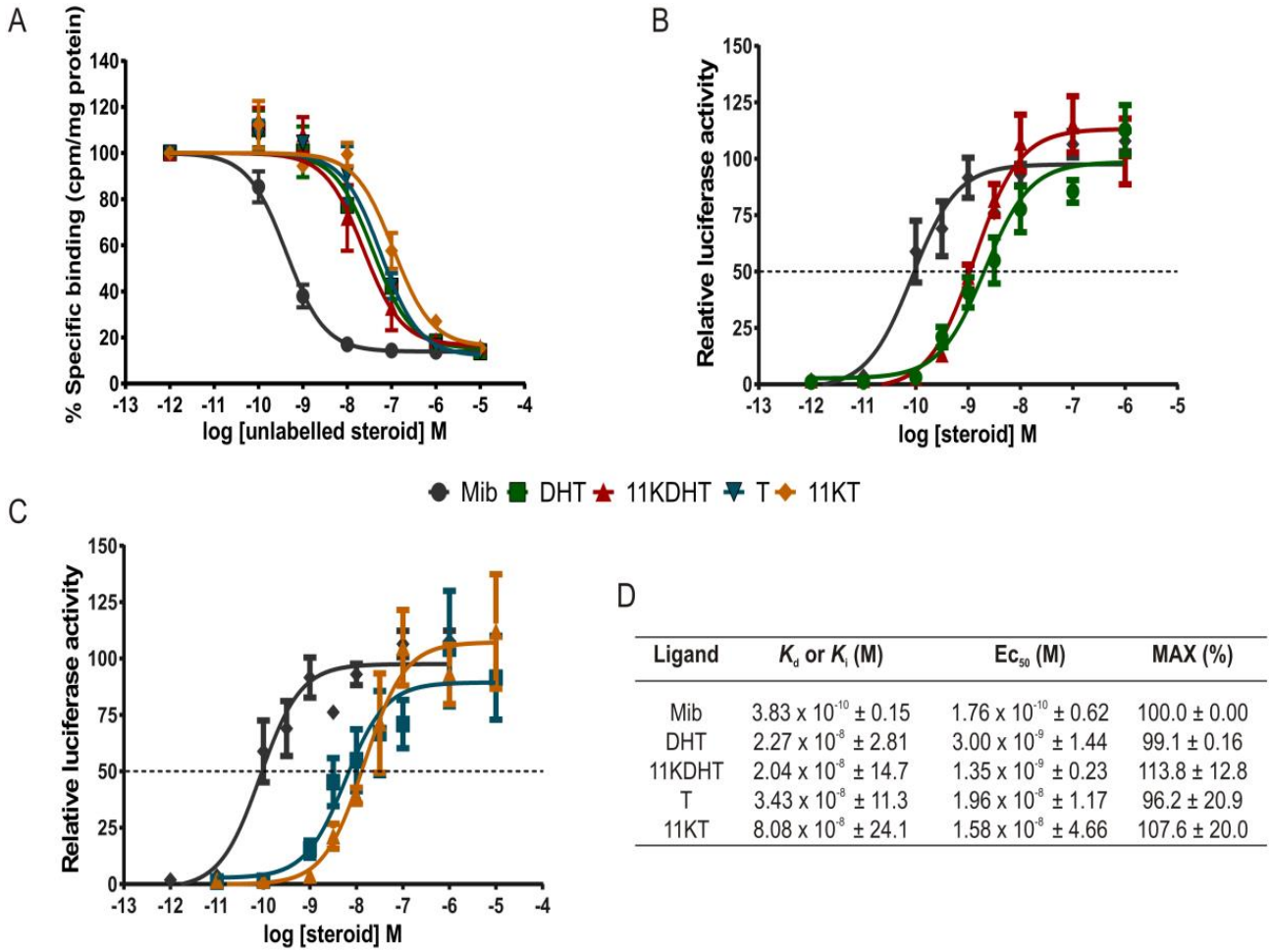

D

Ligand	K_d or K_i (M)	Ec_{50} (M)	MAX (%)
Mib	$3.83 \times 10^{-10} \pm 0.15$	$1.76 \times 10^{-10} \pm 0.62$	100.0 ± 0.00
DHT	$2.27 \times 10^{-8} \pm 2.81$	$3.00 \times 10^{-9} \pm 1.44$	99.1 ± 0.16
11KDHT	$2.04 \times 10^{-8} \pm 14.7$	$1.35 \times 10^{-9} \pm 0.23$	113.8 ± 12.8
T	$3.43 \times 10^{-8} \pm 11.3$	$1.96 \times 10^{-8} \pm 1.17$	96.2 ± 20.9
11KT	$8.08 \times 10^{-8} \pm 24.1$	$1.58 \times 10^{-8} \pm 4.66$	107.6 ± 20.0

Figure 1.10: Binding affinities, agonist potencies and efficacies of DHT, 11KDHT, T and 11KT relative to the synthetic AR agonist mibolerone. Reproduced with permission from: Pretorius, E., Africander, D. J., Vlok, M., Perkins, M. S., Quanson, J., Storbeck, K.-H. (2016) 11-Ketotestosterone and 11-Ketodihydrotestosterone in Castration Resistant Prostate Cancer: Potent Androgens Which Can No Longer Be Ignored. *PLoS One.*

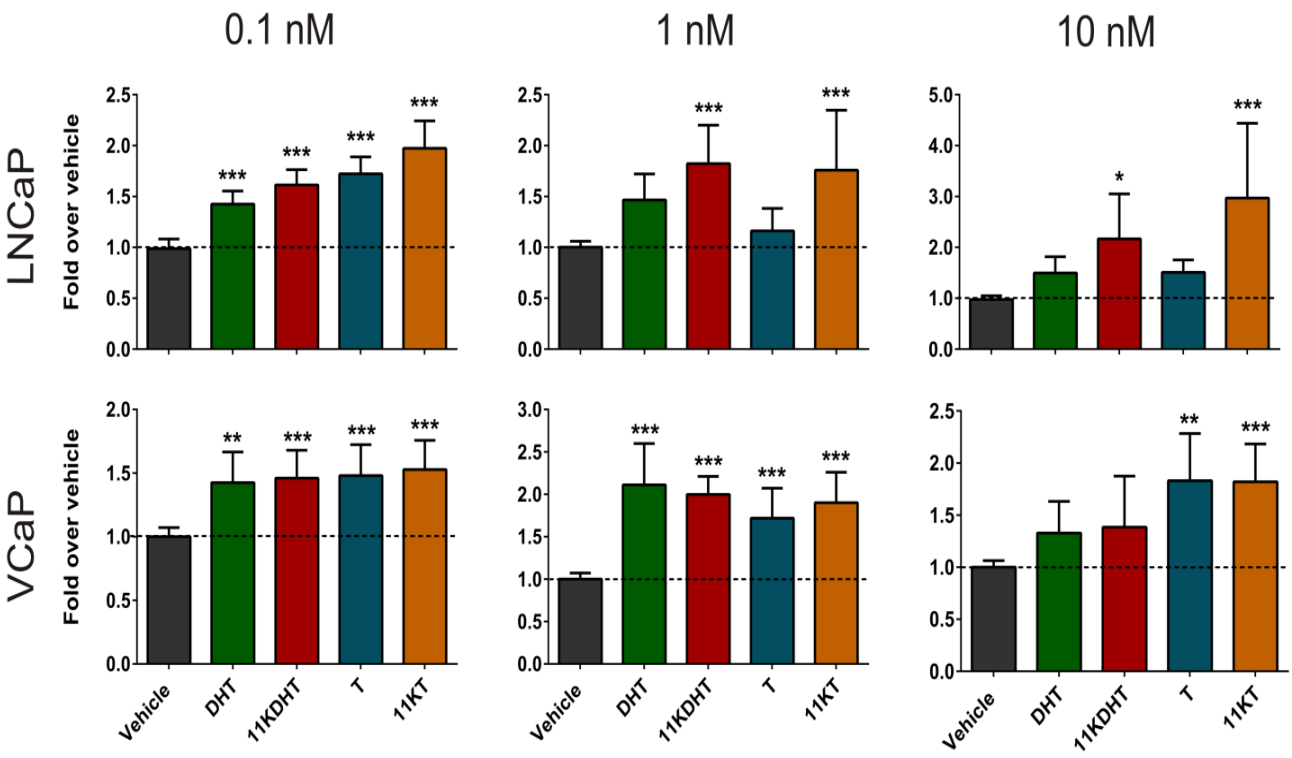

Figure 1.11 Induction of cell proliferation in LNCaP and VCaP cells by DHT, 11KDHT, T and 11KT. Reproduced with permission from: Pretorius, E., Africander, D. J., Vlok, M., Perkins, M. S., Quanson, J., Storbeck, K.-H. (2016) 11-Ketotestosterone and 11-Ketodihydrotestosterone in Castration Resistant Prostate Cancer: Potent Androgens Which Can No Longer Be Ignored. *PLoS One.*

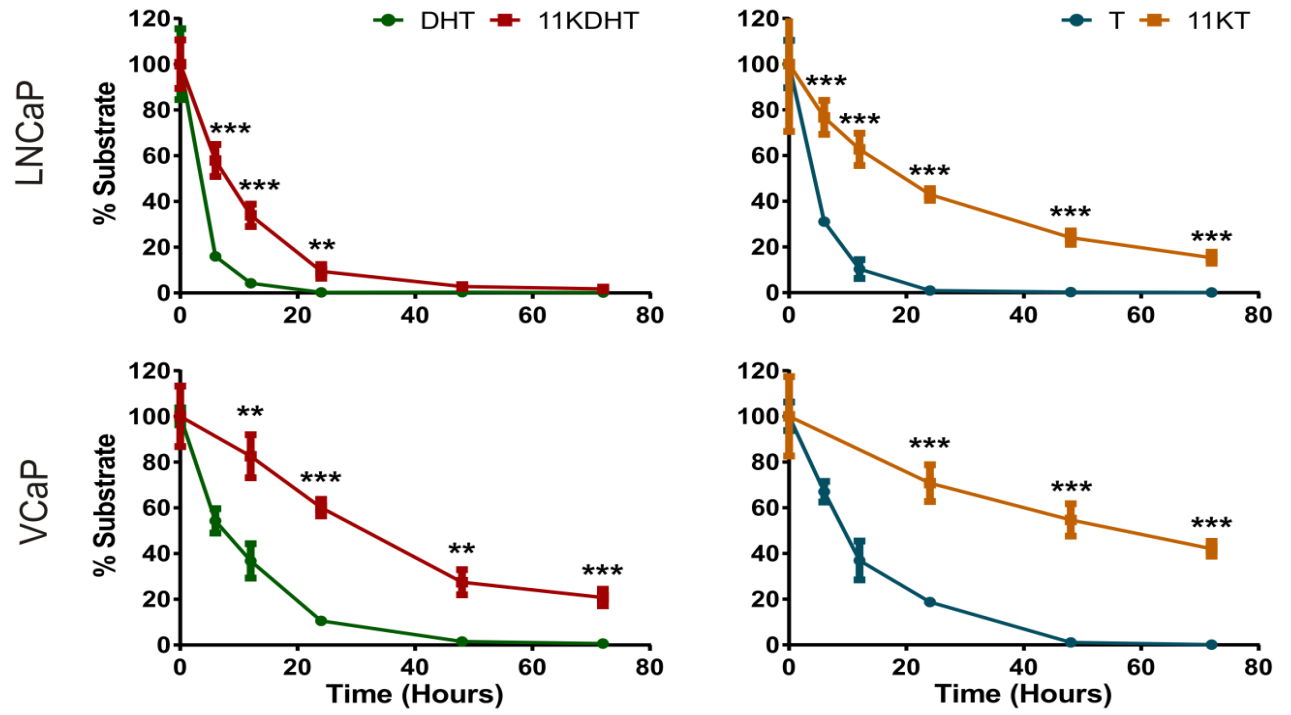

Figure 1.12: Metabolism of DHT, 11KDHT, T and 11KT by LNCaP and VCaP cells. Reproduced with permission from: Pretorius, E., Africander, D. J., Vlok, M., Perkins, M. S., Quanson, J., Storbeck, K.-H. (2016) 11-Ketotestosterone and 11-Ketodihydrotestosterone in Castration Resistant Prostate Cancer: Potent Androgens Which Can No Longer Be Ignored. *PLoS One.*

1.6. The role of 17βHSD2 and AKR1C3 in CRPC

From section 1.5.2. and section 1.5.4. it is clear that both AKR1C3 and 17βHSD2 play vital roles in both the 5α-dione and 11OHA4 pathways. In both pathways AKR1C3 is essential for the conversion of androgen precursors to active androgens, while 17βHSD2 catalyses the reverse reaction, potentially inactivating active androgens.

1.6.1. AKR1C3

AKR1C3 (17βHSD5) was originally considered to be a 3α-Hydroxysteroid dehydrogenase (3αHSD) before being re-classified as an AKR (95, 116, 117). It utilizes NADH and/or NADPH as cofactor and like 17βHSD3, it catalyses the 17-keto reduction of androgen precursors such as A4 to more potent androgens such as T. AKR1C3 also possesses 3α-HSD activity and catalyses the conversion of DHT to the less potent 5α-adiol. Reactions catalysed by AKR1C3 involve the binding of the substrate and cofactor and follow a Bi-Bi sequential reaction mechanism with the cofactor binding before the substrate (118).

Members of the AKR superfamily show high amino acid sequence identity and share a common $(\alpha/\beta)_8$-barrel protein fold. Differences are however observed within the 8 α-helices and 8 β-strands. Three large discorded loops (A, B and C) are visible at the back of the protein structure and undergo a conformational change during the binding of the substrate and cofactor.

The active site of AKR enzymes consists of a large, deep elliptical pocket at the COOH-terminal end of the protein. The active site is highly hydrophobic and favours aromatic and apolar substrates above highly polar molecules. A conserved catalytic tetrad, Y55, H117, D50 and K84 is present at the base of the β-barrel where Y55 acts as a general acid/base catalyst (21, 22). Although the binding site for the cofactor is highly conserved the flexible loops can accommodate assorted structural units. Of the 84 AKR structures listed in the protein-data bank (PDB) a number of structures exists for binary and ternary complexes that form in the reaction mechanism.

While 17βHSD3 is almost exclusively expressed in the testes, AKR1C3 is responsible for the production of extra-testicular conversion of A4 to T in non-steroidogenic peripheral tissues such as the prostate (95, 119). Thus it is no surprise that this enzyme is dominantly expressed in human prostate and mammary gland (120). A previous study by our group found that the conversion of 11KA4 to 11KT by AKR1C3 may be preferred over the conversion of A4 to T (figure 1.13). An investigation into the catalytic activity and substrate preference of AKR1C3 is currently underway in our group.

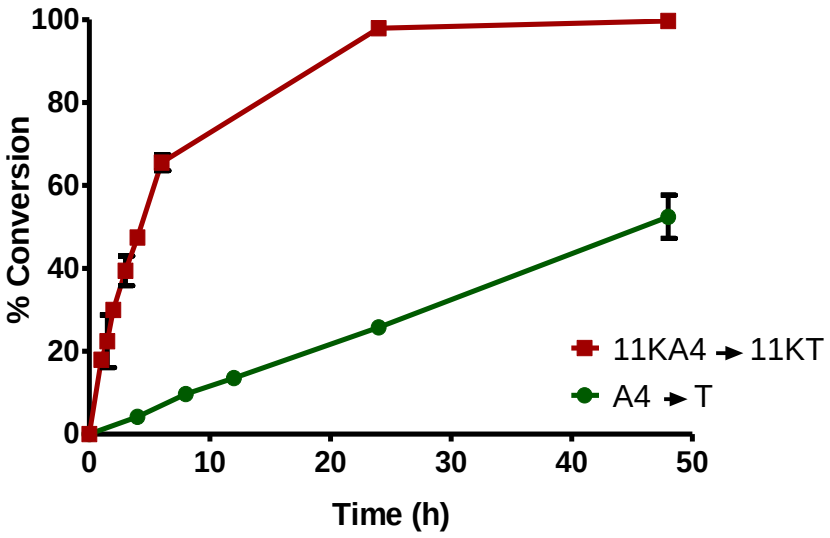

Figure 1.13: The metabolism of A4 and 11KA4 by AKR1C3. A time course for the conversion of 1 μM 11KA4 and A4 to 11KT and T, respectively by AKR1C3 suggests that 11KA4 is the preferred substrate. Unpublished data from the Storbeck laboratory.

The upregulation of AKR1C3 expression in the prostate seems to play an important role in the development of CRPC (table 1.3). Stanbrough *et al.* (121) compared gene expression profiles in 33 patients exhibiting CPRC to that of 22 patients with primary PCa in an attempt to identify altered gene expression profiles which may contribute to the development of CRPC. Results showed an increase in the expression of genes encoding for AKR1C3, SRD5A1 as well as 3βHSD2. Immunohistochemistry confirmed that AKR1C3 expression was increased up to 5.3 fold in CRPC samples (121). Similarly, Jernberg *et al*. (122) investigated altered enzyme expression in CRPC bone metastases samples. Expression levels were analysed using qPCR, immunohistochemistry and immunoblotting. Results indicated significantly higher levels of AKR1C3 mRNA compared to non-malignant and/or malignant prostate tissue.

Immunostaining total score was highly correlated to the AKR1C3 mRNA levels in the corresponding metastases. Pfeiffer *et al.* (123) investigated gene expression profiles in CRPC using microarrays and qPCR and observed an increase in the expression of AKR1C3 in CRPC. Byrns *et al.* (124) investigated the effect of overexpressing AKR1C3 in LNCaP cells which have low levels of endogenous AKR1C3. In the absence of AKR1C3, the LNCaP cells predominantly produced 5α-dione when A4 was given as substrate. These cells ceased to proliferate when treated with the SRD5A inhibitor, finasteride. Conversely, the overexpression of AKR1C3

increased the conversion of A4 to T and resulted in the development of finasteride resistance (124).

Table 1.3: Altered enzyme expression levels observed in prostate cancer (PCa) compared to castration resistant prostate cancer (CRPC) as well as the direction of the reaction catalysed by the enzyme.

Enzyme	Alteration in expression level for PCa	Alterations in expression level for CRPC	Reaction direction
17βHSD1	↑ 3 fold (125, 126)	↑ 3 fold (122, 126)	Weak → Potent
17βHSD2	↓ 7 fold (126, 127)	-	Potent → weak
17βHSD3	↑ 31 fold (122, 126)	-	Weak → Potent
17βHSD6	↑ 2 fold (126, 128)	-	Weak → Potent
AKR1C1	↓ 2-4 fold (126, 129–131)	↑ 3 fold (121, 122, 126)	Potent → Weak
AKR1C2	↓ 16 fold (126, 129–131)	↑ 2-3 fold (121, 122, 126)	Potent → Weak
AKR1C3	↑ 2-5 fold (126, 127)	↑ 5-8 fold (112, 121–123, 126)	Weak → Potent
SRD5A1	↑ 2 fold (121, 126, 132)	↑ 2-3 fold (112, 121–123, 126)	Weak → Potent
SRD5A2	↓ 2-4 fold (66, 121, 126, 133)	↓ 2-9 fold (112, 121–123, 126)	Weak → Potent

It should be noted that AKR1C3 has enzymatic activities other than just 17βHSD activity. AKR1C3 also functions as a reductive 20α-hydroxysteroid dehydrogenase (20α-HSDs) which can reduce PROG and deoxycoricosterone, thereby reducing their affinities for the PROG and mineralcorticoid receptors, respectively (134, 135). In addition to its role in steroid metabolism AKR1C3 functions as an 11-keto prostaglandin (PG) reductase, catalysing the conversion of PGD_2 to 9α,11β-PGF_2 and PGH_2 to $PGF_{2\alpha}$ (135–140).

The active site which facilitates this reaction is quite flexible which helps to accommodate a diverse range of ligands. In the absence of AKR1C3 PGD_2 undergoes spontaneous dehydration reactions leading to the synthesis of PGJ_2. The J series of prostaglandins are ligands for peroxisome proliferator-activated receptors (PPARs), or more specifically PPARγ, which has an anti-proliferation response (139), while PGF_2 is pro-inflammatory and leads to increased proliferation (135). Thus PGJ2 isoforms such as 15-deoxy-$\Delta^{12,14}$ –PGJ_2 ($15dPGJ_2$) are anti-inflammatory as well as anti-neoplastic and promotes differentiation (135). AKR1C3 expression therefore results in increase in the concentration proliferative PGF_2 isomers as well as a concomitant decrease in anti-

proliferative PGJ_2 products and therefore has an impact on hormone dependant as well as hormone independent cancers, making AKR1C3 a prevalent drug target (135) (figure 1.14).

One of the biggest challenges when developing a drug is target site specificity which is complicated due to the high sequence homology between members of the AKR family (135). More specifically an 84% homology between AKR1C3, AKR1C1, AKR1C2 and AKR1C4 requires the drug to be highly specific especially considering that all these enzymes plays a role in steroid metabolism. Inhibition of AKR1C1 and AKR1C2 could promote the development of PCa considering that they act predominantly as 3-ketosteroid reductases which convert active androgens, such as DHT, to inactive metabolites. Inhibition of these enzymes could therefore lead to unwanted activation of the AR (135).

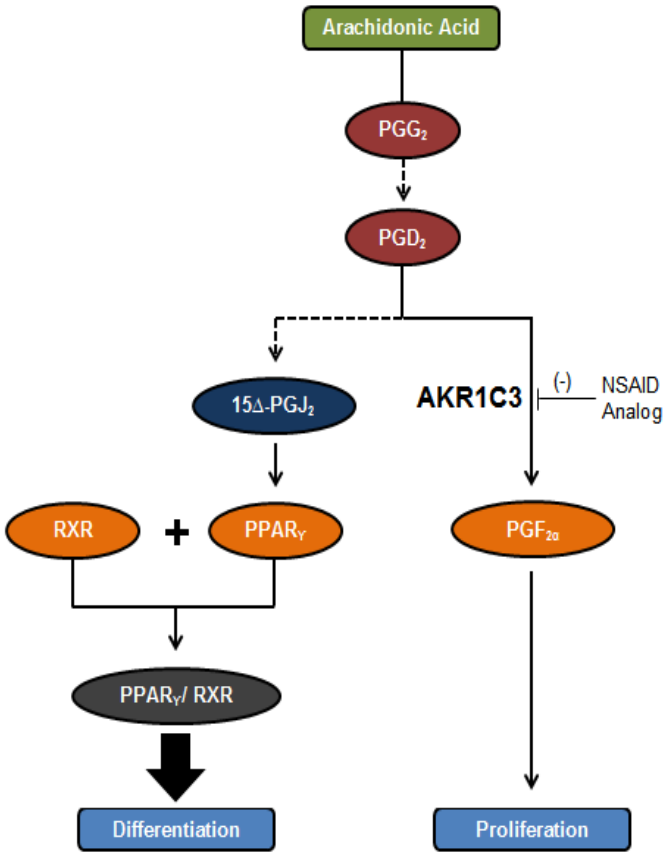

Figure 1.14: AKR1C3 as possible drug target. The inhibition of AKR1C3 activity leads to an increase in PPARγ receptor response which has an anti-proliferation effect, promoting differentiation. Adapted from: Bauman, D. R., Rudnick, S. I., Szewczuk, L. M., Jin, Y., Gopishetty, S., and Penning, T. M. (2004). *Mol. Pharmacol.* 67, 60 – 68.

Studies therefore aim to develop a non-steroidal anti-inflammatory drug (NSAID) analogue which is based on known structure activity relationships and which has a high specificity for AKR1C3. Inhibitors of AKR1C3 that have been considered to date include mefenamic acid and N-phenylanthranilic acid (135). While mefenamic acid is more selective towards the AKR1C isozymes it was still able to inhibit COX isozymes. On the other hand, *N*-Phenylanthranilic acid derivatives were found to be highly specific towards not only AKR1C3 but also other AKR1C isozymes such as AKR1C2 and did not inhibit COX isozymes (141).

A study by Byrns *et al.*, (142) investigated the inhibitory effect of a number of NSAIDs and indomethacin, an AKR1C3 inhibitor, analogues (figure 1.15). Considering structure-activity relationships they identified analogues which do not inhibit COX-1, COX-2, AKR1C1, and AKR1C2, but still exhibit AKR1C3 inhibition. Based on these results they went on to synthesize N-(4-chlorobenzoyl)-melatonin (CBM), which did not inhibit COX-1 or COX-2, but was found to inhibit AKR1C3 with a similar affinity to indomethacin, with no inhibitory effect towards AKR1C1 or AKR1C2.

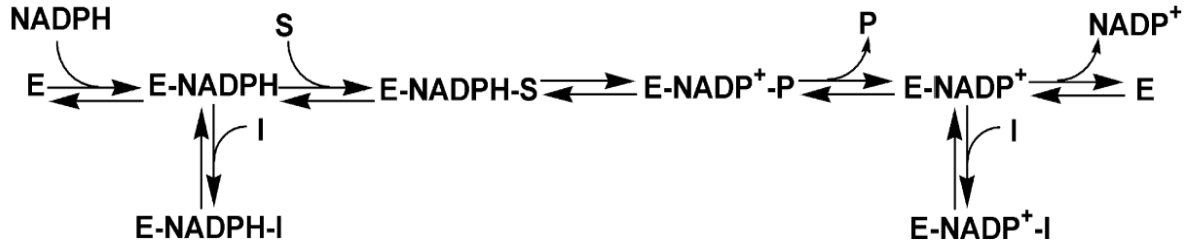

Figure 1.15: The hypothesized formation of inhibitory complexes during reactions catalysed by AKR1C3. Abbreviations: E, enzyme; I, inhibitor; S, substrate; and P, product. Reproduced with permission from: Byrns, M. C., Steckelbroeck, S., and Penning, T. M. (2008) An indomethacin analogue, N-(4-chlorobenzoyl)-melatonin, is a selective inhibitor of aldo-keto reductase 1C3 (type 2 3alpha-HSD, type 5 17beta-HSD, and prostaglandin F synthase), a potential target for the treatment of hormone dependent and hormone independent malignancies. *Biochem. Pharmacol.* 75, 484–493 (142).

1.6.2. 17βHSD2

17βHSD2 is a microsomal oxidase which utilizes NAD^+ to catalyse the inactivation of androgens and estrogens (95). 17βHSD2 was first isolated from prostatic and placenta cDNA libraries (143). Wu *et al.* characterized the 1.4-kilobase cDNA encoding the human 17βHSD2. They showed that it encoded for a 387-amino acid protein with a predicted molecular weight of 42,782 Da. An amino-terminal type 2 signal anchor motif was identified as well as a carboxyl-terminal endoplasmic reticulum retention motif, the latter suggesting that the enzyme is associated with the membrane of the endoplasmatic reticulum. The active site tetrad consist of amino acid residues Asn-Ser-Tyr-Lys at positions 111, 138, 151 and 155 respectively (144). Tyr-151 acts as the catalytic base (145)

while the Ser-138 residue stabilizes the substrate. Lys-155 forms hydrogen bonds with the nicotinamide ribose moiety which results in a lower pKa value of the Tyr-OH and in turn promotes the transfer of protons (144).

17βHSD2 is responsible for the conversion of T to A4, E_2 to estrone (E_1) and DHT to 5α-dione. Our group has also shown that this enzyme can convert 11KT, 11KDHT and 11K-3α-diol to 11KA4, 11K-5α-dione and 11KAST, respectively (95). 17βHSD2 has also been found to exhibit low 20α-hydroxysteroid dehydrogenase activity towards 20α-dihydroprogesterone (95, 143). 17βHSD2 is expressed in the endometrium, liver, placenta, small intestine, colon, kidney, pancreas and prostate (95, 146, 147). Because of 17βHSD2s widespread tissue distribution and broad substrate specificity it is hypothesized that its role in human physiology is to protect tissue from excessive exposure to potent steroid hormones (95, 148). No 17βHSD2 deficiencies have been identified yet and thus the role of this enzyme is thus not fully understood (95).

Wu *et al.* (1993) characterized 17βHSD2 activity towards 7 different substrates including, E_2, T, DHT, 20-α dihydroprogesterone, E_1, A4 and PROG as shown in table 1.4.

Table 1.4 Kinetic constants previously determined for 17βHSD2. Adapted from: Wu, L., Einstein, M., Geissler, W. M., and Chan, H. K. (1993) Expression Cloning and Characterization of Human 178-Hydroxysteroid Dehydrogenase Type 2 , a Microsomal Enzyme Possessing 20a-Hydroxysteroid Dehydrogenase Activity. *J. Biol. Chem.* 268, 12964–12969.

Substrate	K_m (μM)	V_{max} (nmol/min/mg protein)	V_{max}/K_m
E_2	0.21 ± 0.04	38 ± 11	181
T	0.39 ± 0.09	45 ± 15	115
DHT	0.31 ± 0.11	38 ± 4	123
20α-DihydroPROG	0.71 ± 0.06	5.6± 0.2	8
E_1	0.78 ± 0.08	6.6 ± 0.2	8
A4	2.63 ± 0.20	11.5 ± 2	4
PROG	-	<0.3	-

To the best of our knowledge no kinetic data is currently available for the conversion of 11KT or 11KDHT by 17βHSD2. In a different study, Wu *et al.* investigated the optimal temperature and pH conditions for 17βHSD2 activity. They found that the enzyme was sensitive to temperature with an optimal activity at a temperature of 37°C. Furthermore, the authors found that the enzyme was most active at an alkaline pH of 8-10 (143). Research to date has focussed on the expression levels of AKR1C3, which is upregulated in CRPC, while overlooking the role of 17βHSD2 in the development of this disease, considering that the expression levels of this enzyme seem to either remain constant or decrease in CRPC. Very little is known about 17βHSD2's role in the development of CRPC.

1.6.3. Enzyme ratios

The flux through steroidogenic pathways can be influenced or controlled by the expression of HSD enzymes and their relative activity. In many cases there is one HSD which catalyses and activation step, such as the conversion of A4 to T by AKR1C3 (17βHSD5), while another enzyme catalyses the reverse inactivation step, such as the conversion of T to A4 by 17βHSD2. Changes in the relative expression of these enzymes, as is observed in CRPC, therefore have the potential to change the flux through a given pathway.

An example of a study which tested the effect of HSDs on the flux of a pathway was performed by Meittinen *et al*. (146) who investigated the conversion between E_1 and E_2 in a human embryonic kidney cells (HEK293 cells) transfected with 17βHSD type1 and type 2.

17HSD1 acts as a reductase converting E_1 to E_2. In contrast 17HSD2 possesses oxidative activity inactivating E_2 by converting it to the less potent steroid E_1. HEK293 cells transfected with 17βHSD1 demonstrated a high percentage of conversion of E_1 to E_2 while no conversion was found for the reverse reaction. In HEK293 cells only transfected with 17βHSD2 only the reverse reaction was favoured (146).

Meittinen *et al*. (146) next investigated the activity of 17βHSD1 and 17βHSD2 in other cell lines which similar to HEK293 cells do not endogenously express these enzymes. The cell lines HEC-1-B, LNCaP and MCF-7 were transiently transfected with 17βHSD1 or 17βHSD2 and E_1 and E_2 were given as substrates. All cell lines transfected with 17βHSD1 showed high levels of E_1 to E_2 conversion, while the opposite was observed for cell lines transfected with 17βHSD2.

Finally, PC3 cells endogenously expressing the type 2 enzyme were transfected with 17βHSD1. Untransfected PC3 controls resulted in high levels of conversion from E_2 to E_1. No conversion from E_1 to E_2 was observed as expected. The addition of type 1 resulted in a dramatic increase in the conversion of E_1 to E_2 and very low levels of conversion from E_2 to E_1. Next, T-47D, endogenously

expressing 17HSD1 was transfected with 17βHSD2. In contrast to PC3 cells, untransfected T-47D cells converted E_1 to E_2 and no conversion of E_2 to E_1 was observed as expected. When transfected with 17βSD2 the same trend is observed compared to transfected PC3 cells. High levels of E_1 were found to be converted to E_2 and low levels of E_2 was converted to E_1 (146). These results emphasize how the ratio of two enzymes, responsible for the interconversion of substrate/product, can affect one another.

The HSD enzymes have been under the spotlight when investigating the development of PCa and CRPC because of their direct role in intratumoural androgen metabolism. As mentioned above, these enzymes are often considered possible therapeutic targets for the treatment of PCa and CRPC. In the classic pathway, AKR1C3 converts A4 to T, while in the 5α-dione pathway it catalysis the conversion of 5α-dione to DHT. Finally, in the 11OHA4 pathway AKR1C3 converts 11KA4 to 11KT as well as 11K5α-dione to 11KDHT. All of these products have been shown to activate the AR and are considered to have high androgenic activity. On the other hand, 17βHSD2 catalyses the reverse reactions, thereby leading to the inactivation these androgens.

1.7. Project Objectives

Changes in the expression levels of these two enzymes are clear during the development of CRPC, with AKR1C3 being upregulated (124, 149) and 17βHSD2 levels decreasing or remaining constant (127, 150) as discussed earlier in this section, thus favouring androgen production. Although it is clear that these enzymes play vital roles in the respective androgen pathways (classic, 5α-dione and 11OHA4) a comparison of the contribution of these enzymes to the pathways is lacking. The aim of this project was therefore to determine the effect of alterations in AKR1C3 and 17βHSD2 expression which mimic intratumoural enzyme expression in CRPC cells, on the flux through the intratumoral pathways. Furthermore, we set out to characterise the activity of 17βHSD2 towards 11KT and 11KDHT. This study forms part of a larger project in our group, which aims to build a comprehensive mathematical model of intratumoural androgen metabolism which will account for the classic, 5α-dione and 11OHA4 pathways.

Specific aims for this study:

- To develop a high throughput UPC^2-MS/MS method for the separation and quantification of AKR1C3 and 17βHSD2 metabolites.
- To characterize the catalytic activity of 17βHSD2 for substrates from the classic, 5α-dione and 11OHA4 pathways.
- To investigate the effect of different AKR1C3 to 17βHSD2 ratios on metabolism of metabolites from the classic, 5α-dione and 11OHA4 pathways.

- To investigate AKR1C3 and 17βHSD2 activity in PCa and CRPC cell lines.

Chapter 2
Materials and Methods

2.1. Materials

2.1.1. General reagents

Dulbecco's modified Eagles medium (DMEM), HAM's F12K, Roswell Park Memorial Institute media (RPMI-1640), Ampicillin sodium salt, β-glucuronidase from bovine liver, Diethyl pyrocarbonate (DEPC), Dimethyl sulfoxide (DMSO), *tert*-Buthyl methyl ether (MTBE), 2-Propanol and Chloroform were purchased from Sigma Aldrich (St. Louis, MO, USA). Fetal Bovine Serum (FBS), Sodium pyruvate and 4-(2-hydroxyethyl)-1-piperazineethanesulfonic acid (HEPES) were purchased from BioChrom (Camboume, UK). Penicillin-streptomycin and Trypsin-EDTA were purchased from Gibco (Gaithersburg, MD, USA). Wizard® Plus Midipreps DNA Purification System, Recombinant RNasin® Ribonuclease Inhibitor, Oligo(dT)15 Primer, dNTP Mix and ImProm-II™ Reverse Transcriptase were purchased from Promega (Madison, Wisconsin, USA). Restriction endonucleases (*Sal*I, *EcoR*I) were purchased from Fermentas (Burlington, Canada). X-tremeGene HP DNA Transfection Reagent was purchased from Roche Diagnostics (Mannheim, Germany). Tri Reagent® and KAPA SYBR® FAST qPCR Master Mix for LightCycler® 480 were purchased from Zymo Research (Irvine, USA) and KAPA Biosystems (Cape Town, ZAR), respectively. Primers for 17βHSD2 and AKR1C3 were purchased from Inqaba Biotec (Pretoria, ZAR). The Pierce™ BCA Protein Assay kit was purchased from Thermo Scientific™. Absolute Ethanol was purchased from Merck (Darmstadt, Germany) and Methanol was purchased from Romil (Cambridge, UK).

2.1.2. Cell lines

HEK293 and VCaP cells were purchased from the American Type Culture Collections (ATCC) (Manassa, VA, USA). LNCaP and PC3 cells were purchased from the European Collection of Cell Cultures (ECACC) (England, UK). The C4-2B cell line was a generous gift form Professor D Neal (University of Oxford, UK).

2.1.3. Plasmids

A pcDNA3 vector containing AKR1C3, as well as a pcDNA4 vector containing 17βHSD2 were both generous gifts from Prof. J. Adamski (Institute of Experimental Genetics, Germany). A pcDNA3 vector containing AKR1C2 was obtained from Prof. T.M. Penning (University of Pennsylvania, Philadelphia, USA). A pCIneo plasmid containing no insert was available for use in the laboratory.

2.1.4. Steroids and inhibitors

17β-Dihydroandrosterone (5α-androstan-3α,17β-diol; 3α-adiol), Androstanedione (5α-androstan-3,17-dione; 5α-dione), Androstenedione (androsten-3,17-dione; A4), Androsterone (5α-androstan-3α-ol-17-one; AST), Dihydrotestosterone (5α-androstan-17β-ol-3-one; DHT), Drospirenone (17-Hydroxy-6β,7β:15β,16β-dimethylene-3-oxo-17α-pregn-4-ene-21 carboxylic acid, DRSP), Dutasteride ((5α,17β)-*N*-[2,5-Bis(trifluoromethyl)phenyl]-3-oxo-4-azaandrost-1-ene-17-carboxamide), Gestodene (4,15-estradien-17β-ethynyl-18-homo-17α-ol-3-one, GES), Indomethacin (1-(4-Chlorobenzoyl)-5-methoxy-2-methyl-3-indoleacetic acid) and Testosterone (4-androsten-17β-ol-3-one; T) were purchased from Sigma Aldrich (St. Louis, USA). 11-Ketoandrostenedione (4-androsten-3,11,17-trione; 11KA4), 11-ketotestosterone (4-androsten-17β-ol-3,11-dione; 11KT), 11-ketodihydrotestosterone (5α-androstan-17β-ol-3,11-dione; 11KDHT) and 11-ketoandrosterone (5α-androstan-3α-ol-11,17-dione; 11KAST) were purchased from Steraloids (Wilton, USA) and the internal standard testosterone-1,2-d2 (T-d2) was purchased from Cambridge Isotope Laboratories (Andover, USA). All steroids, as well as dutasteride were purchased as a powder and dissolved in 100% absolute ethanol. Indomethacin was purchased as a powder and dissolved in DMSO.

2.2. Methods

2.2.1. Cell Culture

LNCaP cells were cultured in RPMI-1640 media supplemented with 10% FBS, 1.5 g/L $NaHCO_3$, 2.5 g/L D-(+)-Glucose, 1% HEPES, 1% sodium pyruvate and 1% penicillin-streptomycin (stock containing 10 000 U/mL penicillin and 10 000 µg/mL streptomycin) in 75 cm^2 Corning® CELLBIND® surface flasks. C4-2B cells were cultured in RPMI-1640 media supplemented with 10% FBS, 1.5g/L $NaHCO_3$, 2.5 g/L D-(+)-Glucose and 1% penicillin-streptomycin in 75 cm^2 cell culture flasks. HEK293 and VCaP cells were cultured in DMEM media supplemented with 10% FCS, 1.5 g/L $NaHCO_3$, 1% sodium pyruvate and 1% penicillin-streptomycin in 75 cm^2 Corning® CELLBIND®

surface and 75 cm^2 cell culture flasks respectively. PC3 cells were cultured in HAMs F12K media supplemented with 10% FCS, 1.5 g/L $NaHCO_3$ and 1% penicillin-streptomycin in 75 cm^2 cell culturing flasks. All cell lines were grown at 37 °C in 90% humidity and 5% CO_2. All cells were routinely tested for mycoplasma infection as follows: A sterile coverslip was placed in a 10 cm^2 cell culture dish and 3 drops of 80% confluent cell suspension was added to the middle of the slip. Media (6 mL) was carefully placed around the coverslip without disturbing the cells. Cells were then incubated for 4 days and subsequently fixed using methanol:acetic acid in a ratio of 3:1. Cells were then covered with Hoechst Stain Working Solution (2 mL) and incubated at room temperature for 2 min. A drop of mounting solution was subsequently added to the coverslip after which the coverslip was placed, cells facing downwards on a slide. Cells were then viewed at 60x magnification using a Live Cell Imaging Microscope (Olympus IX81 epifluorescent microscope, DAPI filter set, Shinjuku, Tokyo, Japan).

2.2.2. Plasmid DNA preparations

JM109 *E. coli* freezer stocks containing the pcDNA3-AKR1C3, pcDNA3-AKR1C2 and pcDNA4-17βHSD2 constructs were used to inoculate 100 mL Luria-Bertani (LB) media containing 100 g/mL Ampicillin. The cultures were incubated at 37 °C while shaking at 200 rpm for 16 hours (Innova™ 4000 incubator shaker, New Brunswick scientific). The cultures were subsequently centrifuged at 10 000 xg for 10 min at 4 °C (Avanti® JE centrifuge). The pellets were collected after which the plasmid DNA was purified using Wizard® Plus Midiprep DNA Purification System according to the manufacturer's instructions. The concentrations of the purified plasmids were determined spectrophotometrically using a Cary 60 UV-VIS (Agilent technologies). The identity of the plasmid constructs were subsequently confirmed using restriction endonuclease digestion. Restriction endonuclease reactions contained 1 µg plasmid DNA, 10 units of the relevant restriction enzyme and 2 µL of the appropriate BSA containing buffer (x10). The final reaction volume was 20 µL. The reactions were incubated at 37 °C for 1 hour. Digested and undigested samples were analysed using 1% agarose gel electrophoresis. Samples were diluted to a concentration of 2 µg in a total volume of 20 µL, followed by the addition of 10 µL loading buffer (0.2%) containing: 0.1% Orange G (w/v), 20% Ficoll (w/v) and 10 mM EDTA. Electrophoresis was carried out using TAE buffer (40 mM Tris-acetate, 2 mM EDTA and 20 mM acetic acid). The 1% agarose gel was electrophoresed at 110 V for 3 min after which the voltage was decreased to 75 V until the dye was visible as a front approximately 1 cm from the bottom of the gel. The gel was subsequently stained using GR green® and visualised using Vilber Lourmat UV lamp coupled to a Vidamax camera from Omni-Science CC (Randburg, South Africa).

2.2.3. Determination of kinetic constants using initial rates

HEK293 were maintained and grown in a 75 cm^2 flasks until 80% confluent. Cells were subsequently transfected with 17βHSD2 using X-tremeGENE transfection DNA reagent according to the manufacturer's protocol. Twenty-four hours after transfection the cells were re-plated at a density of 5 x 10^4 cells/well (300 µL) in Corning® CELLBIND® 48 well plates. After re-plating, the cells were incubated for a further 24 hours to ensure reattachment. Six different substrates (T, DHT, 5α-adiol, 11KT, 11KDHT and 11K5α-adiol) were added to the cells at six concentrations each (0.25, 0.5, 1, 5, 10 and 20 µM) and time points (150 µL) were collected every 10 min for a total of 40 min for substrate concentrations ≤ 1 µM and every 15 min for a total of 60 min for substrate concentrations > 1 µM.

2.2.3.1. *Determination of a response factor for 11K-5α-dione*

A standard for the steroid 11K-5α-dione was not commercially available. This steroid was therefore quantified relative to the standard curve obtained for the parent compounds by making use of a response factor which was determined as follows: HEK293 cells were transfected with 17βHSD2 or the pCIneo vector, containing no insert, as described above. After 72 hours 0.1, 1 and 10 µM 11KDHT was added to the 17βHSD2 transfected cells. The steroid was also added to the pCIneo transfected cells. The samples were collected after 48 hours of incubation which allowed for the full conversion of substrate to product. d9-PROG (15 ng) and d2-T (15 ng) were added to the samples prior to extraction as describe in section 2.2.6.1 below. The samples were subsequently analysed by Ultra performance convergence chromatography tandem mass spectrophotometry (UPC^2-MS/MS) to verify if all the substrates had been fully converted to their respective products in the case of and 17βHSD2 transfected cells and to confirm that no conversion of substrate to product occurred in the cells transfected with pCIneo. The response factor was subsequently calculated as follows: the peak area of the substrate was divided by the peak area of the internal standard. The ratio of substrate peak area/internal standard peak area (from the pCIneo control) was then divided by the ratio of product peak area/internal standard peak area (from the 17βHSD2 conversions) to determine the response factor (RF) using the following formula:

$$\mathbf{A_s/A_{is} = RF\ (A_p/A_{is})}$$

Where: A_s = area of substrate peak, A_{is} = area of internal standard peak, A_p = area of product peak.

This calculation was performed for eight replicates for all three steroid concentrations and the average response factor calculated.

2.2.3.2. Protein determination

After media was removed for steroid extraction cells were washed twice with phosphate buffered saline (PBS) after which 50 µL passive lysis buffer (0.2% (v/v) Triton, 10% (v/v) glycerol, 2.8% (v/v) TRIS-phosphate-EDTA and 1.44 mM EDTA) was added to the cells. The cells were mixed for 15 min and then frozen at -20 °C until. The cell lysate was thawed and the protein concentration determined using a Thermo Scientific™ Pierce™ BCA Protein Assay kit according to the manufacturer's protocol.

For progress curve analysis HEK293 cells were transfected with 17βHSD2 and re-plated as described above (section 2.2.3). Three different concentrations (0.1, 1 and 10 µM) of T and 11KT were added as substrates to a total volume of 500 µL. Time points (150 µL) were collected at 20, 40, 60, 90, 120, 150, 180, 210, 240, 270, 300 and 360 min.

2.2.4. Ratio experiments

2.2.4.1. HEK293 ratio experiments

HEK293 cells were cultured and grown to 80% confluence in Corning® CELLBIND® surface 75 cm^2 flasks. The cells were subsequently transfected with 17βHSD2, AKR1C3 or pCINeo using X-tremeGENE transfection DNA reagent. After twenty-four hours the cells were counted and combined in different ratios of 17βHSD2:AKR1C3 as shown in table 2.1 before re-plating in Corning® CELLBIND® surface 24 well plates at a density of 2.1 x 10^5 cells per well (500 µL). Cells transfected with the pCINeo plasmid, which contained no insert, were used to ensure all ratios contained an equal number of cells.

After 24 hours the media was removed and replaced with full media (supplemented with 10% FBS and 1% PenStrep) with a final volume of 500 µL, containing 1 µM or 0.1 µM of the steroid substrates A4, 11KA4 and 5α-dione or a combination of A4 and 11KA4, respectively. Time points (500 µL) were collected 24 hours after substrate addition. Samples were stored at 4 °C until further analysis.

Table 2.1: Summary of the HEK293 ratios experiment. HEK293 cells transfected with 17βHSD2 or AKR1C3 were mixed to obtain different ratios of 17βHSD2:AKR1C3. 1 U = 3 x10^4 cells.

Desired ratios	17βHSD2 cells	AKR1C3 cells	pCINeo cells	Total cells added
1:0	3 x 10^4	0	1.8 x 10^5	2.1 x 10^5
0:1	0	3 x 10^4	1.8 x 10^5	2.1 x 10^5
1:1	3 x 10^4	3 x 10^4	1.5 x 10^5	2.1 x 10^5
1:3	3 x 10^4	9 x 10^4	9 x 10^4	2.1 x 10^5
1:4	3 x 10^4	1.2 x 10^5	6 x 10^4	2.1 x 10^5
1:5	3 x 10^4	1.5 x 10^5	3 x 10^4	2.1 x 10^5
1:6	3 x 10^4	1.8 x 10^5	0	2.1 x 10^5
0:0	0	0	2.1 x 10^5	2.1 x 10^5

Additional ratio experiments (0:1, 1:1, 1:4 and 1:6) were performed as described above, but included the addition of the AKR1C3 inhibitor Indomethasin (50 μM). An equivalent amount of DMSO was added to all wells which did not contain Indomethasin.

2.2.4.2. Ratio experiment validation

A mathematical model for the conversion of A4 and 11KA4 by different ratios of AKR1C3:17βHSD2 was constructed using the kinetic parameters for 17βHSD2 determined by this study as well as the kinetic parameters for AKR1C3 determined by our group (unpublished data). These parameters are listed in table 3.4, section 3.4.2. The model was constructed by Prof JL Snoep (Department of Biochemistry, University of Stellenbosch) using Mathematica (Wolfram).

2.2.4.3. PC3 Ratio experiments

PC3 cells were maintained and grown to 80% confluence in 75 cm^2 flasks and subsequently plated in 12 well plates at a density 2 x 10^5 cells/well (1 mL). After 24 hours the cells were transfected with a total of 1 μg plasmid DNA per well. DNA was made up of 0 μg, 0.25 μg, 0.5 μg or 1 μg of the AKR1C3 plasmid. The pCINeo plasmid, which contained no insert, was used to ensure that the cells were transfected with an equal amount of DNA, as shown in table 2.2. Transfections were carried out using X-tremeGENE transfection reagent according to the manufacturer's protocol.

Table 2.2: Summary of the PC3 ratio experiment. PC3 cells, which endogenously express 17βHSD2, were transfected with increasing amounts of AKR1C3.

AKR1C3 added (µg)	pCINeo added (µg)	Total DNA added (µg)
0.00	1.00	1.00
0.25	0.75	1.00
0.50	0.50	1.00
1.00	0.00	1.00

Seventy-two hours after transfection the media was replaced with fresh media (1 mL) containing 0.1 µM of the steroid substrates (A4, 11KA4, T and 11KT) and 10 µM dutasteride, a SRD5A1/2 inhibitor. Time points (500 µL) were collected 24 hours after substrate addition. Samples were stored at 4 °C until further analysis. Media was removed and 400 µL Tri-Reagent® was added to each well. Cells were frozen at -80 °C until RNA isolation.

The potential effect of dutaseride on the activity of AKR1C3 and 17βHSD2 was tested in HEK293 cells transiently transfected with plasmids expressing these enzymes using X-tremeGENE transfection DNA reagent according to the manufacturer's protocol. AKR1C3 activity was assayed using 0.1 µM and 1 µM A4 or 11KA4 as substrates, while 17βHSD2 activity was assayed using 0.1 µM and 1 µM T or 11KT. Assays were conducted in the presence as well as the absence of 10 µM dutasteride. Time points (250 µL) were collected every 10 min for a total of 50 min.

2.2.5. Time courses in PCa cell lines

VCaP and C4-2B cells were grown and maintained in 75 cm^2 flasks while LNCaP cells were cultured in Corning® CELLBIND® surface 75 cm^2 flasks. Cells were plated in 24 well plates at cell density of 1 x 10^5 cells/well (500 µL) for VCaP cells and 2.5 x 10^4 cells/well (500 µL) for C4-2B and LNCaP cells. After 24 hours the media was replaced with media containing 0.1 µM A4, 11KA4, T or 11KT respectively as well as 10 µM dutrastride. Time points (500 µL) were collected every 24 hours for a total of 4 days. Samples were deconjugated prior to extraction. The pH of samples was set to 6.5 using 1% acetic acid. To each sample, 800 units of β-glucuronidase from bovine liver were added after which the samples were incubated at 37 °C for 24 hours. DHT and DHT-G were made up in RPMI 1640 media to a concentration of 1 µM. One of each was deconjugated and

used as a positive control. Internal standards d2-T, GES and DRSP were added to each sample and steroids were extracted as described in section 2.2.6.1 below.

2.2.6. Samples preparation and analysis by UPC^2-MS/MS

2.2.6.1. Steroid extraction

Steroids were extracted from media using MTBE at a ratio of 3:1 (MTBE:media). The samples were shaken for 10 min, allowed to stand for 5 min and then incubated at -80 °C for an hour to allow the aqueous layer to freeze. The MTBE layer containing the steroids was subsequently transferred to a clean test tube and evaporated under a stream of nitrogen gas (N_2). Samples were then re-suspended in 50% methanol and stored at -20 °C prior to analysis by UPC^2-MS/MS. A volume of 150 µL was used to resuspend samples from experiments where substrate concentrations ≤ 1 µM were used, while samples from experiments where substrate concentrations > 1 µM were resuspended in 1 mL.

2.2.6.2. Sample analysis

Steroids were separated using an ACQUITY UPC^2 system (Waters Corporation, Milford, USA) with an ACQUITY UPC^2 BEH 2-EP column (3 mm X 100 mm, 1.7 µm particle size) as previously reported (151). Supercritical CO_2 was used as the primary mobile phase and was combined with methanol which was used as an organic modifier. The gradient profile for the 5 min run is shown in table 2.4. The flow rate was kept constant at 2.0 mL/min and the column temperature and automated back pressure regulator (ABPR) were set to 60 °C and 2000 psi, respectively. The injection volume was 2 µL for all standards and samples. A make-up pump was set to feed 1% formic acid in methanol at a constant flow rate of 0.2 mL/min to the mixer preceding the MS line. A Xevo TQ-S triple quadruple mass spectrometer (Waters, Milford, USA) was used for quantitative mass spectrometric detection. Multiple reaction monitoring (MRM) was used to analyse all steroids with a positive ionization mode electrospray probe (ESI +). Data was collected and analysed using MassLynx 4.1 (Waters Corporation). The capillary voltage was set to 3.8 kV and the source and the desolvation temperature was set to 120 °C and 500 °C respectively, while the desolvation and cone gas were set to a flow rate of 1000 L/h and 150 L/h, respectively.

Table 2.3: MRM mass transitions and mass spectrometer parameters. Parameters for the detection and quantification of C19 steroids by UPC2-MS/MS: retention time (RT) for a (RT_A) 5 min inlet method as well as a (RT_B) 2.5 min inlet method; cone voltages (CV); collision energy (CE).

Steroid	Parent ion	Daughter ion A	CV (V)	CE (eV)	Daughter ion B	CV (V)	CE (eV)	RT_A (min)	RT_B (min)
5α-dione	289.18	253.14	22	16	97.2	30	22	0.52	0.46
A4	287.2	96.9	30	15	108.8	30	15	0.68	0.75
11K5α-dione	303.2	241	35	30	267	35	25	0.96	-
11KA4	301.2	257	35	25	265.2	35	25	1.07	1.08
DHT	291.22	255	25	15	273	25	20	1.16	0.98
AST		273.2>105.4	30	30	291.3>273.3	18	8	1.16	-
T	289.2	97.2	30	22	109	30	22	1.53	1.44
11KAST	305	147.2	30	30	173.1	30	30	1.56	-
11KDHT	305.2	23	30	20	269	30	20	1.84	-
5α-adiol	275.5	257	15	15	175	15	15	2.08	-
11KT	303.2	121	30	20	267	30	20	2.24	2.03
11K5α-adiol	307.2	271	15	10	253	15	10	3.16	-
d9-PROG	324.2	100	30	20	113	30	25	0.65	-
d2-T	291	99.1	30	20	111.2	30	30	1.53	-
GES	311.2	109.4	15	25	135	15	25	1.63	-
DRSP	367.2	97.3	20	30	159.3	20	25	1.82	-

Table 2.4: Binary solvent manager inlet gradient for a 5 min method on the UPC^2-MS/MS.

Step	Time (min)	Flow rate (mL/min)	% Solvent A	% Solvent B	Curve
1	Initial	2	99	1	Initial
2	4	2	91	9	7
3	4:10	2	75	25	6
4	5	2	99	1	6

Table 2.5: Binary solvent manager inlet gradient for a 2.5 min method on the UPC^2-MS/MS.

Step	Time (min)	Flow rate (mL/min)	% Solvent A	% Solvent B	Curve
1	Initial	2	96	4	Initial
2	1.5	2	92	8	6
3	1.6	2	75	25	6
4	2.5	2	96	4	6

Samples collected from kinetic experiments were analysed using a 5 min method developed to separate 19 C19 steroids (151) (table 2.4). Samples containing only A4, T, 11KA4, 11KT, 5α-dione and DHT were separated using a 2.5 min method as shown in table 2.5. All other settings were as described above.

2.2.7. qPCR

2.2.7.1. RNA isolation

Total RNA was isolated using Tri® Reagent. Cells were allowed to thaw in the Tri® Reagent and were lysed by pipetting. The mixture was then transferred to a 1.5 mL RNA free microcentrifuge tube. The samples were incubated at room temperature for 5 min prior to the addition of 80 µL chloroform. The samples were then vortexed to mix the content after which they were incubated at room temperature for an additional 3 min. Samples were subsequently centrifuged at 13 000 rpm using the Biofuge® fresco (Heraeus, Germany) for 30 min at 4 °C. The aqueous phase was then moved to a new 1.5 mL RNA free microcentrifuge tube followed by the addition of an equal volume of isopropanol. The samples were mixed by vortexing and then incubated at room temperature for 15 min. Samples were centrifuged at 13 000 rpm for 20 min at 4 °C after which the supernatant was removed and the pellet washed with 500 µL 75% ethanol. Samples were subsequently vortexed and centrifuged at 8000 rpm at 4 °C for 10 min. The supernatant was removed and samples were centrifuged again at 8000 rpm for 5 min. The pellet was then air dried for 10 min on ice and then re-suspended in 15 µL DEPC treated water. RNA concentration was measure using a Nanodrop 200 spectrophotometer from Thermo Scientific™ (Waltham, Massachusetts, US). Samples were stored at -80 °C until use.

2.2.7.2. cDNA synthesis

The GoScript™ Reverse Transcription System kit was used for first strand cDNA synthesis according to the manufacturer's protocol. The following components were added and mixed in the order as listed in table 2.6 below:

Table 2.6: RNA and Primer mix components for cDNA synthesis.

Component	Volume
Experimental RNA	0.5 µg
Oligo(dT)$_{15}$ primers	1 µL
Nuclease-free water	Up to 5 µL
Total	5 µL

The samples were incubated on a heating block at 70 °C for 5 min after which they were immediately placed on ice for 5 min. Samples were then vortexed for 10 seconds and stored on ice while the rest of the components were prepared. The reverse transcription reaction mix was prepared as shown in table 2.7 below.

Table 2.7: Components of the reverse transcriptase mix. Volumes are shown per reaction.

Component	Volume
GoScript™ 5X Reaction Buffer	4.0 µL
$MgCl_2$ (final concentration, 1.5-5.0 mM)	1.2-6.4 µL
PCR Nucleotide Mix (final concentration 0.5 mM each dNTP)[2]	1.0 µL
Recombinant RNasin® Ribonuclease Inhibitor	20 units
GoScript™ Reverse Transcriptase	1.0 µL
Nuclease free water	Up to 15 µL
Final volume	15 µL

The prepared reverse transcriptase mix was added to the template and primer mix and the reactions were incubated at 25 °C for 5 min and then at 42 °C for one hour. Reactions were

subsequently stopped by incubation at 70 °C for 15 min. Samples were stored at -20 °C until further use.

2.2.7.3. Primers

Primers for the relative quantification of 17βHSD2 and AKR1C3 were selected from literature. Primers for the amplification of the reference gene ALAS (delta-aminolevulinate synthase) were previously aselected from literature and were available for use in the laboratory (107). Primer sequences are shown in table 2.8.

Table 2.8: List of all qPCR primer sequences

Primer	Oligonucleotide sequence (5′ → 3′)	References
17βHSD2 (forward)	TCTTTGGAACTGTGGAGGTCACAAAGACGT	(152)
17βHSD2 (reverse)	AGAGAAGTCCTTGCTGGCTAACGAGTTGAT	
AKR1C3 (forward)	AGCCAGGTGAGGAACTTTC	(138)
ACR1C3 (reverse)	ATCACTGTTAAAATAGTGGAG	
ALAS (forward)	TTCCACAGGAGCCAGCATAC	(107)
ALAS (reverse)	GGACCTTGGCCTTAGCAGTT	

2.2.7.4. PCR optimisation

Real-time PCR was performed using the KAPA SYBR® FAST qPCR Master Mix for LightCycler® and a LightCycler® 96, rapid thermal cycler instrument (Roche Life Science). Each qPCR reaction mixture was prepared as shown in table 2.9 below.

The qPCR profile consisted of a pre-incubation at 95 °C for 3 min followed by amplification which consisted of: denaturation at 95 °C for 10 seconds; primer annealing using a temperature gradient (50-62 °C) for 20 seconds; and extension at 72 °C for 1 second. Forty-five cycles were typically used for amplification and was followed by melting curve analysis. Melting curve analysis was performed by denaturing the samples at 95 °C for 5 seconds followed by annealing at 65 °C for 60 seconds. The samples were then heated from 65 °C to 97 °C at a ramp rate of 2.2 °C per second.

Table 2.9: Components of qPCR Master mix. Volumes are shown per reaction.

Components	Volume
PCR grade water	1µL
Primer Forward (5 µM stock)	1µL
Primer Reverse (5 µM stock)	1µL
KAPA SYBR® FAST qPCR Master Mix (2X)	5µL
cDNA template	2µL
Total	10µL

Table 2.10 contains the melting temperatures and GC content for each primer set from both the synthesis report as well as the Primer-BLAST search. A temperature gradient of 50-62 °C was used to determine the ideal annealing temperature for each primer set and the optimal annealing temperatures are shown in table 2.10.

Table 2.10: Summary of theoretical melting temperatures and experimentally determined annealing temperatures for all primers.

Primer	Primer synthesis report		Primer-BLAST		
	Melting temp (°C)	% GC content	Melting temp (°C)	% GC content	Optimal annealing temperature (°C)
17βHSD2 (forward)	67.81	46.67	67.37	46.67	60
17βHSD2 (reverse)	67.38	46.67	67.37	46.67	60
AKR1C3 (forward)	56.96	52.63	60.16	52.63	58
AKR1C3 (reverse)	50.59	33.33	54.76	33.33	58
ALAS (forward)	62.45	55.00	59.96	55.00	60
ALAS (reverse)	62.45	55.00	59.96	55.00	60

2.2.7.5. PCR efficiencies

PCR efficiencies were determined by using a serial dilution of cDNA template prepared in nuclease free water. Standard curves for each primer set were then generated by plotting the cycle threshold (Ct) values against the log of the cDNA starting concentrations. The efficiency was then calculating using the gradient of the standard curves generated using the formula shown below:

$$\boldsymbol{Efficiency = \left(10^{\left(-\frac{1}{slope}\right)} - 1\right)100}$$

2.2.7.6. Relative qPCR quantification

Optimized parameters and qPCR efficiencies were used to perform relative quantification. A reference gene was used to determine relative target gene expression. This was done using a modified form of the model constructed by Pfaffl (153) which takes into account the differences in PCR efficiencies. Inter-experimental variation was accounted for by applying mean-centering (154) to the data which was represented as fold change over the control.

$$\boldsymbol{Ratio = \frac{(Efficiency\ target)^{\Delta Ct\ (b\ value - sample)}}{(Efficiency\ ref\ )^{\Delta Ct\ (b\ value - sample)}}}$$

The b values are a representation of the y-intercept of the standard curve generated for each primer set using a dilution series.

2.2.8. Statistical analysis

All data manipulations, graphical representations and statistical analysis were performed using GraphPad Prism® software (Version 4). Linear regression was used to determine the initial rates for kinetic data. Resulting initial rates were plotted against the respective substrate concentrations using the Michaelis Menten equation. qPCR data was processed as described 2.2.7.6. and subsequently analysed using one-way ANOVA followed by Tukey's multiple comparisons test. Data from all ratio experiments were analysed using one-way ANOVA followed by Tukey's multiple comparisons test. The effect of inhibitors on steroid metabolism was analysed using Student's t tests.

Chapter 3

Results

3.1. Quantitative PCR

3.1.1. Primer design

Primer sequences for the relative quantification of AKR1C3 (138) and 17βHSD2 (127) by qPCR were obtained from literature. Primer sequences were subjected to analysis by Primer-BLAST to confirm that each primer annealed in different exons (figure 3.1) as to ensure that genomic DNA would not be amplified due to the presence of large intron sequences. A primer set for the relative quantification of the reference gene, ALAS, was previously designed by our group and was available for use in the laboratory (115).

Figure 3.1 Primer-BLAST analysis of (A) 17βHSD2 and (B) AKR1C3 primers. All primers were shown to bind in different exons, thus preventing the amplification of genomic DNA.

3.1.2. Primer optimization

The optimal annealing temperature for each primer set was determined (figure 3.2, red line) using a gradient PCR. Amplifications yielding only a single product as determined by melting curve analysis were considered to be optimal, but in some cases nonspecific amplification and/or primer

dimers could not be eliminated completely. An optimal annealing temperature of 60 °C was determined for 17βHSD2 and ALAS, while the optimal annealing temperature for AKR1C3 was found to be 58°C.

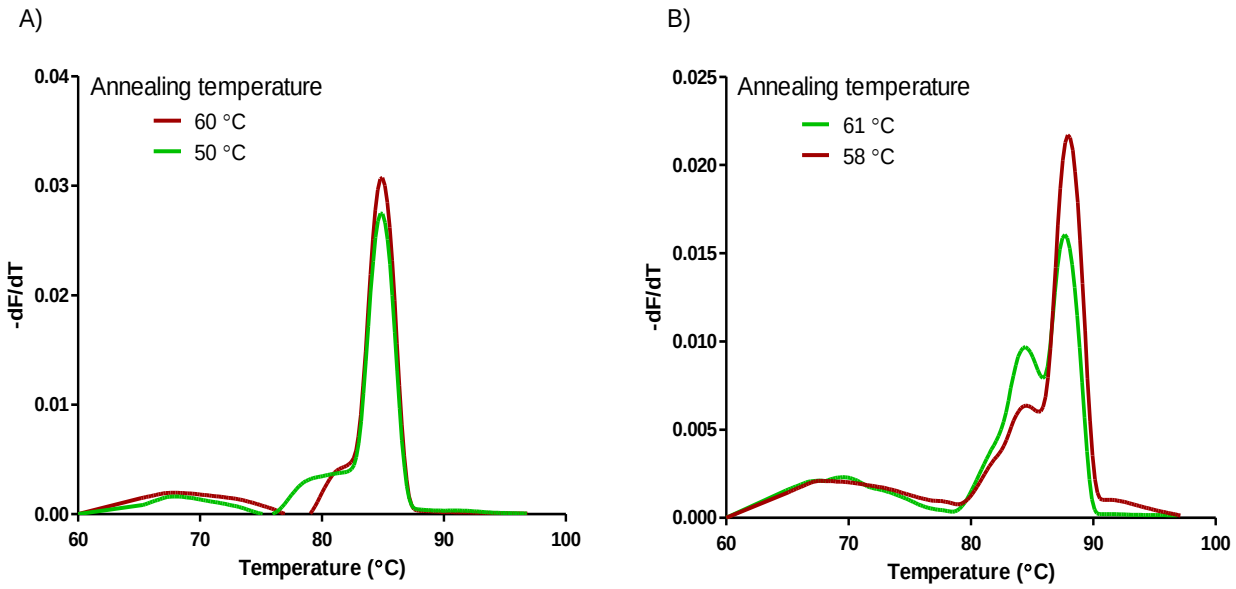

Figure 3.2: Melting curves for 17βHSD2 and AKR1C3. Example of melting curve analysis of 17βHSD2 (A) and AKR1C3 (B) primer sets at two different annealing temperatures. Nonspecific amplicons and/or primer dimers can be observed as a peak to the left of the amplified product.

3.1.3. qPCR efficiency

A serial dilution (X2) series of template cDNA was used to determine the qPCR efficiency for each primer set. A single qPCR reaction was performed for each dilution. The resulting Ct values were subsequently plotted against the log of the cDNA concentration (figure 3.3). The resulting gradients from linear regression analysis were used to determine the qPCR efficiencies (table 3.1), which were all found to be equal to or above 91%: 17βHSD2, 91%; AKR1C3, 96%; and ALAS, 91%.

Table 3.1: Primer set efficiencies

Primer set	Slope	Efficiency (%)
17βHSD2	-3.5578	91
AKR1C3	-3.4116	96
ALAS	-3.5511	91

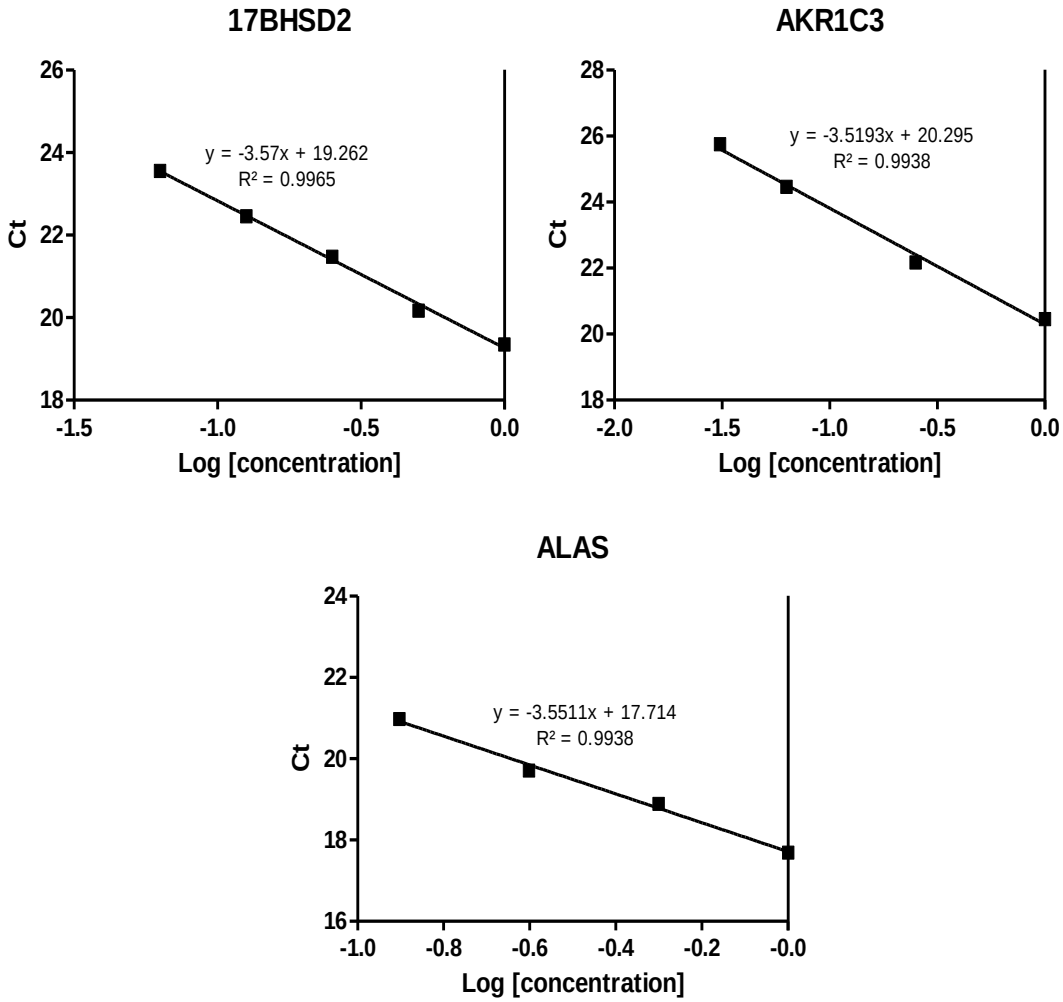

Figure 3.3: Calibration curves for 17βHSD2, AKR1C3 and ALAS. The gradients were used to determine the qPCR efficiency. The following equation was used to determine the qPCR efficiency: Efficiency = $(10^{(-1/slope)}-1)100$.

3.2. High throughput UPC^2-MS/MS method development

A high throughput UPC^2-MS/MS method for the separation and quantification of nineteen C19 steroids was previously developed in our laboratory (151). As the majority of experiments conducted in this study required only the separation and quantification of 6 of these steroids, this method was modified to further increase the throughput for this study. Six structurally related C19 steroids were separated in 2.5 min (figure 3.4A and 3.4B).

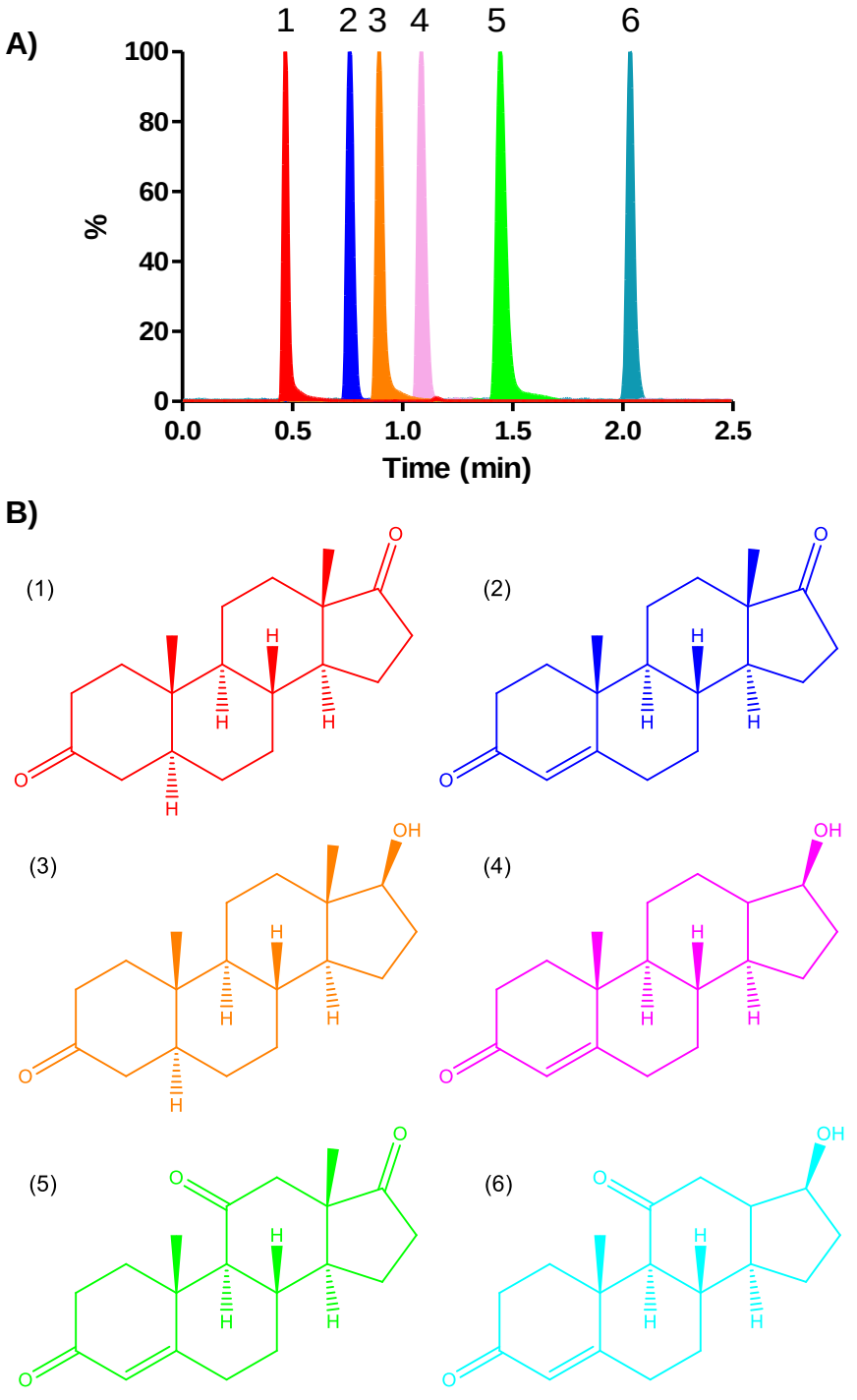

Figure 3.4: (A) The separation profile of six C19 steroids by UPC^2-MS/MS. The elution order is as follows: 5α-dione (1), A4 (2), DHT (3), T (4), 11KA4 (5) and 11KT (6). **(B) The structures of six C19 steroids separated on the UPC^2-MS/MS in 2.5 min**. The order is as follows: 5α-dione (1), A4 (2), DHT (3), T (4), 11KA4 (5) and 11KT (6).

3.3. The characterisation of 17βHSD2 activity

Since the activity of 17βHSD2 towards 11-oxygenated C19 steroids has not previously been characterised, we set out to determine the apparent K_m ($K_{m,\ app}$) and apparent V_{max} ($V_{max,\ app}$) values using the 11-oxygenated steroids 11KT and 11KDHT as substrates. The classical steroids T, DHT and 5α-adiol were included in all experiments for comparative purposes. The response factor used to quantify 11K-5α-dione, which was not available commercially, is shown in table 3.2.

Table 3.2: Response factor calculated for 11K-5α-dione.

Substrate	Product
	11K-5α-dione
11KDHT	0.188 ± 0.01

Initial rates (V_0) were determined for six substrate concentrations per steroid (figure 3.5) and were subsequently used to determine the $K_{m,\ app}$ and $V_{max,\ app}$ values. V_0 was plotted against the respective substrate concentrations and a Michaelis Menten equation was fitted using non linear regression. The resulting Michaelis Menten fits are shown in figure 3.6 and the respective kinetic parameters are summarized in table 3.3.

It is clear from the kinetic parameters summarized in table 3.3, that 17βHSD2 tended to have the highest affinity for DHT ($K_{m,\ app}$ = 3.18 ± 0.48 µM) closely followed by T ($K_{m,\ app}$ = 3.35 ± 0.81 µM) and 5α-adiol ($K_{m,\ app}$ = 3.39 ± 0.94 µM). Overall the affinity of 17βHSD2 for the 11-oxygenated C19 substrates tended to be lower than for the classical C19 steroids, however, these differences were not statistically significant. For example, a 69% lower affinity was observed for 11KT ($K_{m,\ app}$ = 5.48 ± 1.13 µM) when compared to the affinity of 17βHSD2 for T. The affinity of 17βHSD2 for 11KDHT ($K_{m,\ app}$ = 20.46 ± 3.56 µM) was also significantly lower than that of DHT ($K_{m,\ app}$ = 3.18 ± 0.48). It should, however, be noted that the $K_{m,\ app}$ for 11KDHT is only an estimate given the fact that no commercial standards were available for the product 11K-5α-dione and analyses therefore relied on a response factor which may have introduced additional error into the data.

Interestingly, despite differences in affinities, no significant difference was found for the V_{max} values for T ($V_{max,\ app}$ = 131 ± 9.52 µmol/hour/mg protein) and 11KT ($V_{max,\ app}$ = 143 ± 10.2 µmol/hour/mg protein). The $V_{max,\ app}$ value for 5α-adiol ($V_{max,\ app}$ = 136 ± 11.4 µmol/hour/mg protein) was also similar to that of T and 11KT. 17βHSD2 had a substantially lower V_{max} value for DHT ($V_{max,\ app}$ = 87.3 ± 3.97 µmol/hour/mg protein) compared to that of the other substrates. Conversely, a high V_{max} value ($V_{max,\ app}$ = 491 ± 50.7 µmol/hour/mg protein) was observed for 11KDHT although the accuracy of this needs to be confirmed.

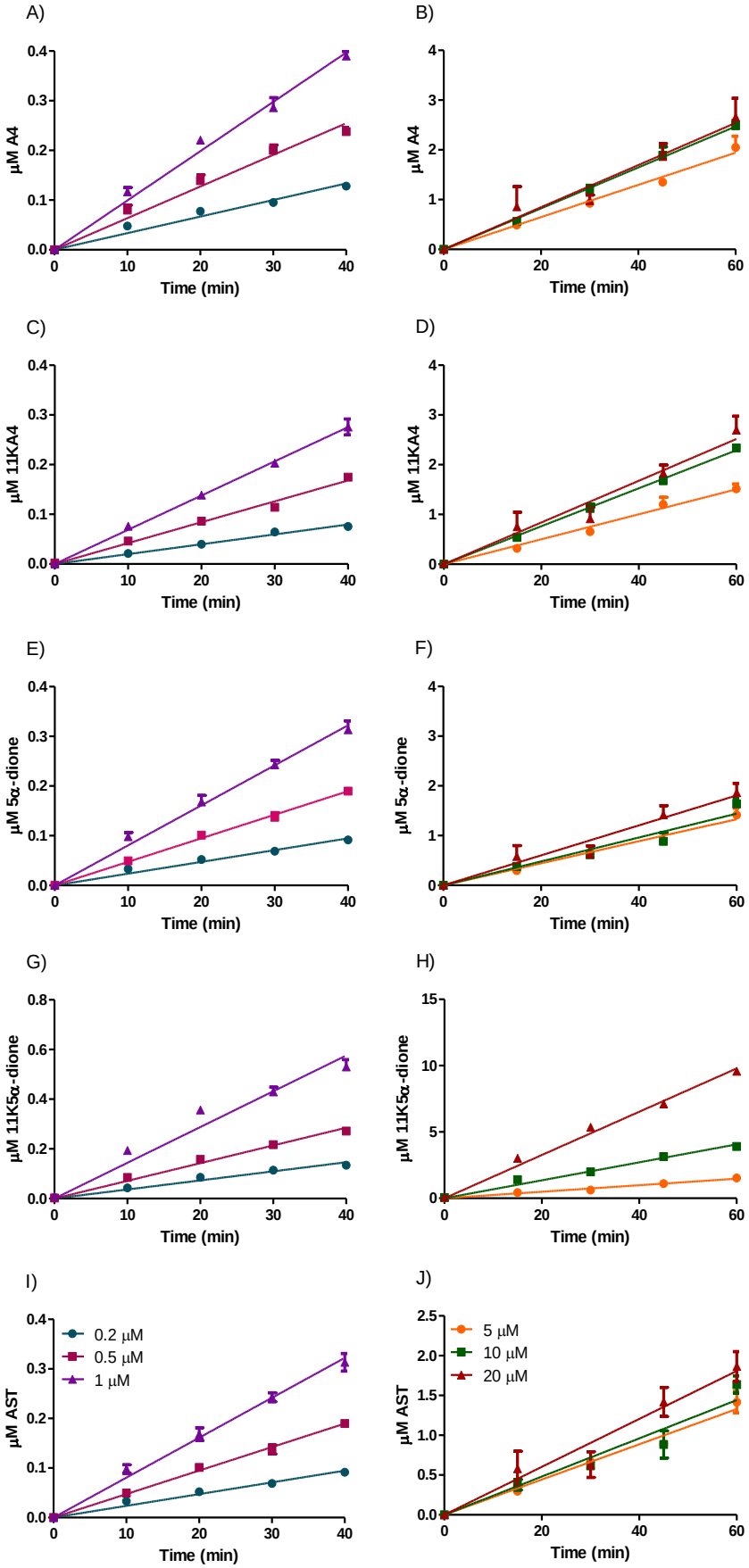

Figure 3.5 Initial rates for the conversion of (A & B) T to A4, (C & D) 11KT to 11KA4, (E & F) DHT to 5α-dione, (G & H) 11KDHT to 11K5α-dione and (I & J) 5α-adiol to AST by HEK293 cells expressing 17βHSD2. Steroids were extracted and measured by UPC^2-MS/MS. Linear regression lines were fitted in GraphPad Prism. The results are from a single experiment performed in triplicate and are expressed as the mean ± SD.

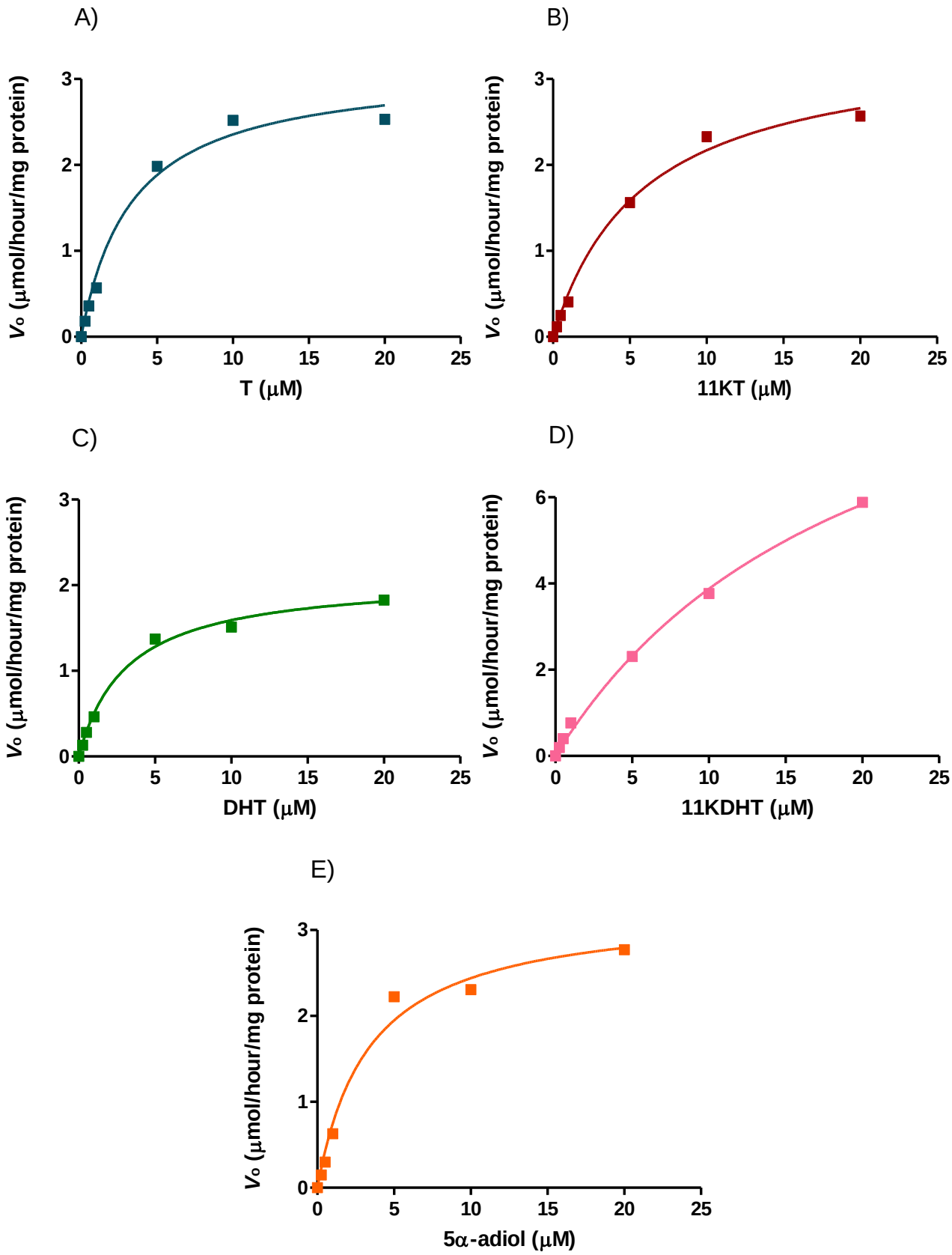

Figure 3.6: Michaelis-Menten plots for the metabolism of (A) T, (B) 11KT, (C) DHT, (D) 11KDHT and (E) 5α-adiol by 17βHSD2.

The catalytic efficiency (K_{cat}/K_m) could not be calculated as the enzyme concentration could not be determined. However, all kinetic data was generated during a single experiment in which cells were mixed after transfection. It can therefore be assumed that enzyme concentration was constant for all substrates and time points and as such catalytic efficiency can be approximated by the V_{max}/K_m values. The highest V_{max}/K_m values were determined for the conversion of 5α-adiol (V_{max}/K_m = 40.1) and T (V_{max}/K_m = 39.1). The V_{max}/K_m values for DHT, 11KT and 11KDHT were all similar (27.5, 26.1 and 24.0 respectively). This data shows that the conversion of T to A4 and 5α-adiol to AST are the most favoured reactions by catalysed 17βHSD2, but that 17βHSD2 can also efficiently catalyse the conversion of the 11-oxygenated steroids 11KT and 11KDHT.

Table 3.3: The apparent kinetic parameters ($K_{m, app}$ and $V_{max, app}$) for 17βHSD2. Letters a and b represents significant differences between samples (p>0.05), while values which do not significantly differ are assigned the same letter.

Substrate	Product	$K_{m, app}$ (μM)	Stats. K_m	$V_{max, app}$ (μmol/hour/mg protein)	Stats. V_{max}	V_{max}/K_m
T	A4	3.35 ± 0.81	a	131 ± 9.52	a	39.1
11KT	11KA4	5.48 ± 1.13	a	143 ± 10.2	a	26.1
DHT	5α-dione	3.18 ± 0.48	a	87.3 ± 3.97	a	27.5
11KDHT	11K5α-dione*	20.46 ± 3.56	b	491 ± 50.7	b	24.0
5α-adiol	AST	3.39 ± 0.94	a	136 ± 11.4	a	40.1

**No commercial steroids available, calculated using a response factor.*

The difference in the estimated catalytic efficiency for T and 11KT could clearly be observed during time courses conducted with three different concentrations of substrate. Figure 3.7 shows the conversion of T and 11KT to their respective products, A4 and 11KA4 by HEK293 cells expressing 17βSHSD2. Preliminary experiments (results not shown) indicated full conversion of both substrates T and 11KT after 6 hours, thus the conversion of T and 11KT to their respective products was determined at 20, 40, 60, 90, 120, 150, 180, 210, 240, 270, 300 and 360 min. After the first 20 min 56% of the 0.1 μM T was converted to A4 while in the same period of time only 33% of 11KT was converted to 11KA4. Similar for 1 μM substrates, 91% of T was converted to A4 in one hour compared to 66% of 11KT converted to 11KA4 in the same period of time. The same trend was observed at a saturating substrate concentrations.

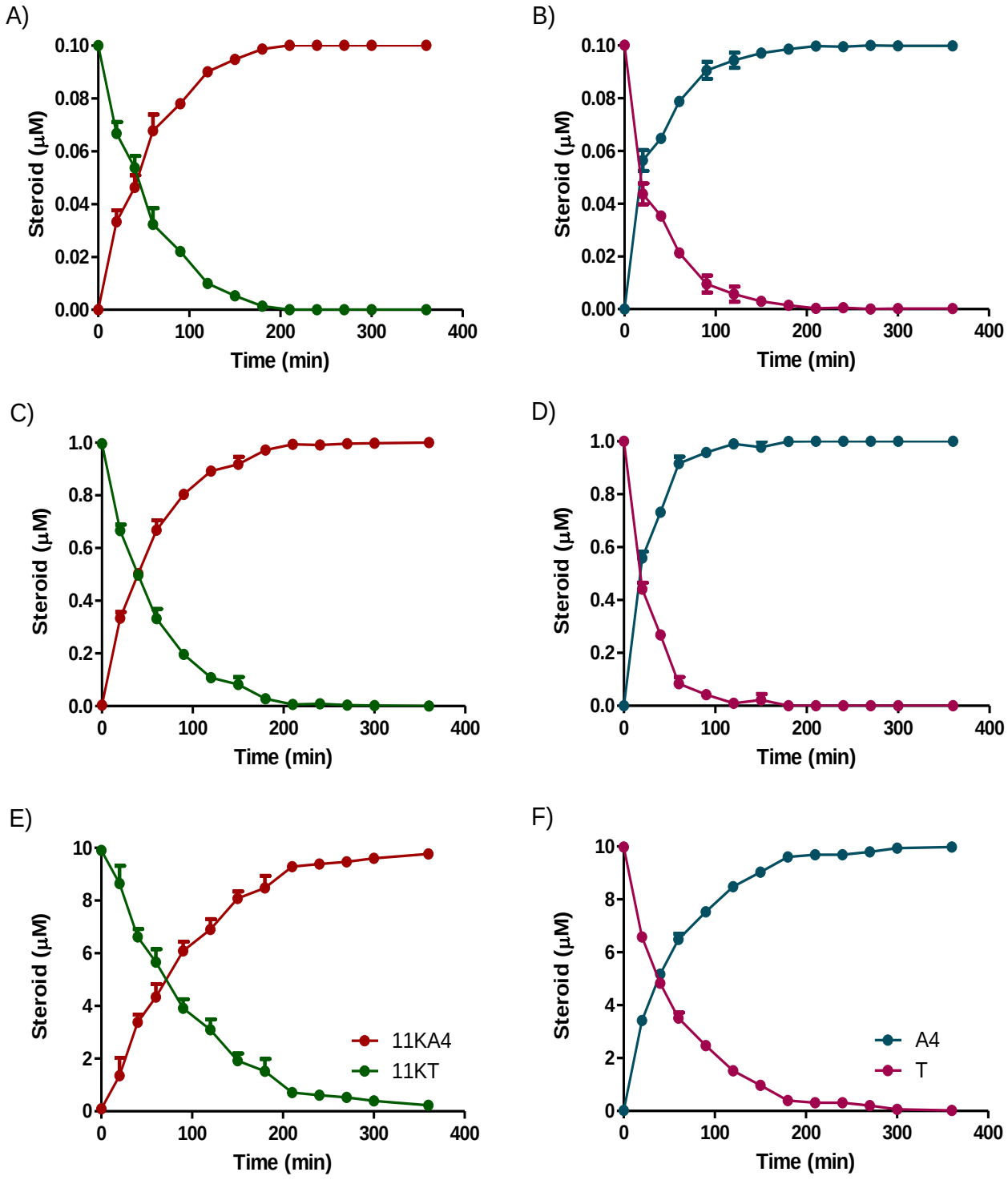

Figure 3.7: Time courses for the conversion of T and 11KT by 17βHSD2. Time course for the metabolism of T and 11KT at (A & B) 0.1 µM, (C & D) 1 µM and 10 µM (E & F) by 17βHSD2 expressed in HEK-293 cells. The results are from a single experiment performed in triplicate and are expressed as the mean ± SD.

3.4. The effect of different AKR1C3:17βHSD2 ratios on steroid metabolism

It is well known that AKR1C3 catalysis the 17β-reduction of A4 to T. Previous studies in our laboratory have also shown that the 11-oxygenated steroid 11KA4 is also a substrate for this enzyme and that 11KA4 may in fact be the preferred substrate (107, 108). Our group subsequently showed that the product of this reaction, 11KT, is an androgen and is equipotent to T (115). AKR1C3 expression has been shown to be upregulated in CRPC while the expression of 17βHSD2, which catalyses the reverse reaction, decreases or remains unaltered, thus leading to an increase in the pool of potent androgens (121–124). We therefore hypothesized that given the apparent preference of AKR1C3 for 11KA4 an increase in the expression of AKR1C3 will result in higher levels of 11KT being produced than T and that this effect would be further enhanced by the preference of 17βHSD2 for T as substrate. We therefore investigated this by measuring the effect of AKR1C3/17βHSD2 ratios in nonsteroidogenic HEK293 cells and the PCa cell line PC3 on the metabolism of A4 and 11KA4.

3.4.1. AKR1C3:17βHSD2 ratios in HEK293 cells

Nonsteroidogenic HEK293 cells were transfected with AKR1C3, 17βHSD2 and pCINeo, respectively and subsequently mixed to obtain different ratios of AKR1C3 to 17βHSD2 while keeping the total number of transfected cells constant. The metabolism of A4 and 11KA4 were then assayed using two different substrate concentrations (1 μM and 0.1 μM).

After 24 hours, cells expressing only AKR1C3 (1:0) converted only 2% of the 1 μM A4 to T while in the same time 14% 11KA4 was converted to 11KT, confirming previous observations that 11KA4 is the preferred substrate as shown in figure 3.8. Cells transfected with only 17βHSD2 (0:1) were given T and 11KT as substrate in order to confirm the expression and activity of this enzyme (figure 3.8, insert). A negative control (0:0) consisting of only cells transfected with the pCINeo vector, which contained no insert, was included in all experiments and confirmed that the HEK293 were nonsteroidogenic.

No difference was observed on the amount of A4 converted to T when cells expressing AKR1C3 and 17βHSD2 were combined in different ratios (figure 3.8A). In contrast, increased ratios of AKR1C3 to 17βHSD2 resulted in increased levels of 11KT being produced. The amount of 11KT produced increased significantly from 10% at a 1:1 ratio to 30% at a ratio of 6:1 (figure 3.8B).

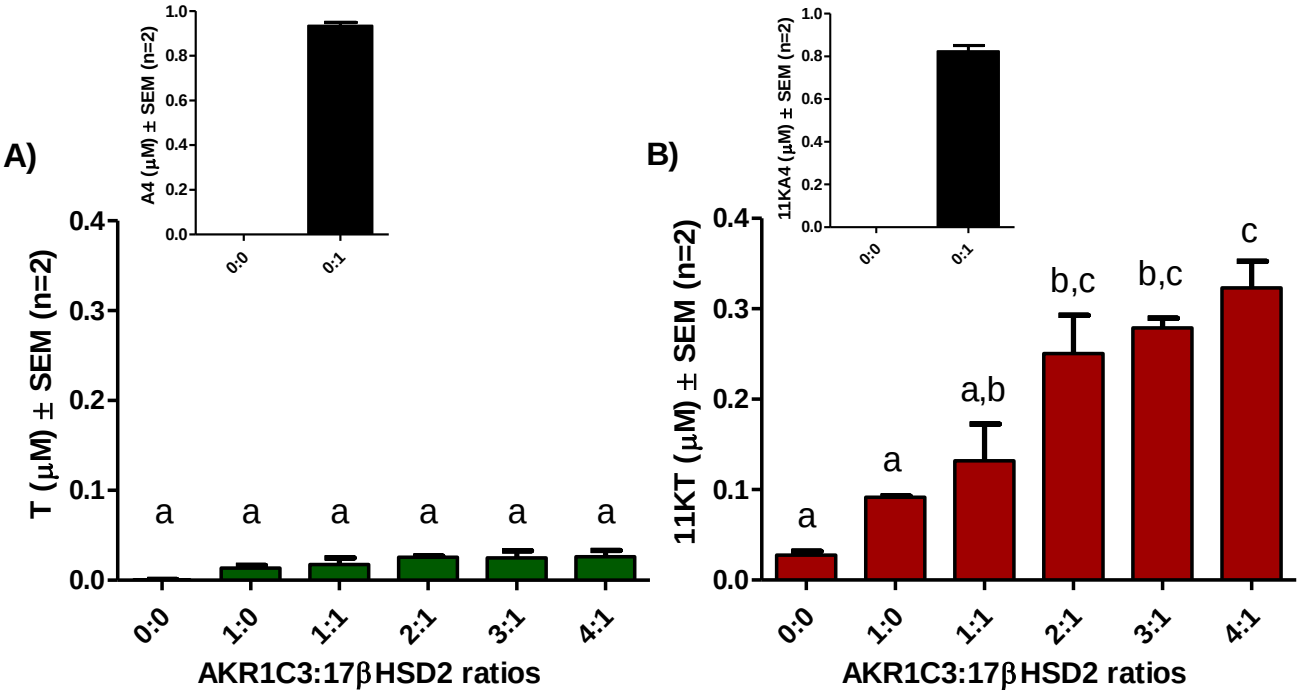

Figure 3.8: The metabolism of 1 µM A4 (A) and 11KA4 (B) by different ratios of HEK293 cells expressing AKR1C3 and 17βHSD2. Steroids were extracted and measured by UPC^2-MS/MS. The results are from two independent experiments performed in triplicate and are expressed as the means ± SEM. Letters a, b, c and d represents significant differences between samples (p>0.05), while values which do not significantly differ are assigned the same letter.

Repeating these experiments using a 0.1 µM substrate yielded similar to results to the experiments with 1 µM substrate described above. Increased ratios of AKR1C3 to 17βHSD2 had no effect on the production of T, but resulted in significantly higher levels of 11KT being produced as seen in figure 3.9A and figure 3.9C respectively. In the alternative 5α-dione pathway A4 is converted to 5α-dione by SRD5A1, which is in turn converted to DHT by AKR1C3. This route completely bypasses the production of T and is believed to be the main contributor to the intraprostatic androgen pool after ADT. We therefore also investigated the effect of different AKR1C3 to 17βHSD2 ratios on the conversion of 5α-dione to DHT. Similar to the conversion of A4 to T, the conversion of 5α-dione to DHT remained low even with an increase in AKR1C3 levels. No significant change in conversion was found for any of the ratios (figure 3.9B).

As there was no difference between the results obtained for T and 5α-dione and as AKR1C3 catalyses the conversion of A4 and 5α-dione with similar efficiencies (unpublished data) and 17βHSD2 catalyses the conversion of T and DHT with similar efficiencies (table 3.3), all further experiments were carried out with T.

We subsequently confirmed that the increase in 11KT production observed above was due to the increase in AKR1C3 expression. Three different ratios of cells expressing AKR1C3 and 17βHSD2 were incubated with 0.1 µM A4 or 11KA4 with and without 50 µM of the AKR1C3 inhibitor,

Indomethacin (figure 3.10). Indomethacin had little effect on the already low conversion of A4 to T, but significantly inhibited the conversion of 11KA4 to 11KT as was expected.

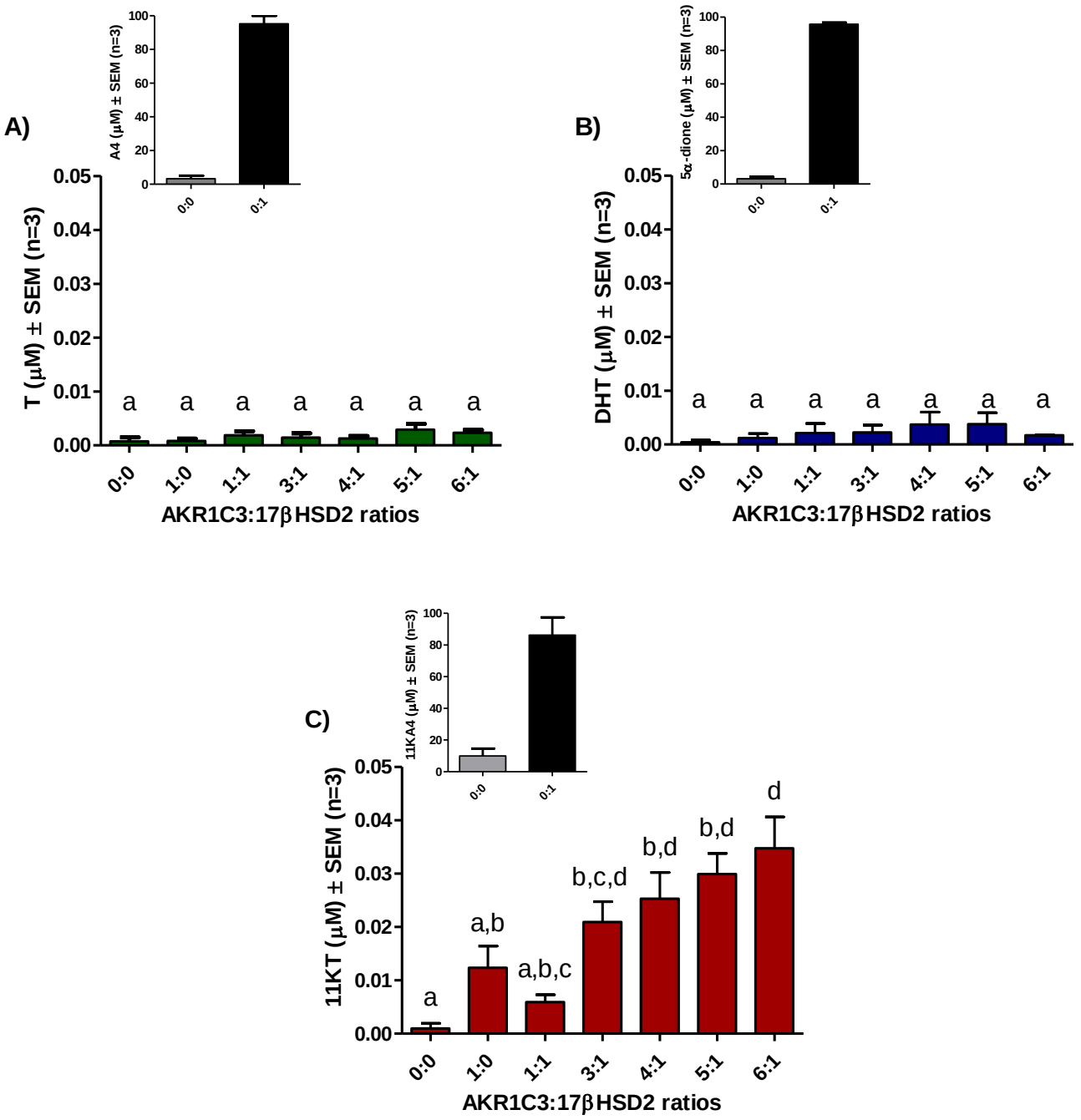

Figure 3.9: The metabolism of 0.1 µM A4 (A), 5α-dione (B) and 11KA4 (C) by different ratios of HEK293 cells expressing AKR1C3 and 17βHSD2. Steroids were extracted and measured by UPC^2-MS/MS. Results are shown as means ± SEM of three independent experiments performed in triplicate. Letters a, b, c and d represents significant differences between samples (p>0.05), while values which do not significantly differ are assigned the same letter.

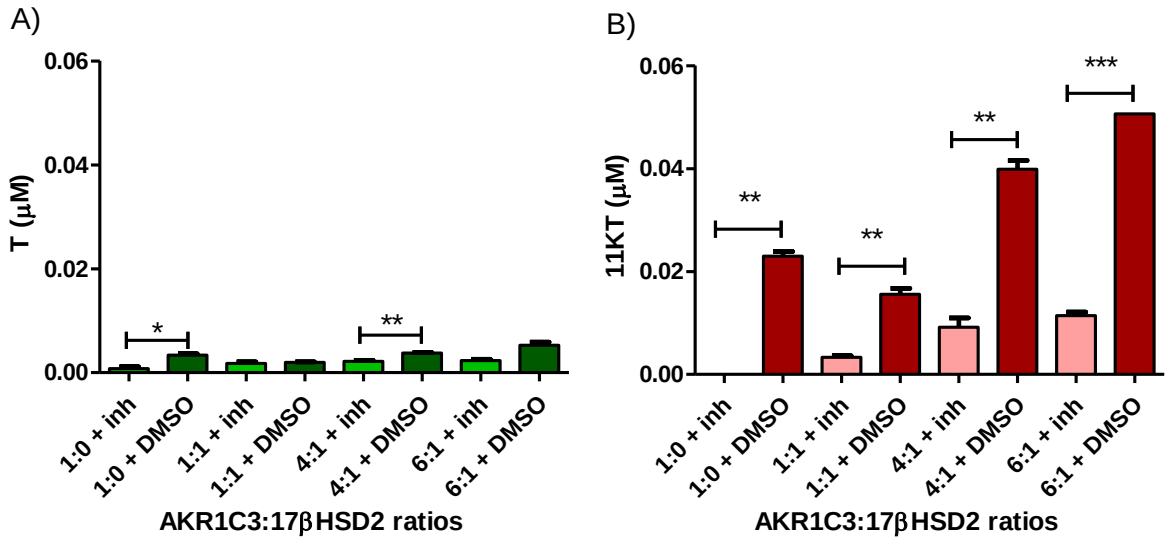

Figure 3.10: The metabolism of 0.1 µM A4 (A) and 11KA4 (B) by different ratios of HEK293 cells expressing AKR1C3 and 17βHSD2 in the presence (inh) or absence (DMSO) of the AKR1C3 inhibitor, Indomethacin. Steroids were extracted and measured by UPC^2-MS/MS. Results are from a single experiment performed in triplicate and is expressed as the mean ± S D. Statistically significant differences are indicated by *, ** or *** for p<0.05, p<0.01 or p<0.001, respectively.

In vivo, enzymes are exposed to more than one substrate at a time. We therefore assessed the simultaneous metabolism of 0.1 µM A4 and 0.1 µM 11KA4 using different ratios of HEK293 cells expressing AKR1C3 and 17βHSD2 as described above.

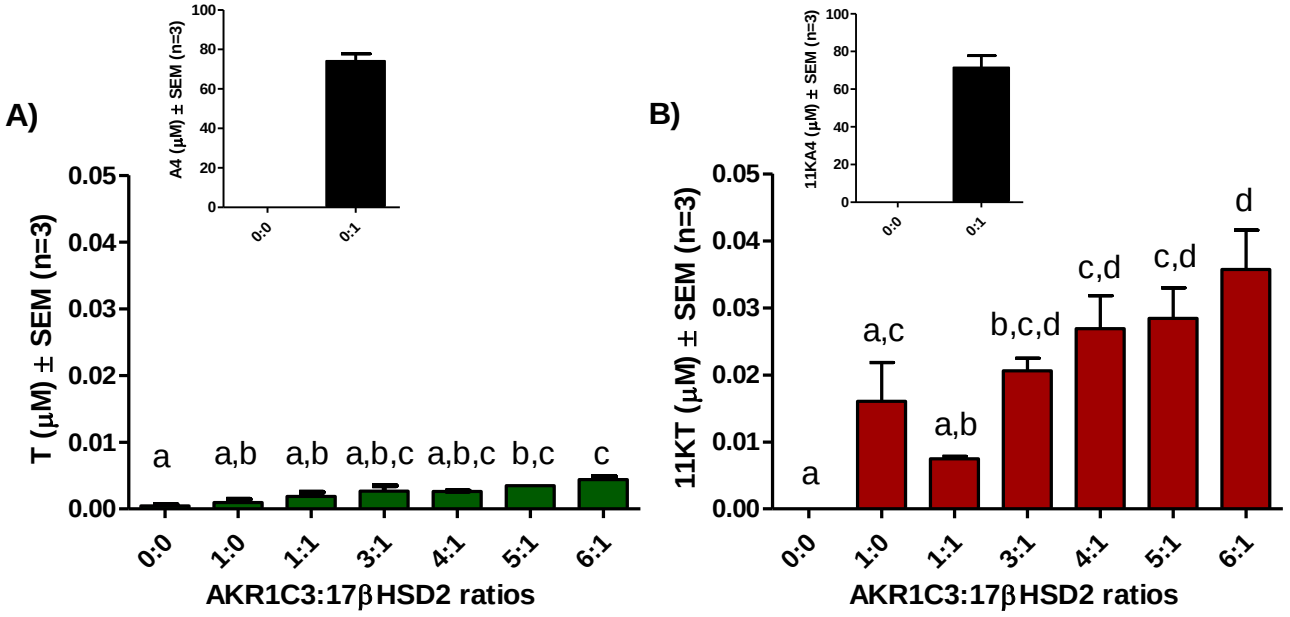

Figure 3.11: The metabolism of 0.1 µM A4 (A) and 11KA4 (B) by different ratios of HEK293 cells expressing AKR1C3 and 17βHSD2. Cells were incubated simultaneously with both substrates. Steroids were extracted and measured by UPC^2-MS/MS. Results are from three independent experiments each performed in triplicate and are shown as the means ± SEM. Letters a, b, c and d represents significant differences between samples (p>0.05), while values which do not significantly differ are assigned the same letter.

A similar pattern was observed as when the substrates where added individually (figure 3.11). The conversion of A4 to T remained relatively constant even when AKR1C3 levels increased, while increased levels of 11KT were observed as the ratio of AKR1C3:17βHSD2 increased. These results show that even in the presence of both substrates an increase in AKR1C3 levels with constant levels 17βHSD2 strongly favours the conversion of 11KA4 to the potent androgen 11KT.

3.4.2. Model of AKR1C3:17βHSD2 ratios

A mathematical model for the conversion of A4 and 11KA4 by different ratios of AKR1C3:17βHSD2 was constructed in Mathematica (Wolfram). The model was based on the kinetic parameters for 17βHSD2 determined by this study as well as the kinetic parameters for AKR1C3 determined by our group (unpublished data). As V_{max} is dependent on enzyme concentration, the V_{max} was scaled according to the number of transfected cells used in the HEK293 ratio experiments described in section 2.2.4. In other words the V_{max} value for AKR1C3 and 17βHSD2 was calculated for each ratio depending on the number of transfected cells present per ratio (table 3.4). The resulting model was then used to predict the metabolism of 0.1 µM A4 or 11KA4.

Table 3.4: The kinetic parameters for AKR1C3 and 17βHSD2 used for the construction of a mathematical model.

Enzyme	Substrate	$K_{m,\ app}$ (µM)	$V_{max,\ app}$ values of AKR1C3:17βHSD2 ratios (µmol/hour)					
			1:0	1:1	3:1	4:1	5:1	6:1
AKR1C3*	A4	1.11	0.012042	0.012042	0.036126	0.048168	0.060210	0.072252
	11KA4	2.87	0.148860	0.148860	0.446580	0.595440	0.744300	0.893160
17βHSD2	T	3.35	0.000000	1.886400	1.886400	1.886400	1.886400	1.886400
	11KT	5.84	0.000000	2.062800	2.062800	2.062800	2.062800	2.062800

*unpublished data from a separate study in our group.

The resulting model, as seen in figure 3.12, predicted that an AKR1C3:17βHSD2 ratio of 1:0 (only AKR1C3) would slowly convert A4 to T, with 20% conversion being achieved after 24 hours. In contrast, the model predicted that 11KA4 would rapidly be converted to 11KT with 70% conversion

being achieved after 24 hours. The inclusion of 17βHSD2 resulted in a steady state being reached for all ratios and both substrates. Increased AKR1C3:17βHSD2 ratios had little effect on the metabolism of A4 to T and the maximum conversion of A4 to T at steady state was only 10%. In contrast, increased AKR1C3:17βHSD2 ratios significantly shifted the steady state from 10% 11KT (1:1 ratio) to 45% 11KT (6:1 ratio).

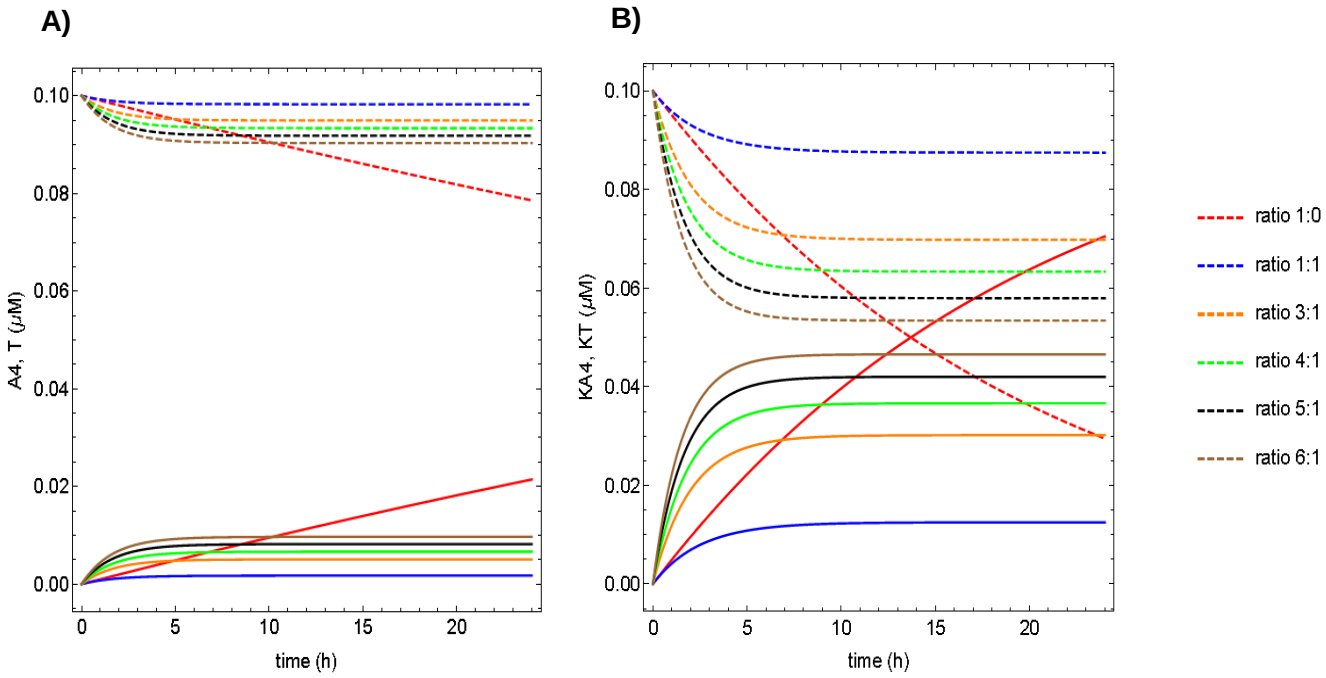

Figure 3.12: A model used to predict the metabolism of (A) A4, and (B) 11KA4 by increasing AKR1C3:17βHSD2 ratios. The model was constructed by Prof JL Snoep, Biochemistry department, Stellenbosch University.

3.4.3. AKR1C3:17βHSD2 ratios in PC3 cells

The androgen independent PCa cell line, PC3, endogenously expresses 17βHSD2, but does not express AKR1C3 (155). This cell line was therefore used to further investigate the effect of AKR1C3:17βHSD2 ratios on the metabolism of A4 and 11KA4 by transiently transfecting the cells with increasing concentrations of AKR1C3. The cells were incubated with 0.1 µM A4 or 11KA4 in the presence of 10 µM of the SRD5A inhibitor, dutasteride, which was included to prevent the downstream metabolism of either the substrates or products. The levels of 17βHSD2 and AKR1C3 were confirmed by qPCR.

Results showed that the expression of endogenous 17βHSD2 remained constant (figure 3.13A). The expression of AKR1C3 was low in control samples (pCINeo transfected cells), but increased significantly after transfection. Furthermore, the levels of AKR1C3 increased proportionally (2-fold) when 0.25, 0.5 or 1 µg AKR1C3 plasmid DNA was added (figure 3.13B).

The metabolism of A4 and 11KA4 in PC3 cells transfected with increasing concentrations of AKR1C3 was found to mirror the results of the HEK293 ratio experiments described above (section 3.4.1). Only very low levels of A4 were converted to T under all conditions, while the amount of 11KT produced increased significantly when the cells were transfected with 0.5 and 1 µg AKR1C3 (figure 3.14).

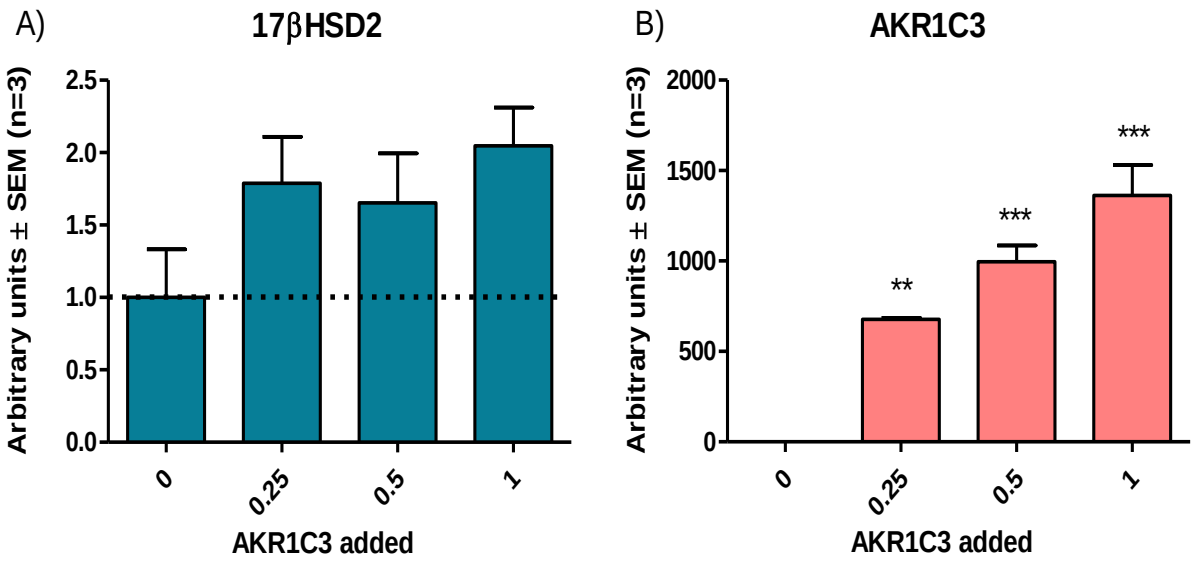

Figure 3.13: qPCR analysis of (A) 17βHSD2 and (B) AKR1C3 in PC3 cells. Results are shown as means ± SEM of three independent experiments each performed in triplicate. Data from the individual experiments was normalized using log transformation and mean centering prior to analysis (154). Statistically significant differences are indicated by *, ** or *** for p<0.05, p<0.01 or p<0.001, respectively.

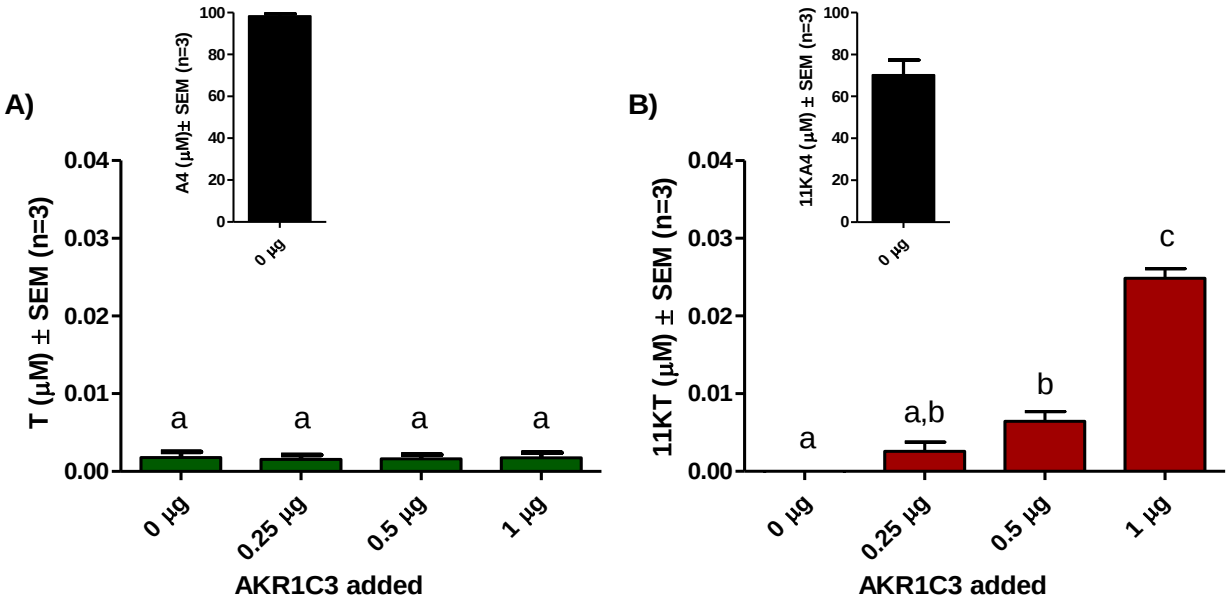

Figure 3.14: The metabolism of 0.1 µM A4 (A) and 11KA4 (B) by PC3 cells transfected with increasing amounts of AKR1C3. Steroids were extracted after 24 hours and analysed using UPC^2-MS/MS. Results are shown as means ± SEM of three independent experiments each performed in triplicate. Letters a, b, c and d represents significant differences between samples (p>0.05), while values which do not significantly differ are assigned the same letter.

It should be noted that these experiments were conducted in the presence of the SRD5A inhibitor, dutasteride, which was added to prevent downstream metabolism of the substrates and products. We therefore confirmed that dutasteride has no effect on the activity of either 17βHSD2 or AKR1C3 by assaying the conversion of T and 11KT or A4 and 11KA4 in HEK293 cells transiently transfected with either enzyme, respectively, in both the presence and absence of 10 µM dutasteride (figure 3.15 and 3.16). No significant differences were observed between control samples and those treated with dutasteride, thereby confirming that this SRD5A inhibitor has no significant effect on the activity of AKR1C3 or 17βHSD2. Thus results obtained from the experiments performed in the presence of dutasteride were not influenced by the presence of the inhibitor.

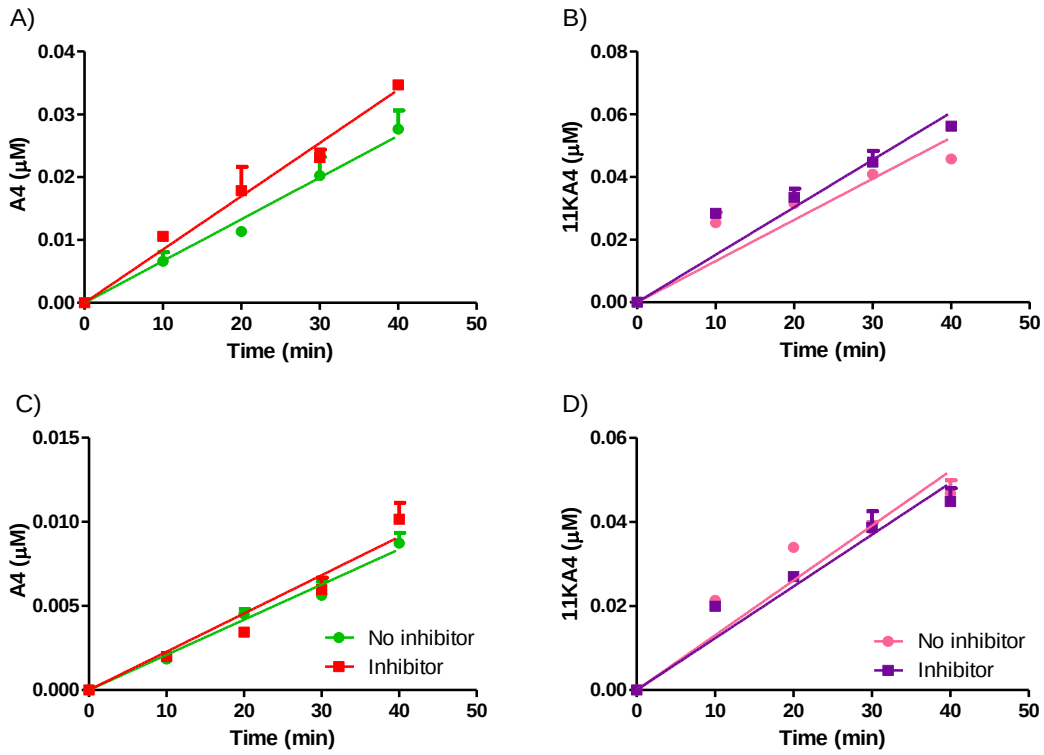

Figure 3.15: The effect of dutasteride on 17βHSD2 activity. Initial rates for the conversion of (A & B) 0.1 µM and (C & D) 1 µM T and 11KT in the presence and absence of 10 µM dutasteride by HEK293 cells expressing 17βHSD2. Steroids were extracted and measured by UPC2-MS/MS. Linear regression lines were fitted in GraphPad Prism. The results are from a single experiment performed in triplicate and are expressed as the mean ± SD.

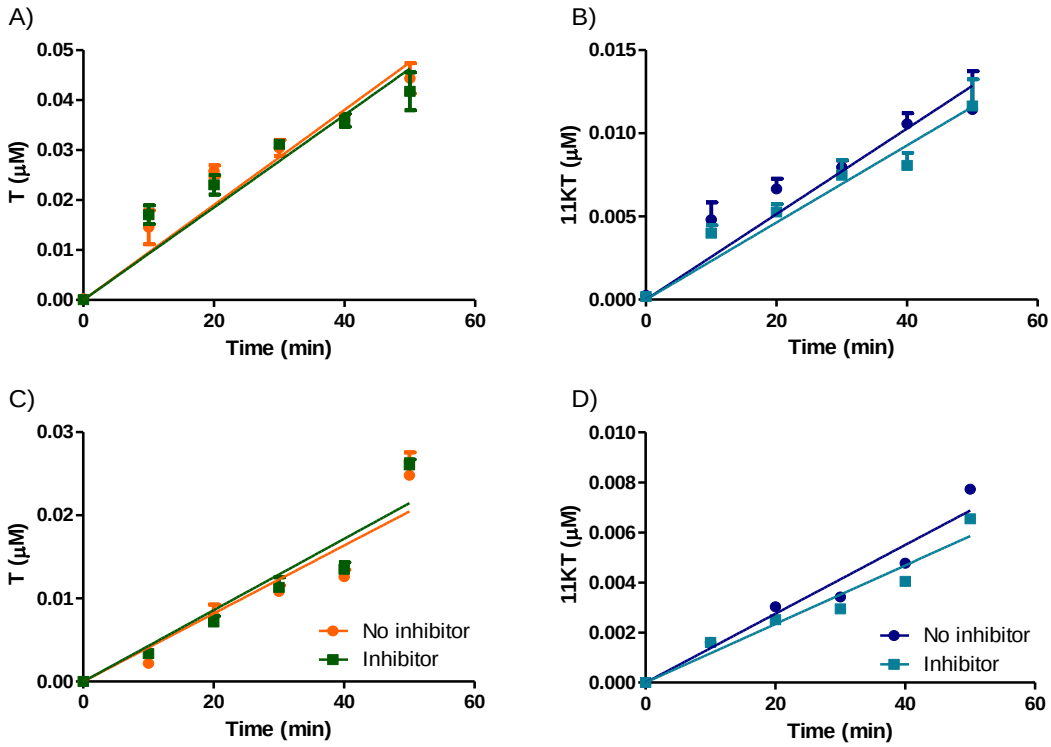

Figure 3.16: The effect of dutasteride on AKR1C3 activity. Initial rates for the conversion of (A & B) 0.1 µM and (C & D) 1 µM A4 and 11KA4 in the presence and absence of 10 µM dutasteride by HEK293 cells expressing AKR1C3. Steroids were extracted and measured by UPC2-MS/MS. Linear regression lines were fitted in GraphPad Prism. The results are from a single experiment performed in triplicate and are expressed as the mean ± SD.

3.5. The metabolism of T and 11KT in PCa cell lines endogenously expressing AKR1C3 and 17βHSD2.

Three PCa cell lines were chosen to validate the results obtained by the ratio experiments described above (sections 3.4.1 and 3.4.2) by investigating the effect of endogenous AKR1C3 and 17βHSD2 activity on the metabolism of A4, T, 11KA4 and 11KT.

LNCaP cells were originally derived from a needle biopsy taken from the left supraclavicular lymph node of a 50-year old Caucasian male (156). LNCaP cells are relatively slow growing cells, which express a mutated AR (T877A) and are androgen responsive. The cell line C4-2 (not included in this study) was derived from a tumour which developed in castrated nude mice injected with LNCaP cells. The C4-2B cell line was derived from a bone metastasis after the orthotopic transplant of the C4-2 cells in nude mice 5. C4-2B is thus a metastatic derivative of the LNCaP cell line and are considered to be a model of CRPC (157).

The VCaP cell line was obtained from a patient who underwent androgen deprivation by groserelin acetate plus flutamide as well as three different regimens of chemotherapy. VCaPs are thus

considered to be a model of CRPC. They are a slow growing cell line and overexpress the wild type AR.

The levels of endogenous 17βHSD2 and AKR1C3 expression in VCaP, C42B and LNCaP cell lines were investigated using qPCR. No statistical significant difference was observed in the levels of 17βHSD2 expressed in the three cell lines although it appeared that LNCaP cells express higher levels of 17βHSD2 compared to the VCaP or C42B cells (figure 3.17A). The endogenous expression of AKRC3 was higher than that of 17βHSD2 in all three cell lines. Significantly higher levels of AKR1C3 were observed in VCaP cells when compared to C42B and LNCaP cells (figure 3.17B).

The ratio of AKR1C3 to 17βHSD2 expression in each cell line was subsequently calculated. The results showed that VCaP cells have a significantly higher ratio of AKR1C3 to 17βHSD2 compared to C42B and LNCaP cells. No significant difference in the ratio of AKR1C3 to 17βHSD2 was observed between C42B cells and LNCaP cells (figure 3.18).

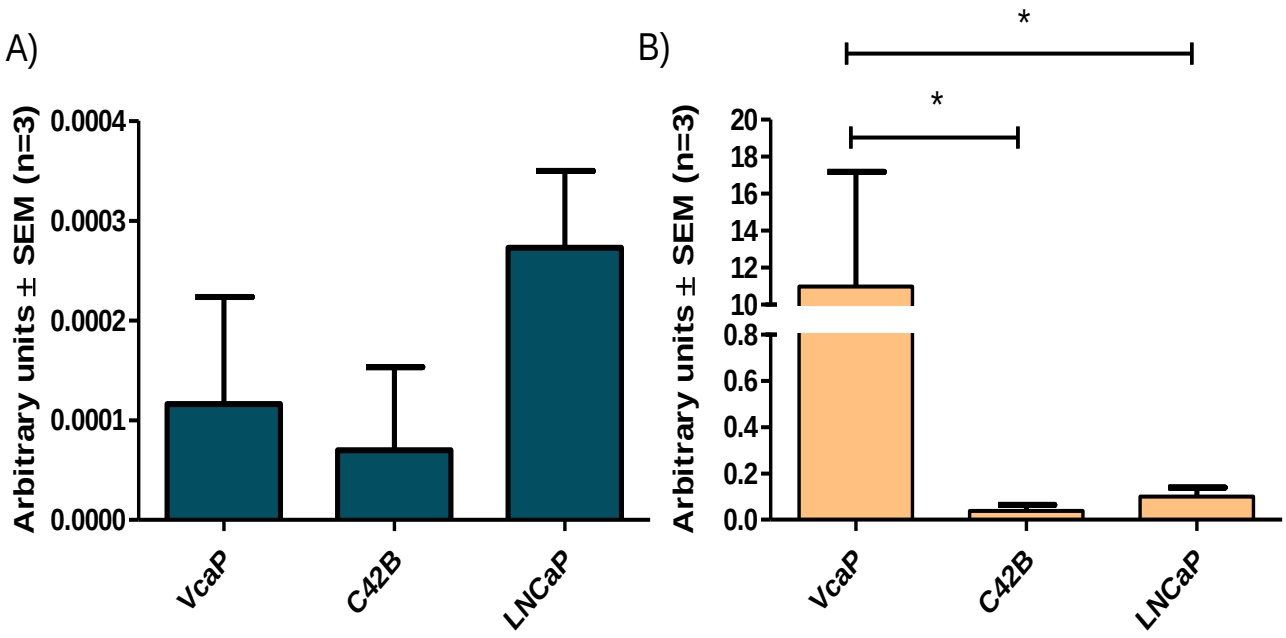

Figure 3.17: qPCR analysis of (A) 17βHSD2 and (B) AKR1C3 expression VCaP, C42B and LNCaP cells. Results are shown as means ± SEM of three independent experiments each performed in triplicate. Statistically significant differences are indicated by *, ** or *** for $p<0.05$, $p<0.01$ or $p<0.001$, respectively.

The cells were subsequently all incubated with 0.1 µM of each substrate (A4, 11KA4, T and 11KT) in the presence of dutasteride to inhibit the downstream metabolism of substrates or products. Time points where collected every 24 hours for a period of 4 days. As expected significantly higher rates of conversion were observed for 11KA4 when compared to A4 in all three cell lines. Overall the highest levels of conversion were observed in the VCaP cells which are not surprising given

that these cells express the highest levels of AKR1C3 and had the highest ratio of AKR1C3 to 17βHSD2 (figure 3.18). After 96 hours only 12% A4 was converted to T, while 80% 11KA4 was converted to 11KT during the same time the same time (figure 3.19). Interestingly, although VCaP cells express only low levels of 17βHSD2, T was efficiently converted to A4 when added as a substrate (88% metabolised after 96 hours). In contrast, only low levels of 11KA4 were produced when 11KT was added as a substrate (14% metabolised after 96 hours) (figure 3.19). While these conversions are likely due to 17βHSD2, the potential role of other oxidative 17βHSD cannot be excluded at this stage.

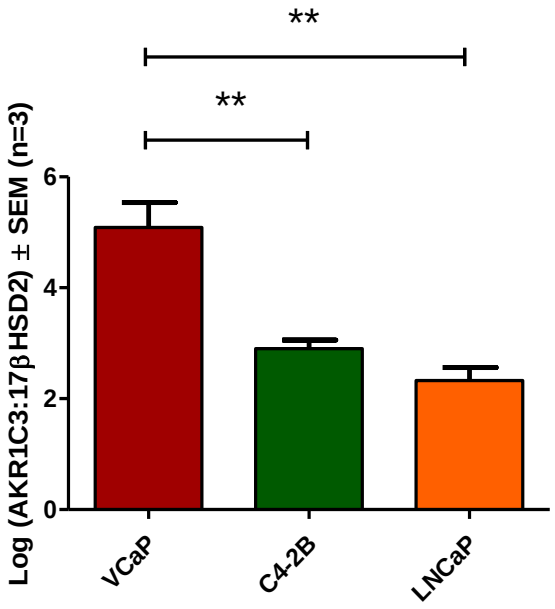

Figure 3.18: qPCR analysis of the endogenous expression of AKR1C3:17βHSD2 in VCaP, C42B and LNCaP cell lines. Results are shown as means ± SEM of three independent experiments performed in triplicate (n=3). Statistically significant differences are indicated by *, ** or *** for p<0.05, p<0.01 or p<0.001, respectively.

The conversion of A4 and 11KA4 to T and 11KT, respectively, were substantially lower in C4-2B and LNCaP cells, which both express significantly less AKR1C3 than VCaP cells. Nevertheless, the same trend was observed with both cell lines showing a preference for the conversion of 11KA4 (figure 3.19). Similar to the results in the VCaP cells, when T and 11KT were given as substrates a preference was observed for the conversion of T in both C4-2B and LNCaP cells. Also it is interesting to note that the highest level of conversion from 11KT to 11KA4 was observed in LNCaP cells (figure 3.19) which correlates to the observation that this cell line expresses the highest levels of 17βHSD2.

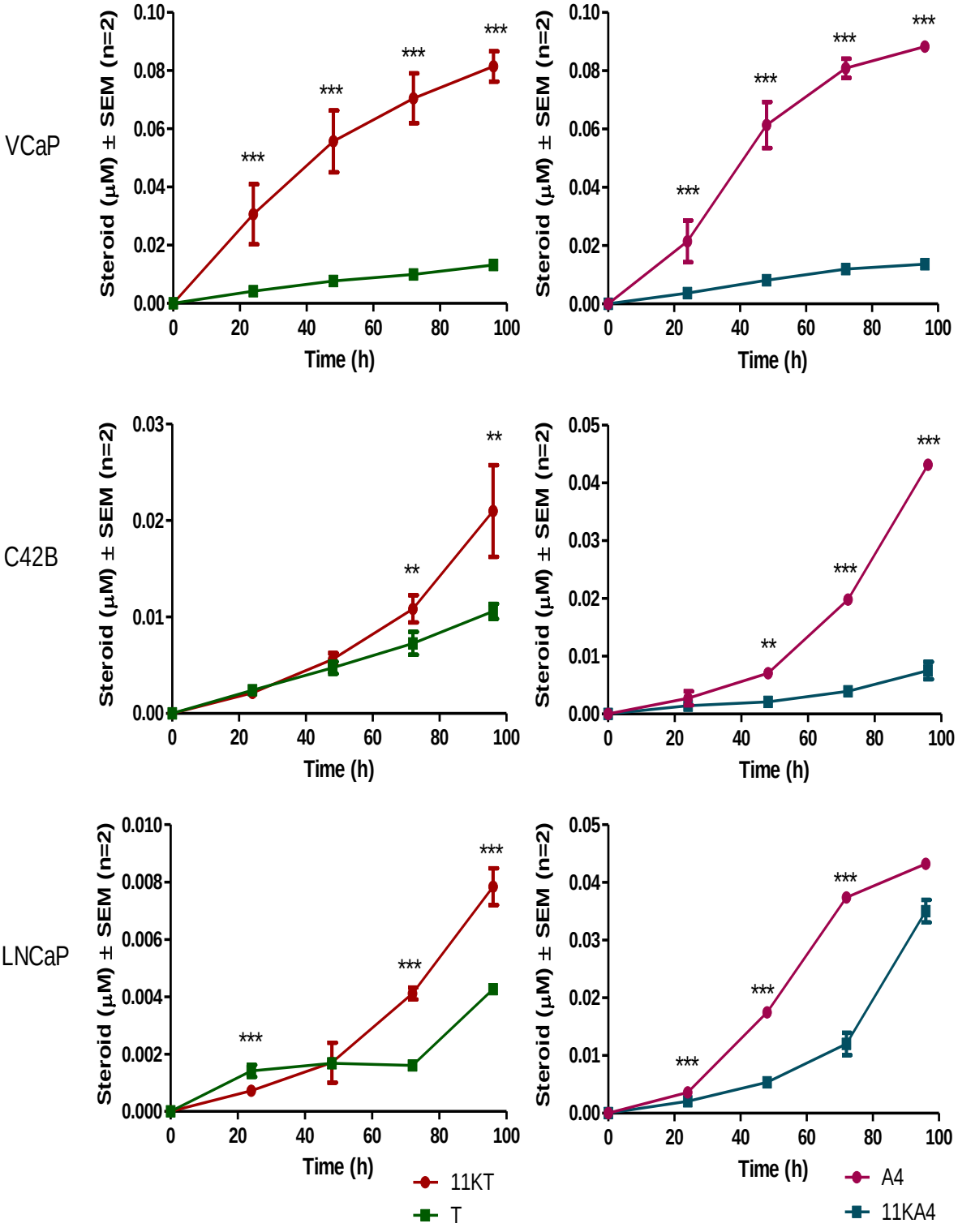

Figure 3.19: The metabolism of 0.1 µM A4, 11KA4, T and 11KT by VCaP, C42B and LNCaP cells in the presence of dutasteride. Steroids were extracted and analyzed using UPC^2-MS/MS. Results are shown as means ± SEM of two independent experiments each performed in triplicate. Statistically significant differences are indicated by *, ** or *** for p<0.05, p<0.01 or p<0.001, respectively.

Chapter 4
Discussion

Introduction

PCa is a hormone dependent cancer. ADT is therefore used to treat the advanced stages of this disease and is accomplished through either chemical or physical castration (27). While ADT initially yields excellent results, in many cases the PCa later returns despite the castrate levels of T and is then known as CRPC (42). Although CRPC was initially thought to be androgen independent, many recent studies have shown that in the majority of cases this is in fact not true (57, 74). Instead CRPC is fuelled by androgen precursors of adrenal origin. CRPC tissue has been shown to convert the androgen precursors DHEA and A4 to the potent androgen DHT via the alternate 5α-dione pathway (158). Our laboratory has also recently suggested that the intratumoural conversion of the adrenal steroid 11OHA4 to the potent androgens 11KT and 11KDHT may contribute to the development and maintenance of CRPC (107, 115). Both the 5α-dione and 11OHA4 pathways rely on the activity of key steroidogenic enzymes, the majority of which are shared by both pathways. Consequently, the study and characterization of these enzymes is vital for our understanding of disease development and progression and may even lead to new targets being identified for drug development.

Many of the key steps in intratumoural androgen metabolism are catalysed by 17βHSD enzymes. For the most part C19 steroids with a keto group at carbon 19 have little to no androgenic activity, while C19 steroids with a beta hydroxyl group at this position are androgenic. The enzyme AKR1C3 (17βHSD5) catalyses the conversion of inactive 17-keto C19 steroids to the more active 17β-hydroxy C19 steroids, while the reverse reaction is catalysed by 17βHSD2. Together these enzymes therefore play a vital role in regulating the intratumoural pool of active androgens. Numerous studies have shown that the expression levels of these enzymes are altered during the development of CRPC (112, 121–123, 126). A significant increase in the expression of AKR1C3 has been observed (124, 149), while the levels of 17βHSD2 appear to remain constant or decrease (127, 150). A study by Stanbrough *et al.* (121) found that AKR1C3 is the most upregulated enzyme which is involved in androgen biosynthesis in CRPC patients at both RNA and protein levels within tumour and soft tissue metastasis. Using microarrays, they found a 5.3 fold increase in the expression of AKR1C3 in CRPC. Immunohistochemical analysis showed that only 5.6% of primary tumours stained strongly for AKR1C3 compared to the 58% of CRPC samples. It

has thus been suggested that this phenomenon acts as a mechanism to compensate for the reduced levels of androgens observed after ADT.

Although both AKR1C3 and 17βHSD2 have been well characterized using classical substrates such as those found in the 5α-dione pathway, the activity of these enzymes towards metabolites from the novel 11OHA4 pathway has not yet been investigated. Furthermore, the relative contribution of these enzymes to the 5α-dione and 11OHA4 pathways is unknown. The comprehensive characterization of these enzymes will therefore not only elucidate the activity of the individual enzymes, but will also provide a better understanding of intratumoural androgen metabolism.

The characterization of 17βHSD2 activity towards 11-oxygenated substrates

The activity of 17βHSD2 towards the 11-oxygenated substrates 11KT and 11KDHT as well as classical substrates T, DHT and 5α-adiol was characterized in this study. Interestingly although not statistically significant, 17βHSD2 tended to have slightly higher affinity for the classical substrates: DHT ($K_{m,\ app}$ = 3.18 ± 0.48 µM), T ($K_{m,\ app}$ = 3.35 ± 0.81 µM) and 5α-adiol ($K_{m,\ app}$ = 3.39 ± 0.94 µM) than for the 11-oxygenated substrates: 11KDHT ($K_{m,\ app}$ = 20.46 ± 3.56 µM) and 11KT ($K_{m,\ app}$ = 5.48 ± 1.13 µM). Our results agree with previous studies by Wu *et al.* (143) and Lu *et al.* (159) which both showed that 17βHSD2 has a higher affinity for DHT than T. However, the K_m values obtained by these previous studies were up to 10-fold lower that the values obtained in this study. Wu *et al.* (143) measured $K_{m,\ app}$ values of 0.31 µM and 0.39 µM for DHT and T, respectively, while the values determined by Lu *et al.* (159) were 0.25 µM and 0.61 µM for DHT and T, respectively. Differences in K_m and V_{max} values between this study and those of previous studies can be attributed to the differences in experimental procedure. The current study was conducted *in vitro* using HEK293 cells transiently transfected to express 17βHSD2, while Wu *et al.* assayed 17βHSD2 activity using homogenates from transfected cells and added the cofactor NAD^+ to initiate the reaction. Similarly, the experiments conducted by Lu *et al.* also made use of homogenates and added cofactor (NAD^+). The current study forms part of a larger study which aims to characterise all the relevant androgen metabolizing enzymes in CRPC under cellular conditions and thus did not make use of additional cofactors, but instead relied on intracellular cofactor concentrations. In this study cells were first plated in 75 cm^2 flasks, transfected and then detached and mixed prior to replating in 48 well plates, thus ensuring the equal distribution of transfected cells. All kinetic studies were thus conducted in cells expressing the same amount of 17βHSD2 therefore allowing for the comparison of the determined kinetic constants.

It was interesting to note that the affinity of 17βHSD2 for the 11-oxygenated substrate, 11KT ($K_{m,\ app}$ = 5.84 ± 1.13 µM) was lower than that of the classical substrates described above although no

statistical significance was found for results. While the affinity of 17βHSD2 for 11KDHT ($K_{m,\ app}$ = 20.46 ± 3.56 µM) was even lower than that of 11KT, the accuracy of this parameter needs to be confirmed when commercial standards become available for the product 11K-5α-dione. The substrate 11K-5α-adiol was not commercially available for purchase and thus was not included in this study.

The $V_{max,\ app}$ values for T, 5α-dione and 11KT were similar (ranging from 131 ± 9.52 to 143 ± 10.2 µmol/hour/mg protein) while that of DHT was lower (140 ± 6.26 µmol/hour/mg protein) and that of 11KDHT was higher (491 ± 50.7 µmol/hour/mg protein) as seen in table 3.3.

Catalytic efficiency, defined as K_{cat}/K_m, is perhaps the most appropriate way to compare the activity of an enzyme towards different substrates (160). The determination of K_{cat} is however dependent on the enzyme concentration being determined, which was not possible in this study as 17βHSD2 was expressed in mammalian cells and protein determinations thus reflected the total protein content of the cells. The ratio of V_{max}/K_m could however be used to estimate the catalytic efficiency. This was possible as the K_m and V_{max} for all substrates were determined during the same experiment using methodology which ensured that the concentration of 17βHSD2 was constant as described above. The resulting estimated catalytic efficiencies (V_{max}/K_m) revealed that the preferred substrates were T (V_{max}/K_m = 39.1) and 5α-adiol (V_{max}/K_m = 40.1). Interestingly, estimated catalytic efficiencies for 11KT (V_{max}/K_m = 26.1), DHT (V_{max}/K_m = 27.5) and 11KDHT (V_{max}/K_m = 24.0) were all similar.

Taken together this data showed for the first time that 17βHSD2 efficiently catalyses the conversion of 11-oxygenated C19 steroids from the 11OHA4 pathway, albeit less efficiently than some of the classical substrates.

The effect of different AKR1C3:17βHSD2 ratios on the metabolism of T and 11KT

The focus of this study was to compare the effect of different AKR1C3:17βHSD2 ratios on the flux through the alternate 5α-dione and 11OHA4 pathways. One substrate was thus selected for each of the pathways. 11KA4 was selected in the case of the 11OHA4 pathway as unpublished data from our group has demonstrated that the flux through the pathways results in the production of 11KA4, which is further metabolized by AKR1C3 yielding 11KT. Although the flux through the alternate 5α-dione pathway bypasses the conversion of A4 to T by AKR1C3, and instead follows the 5α-reduction of A4 to 5α-dione prior to the conversion of 5α-dione to DHT by AKR1C3, A4 was selected as the representative substrate for the experiments conducted in this study for the following reasons. First, unpublished data from our group has shown that the affinity and catalytic efficiency of AKR1C3 towards A4 and 5α-dione is comparable, while this study has shown that the affinity and catalytic efficiency of 17βHSD2 were similar for T and DHT. Second, the downstream

metabolism of A4, T, 11KA4 and 11KT by SRD5A1 in PCa cell lines can be inhibited using an SRD5A inhibitor such as dustasteride, thus permitting only the conversion of these steroids by the 17βHSD enzymes to be measured, while not affecting the activity of AKR1C3 or 17βHSD2. In contrast, both DHT and 5α-dione can be subjected to metabolism which cannot be blocked due to a lack of specific inhibitors for AKR1C2, which catalyses the 3α-reduction of these steroids. AKR inhibitors would lead to the inhibition of isozyme AKR1C3, which would compromise the results of this study. Third, the lower limits of detection of the UPC^2-MS/MS method employed in this study were significantly lower for A4 and T than 5α-dione and DHT, as Δ^4-steroids ionize better than 5α-reduced steroids. Finally, experiments which did include both A4 and 5α-dione as substrates yielded nearly identical results, thus validating the use of A4 instead of 5α-dione (figure 3.9B).

Three different systems were used to compare the effect of AKR1C3:17βHSD2 ratios on the metabolism of A4 and 11KA4 to T and 11KT, respectively. First, HEK293 cells, which do not endogenously express either AKR1C3 or 17βHSD2, were transfected individually with both enzymes after which the transfected cells were mixed to obtain different AKR1C3:17βHSD2 ratios. Second, PC3 cells, which endogenously express 17βHSD2, were transfected with increasing amounts of AKR1C3 to obtain different AKR1C3:17βHSD2 ratios. Lastly, the PCa cell lines, VCaP, C4-2B and LNCaP, were also used as *in vitro* model systems as all three cell lines endogenously express both enzymes, but at different ratios.

The results from both the ratio experiments performed in the HEK293 cells (figure 3.9) and PC3 cells (figure 3.14) were similar. In both systems the conversion of 11KA4 to 11KT increased significantly as the ratio of AKR1C3:17βHSD2 increased, while the conversion of A4 to T remained unchanged. The same results were observed irrespective of substrate concentration (0.1 μM or 1 μM), as seen in figures 3.9 and 3.8 and whether the substrates were added individually or in combination (figure 3.11). These results were then confirmed in three PCa cell lines expressing different ratios of AKR1C3:17βHSD2 (figure 3.18). 11KA4 was converted to 11KT significantly faster than A4 was converted to T in each cell line. What's more the rate of conversion correlated well with the AKR1C3:17βHSD2 ratios determined by qPCR. For example, the conversion of 11KA4 to 11KT was the fastest in the VCaP cell line which was shown to express the highest AKR1C3:17βHSD2 ratio (figure 3.18). 11KT was also metabolized to 11KA4 at a lower rate than T was metabolized to A4 in all three cell lines when 11KT and T were used as substrates (figure 3.19). This was not unexpected as AKR1C3 converts 11-keto substrates more efficiently than classical substrates. Thus, the conversion from 11KT to 11KA4 by 17βHSD2 is countered by the highly efficient conversion from 11KA4 back to 11KT. Also, the conversion of 11-keto substrates by 17βHSD2 is less efficient than the conversion of substrates from the classical pathway (table 3.3).

A mathematical model was also constructed to predict the metabolism of A4 and 11KA4 in the presence of increasing AKR1C3:17βHSD2 ratios. The model predicted that the co-expression of

AKR1C3 and 17βHSD2 would lead to the establishment of a steady state where the rate catalysed by each enzyme is equal. The predicted steady states for the conversion of A4 to T ranged from ± 1% T (1:1 ratio) to ± 10% T (6:1 ratio) (figure 3.12). In contrast the predicted steady states for the conversion of 11KA4 to 11KT ranged from ± 12% 11KT (1:1 ratio) to ± 45% 11KT (6:1 ratio) (figure 3.12) thus confirming what was observed experimentally (figures 3.9A and 3.9C). The model clearly demonstrates that the increased AKR1C3:17βHSD2 ratios have a substantially greater effect on the conversion of 11KA4 than A4.

This can be explained by the observation that AKR1C3 is significantly more efficient at catalysing the conversion of 11KA4 to 11KT than A4 to T (unpublished data) and the effect is confounded by the activity of 17βHSD2. The catalytic efficiency of AKR1C3 for the conversion of 11KA4 to 11KT is similar to that of the catalytic efficiency of 17βHSD2 for the conversion of 11KT to 11KA4. Thus, changes in the ratios of the enzymes will have significant effects on the flux. In contrast, the catalytic efficiency for 17βHSD2 for T is substantially higher that of AKR1C3 for A4 and as a result elevated levels of AKR1C3 has a minimal effect on the conversion of A4 to T due to the rapid conversion of T back to A4 by 17βHSD2. Elevate AKR1C3 levels alone may therefore not be sufficient to increase the flux through the 5α-dione pathway as was previously suggested.

Taken together these results show that the upregulation of AKR1C3 observed in CRPC may have less of an effect on the 5α-dione pathway, but may favour the production of more potent androgens by the 11OHA4 pathway. Furthermore, these results show for the first time that 17βHSD2 expression may play a vital role in regulating intratumoral androgen production in CRPC.

Implications for CRPC

To date the alternate 5α-dione pathway is believed to make the biggest contribution to the maintenance of the intratumoural androgen pool which drives the development and progression of CRPC. Previous studies by our group have, however, suggested that the overlooked 11OHA4 pathway, which results in the production of the potent androgens 11KT and 11KDHT, may play a previously unrecognized role in the maintenance of intratumoural androgen levels.

While more work is required to elucidate the role of the 11OHA4 pathway in the development and progression of CRPC the current study provides further evidence of the importance of this pathway. The most striking finding was that while altered enzyme expression of AKR1C3 and 17βHSD2 is believed to facilitate the production of T and DHT this was not observed in any of the models employed in this study suggesting that the alternative 5α-dione pathway as well as the classical pathway may not be the main contributors to the pool of potent androgens after ADT as previously assumed. Conversely, significant increases in the conversion of 11KA4 to 11KT were

observed in all models used in this study to investigate the effect of altered AKR1C3:17βHSD2 ratios.

It should, however, be noted that in the classical and alternative 5α-dione pathways, the precursor androgen A4 is converted to DHT either via the production of T or 5α-dione and thus requires two enzymatic steps catalysed by SRDA1 and AKR1C3. In contrast an extra step is required in the 11OHA4 pathway as 11OHA4 first needs to be converted to 11KA4 by 11βHSD2 before the latter can be converted to 11KT by AKR1C3 and the 11KDHT by SRD5A1. This step is necessary as our group has shown that neither AKR1C3 nor 17βHSD3 can catalyse the conversion of 11OHA4 to 11OHT ((113), unpublished data). Even so, preliminary data from our group has shown that the initial conversion of 11OHA4 to 11KA4 is highly efficient and thus should not limit the flux through the 11OHA4 pathway. Also it is interesting to note that the adrenal produces higher levels of 11OHA4 compared to A4 under both normal and ACTH-stimulated conditions (106, 107) and more substrate could therefore be available for the 11OHA4 pathway. Both DHEAS and DHEA can also be used as substrates for the alternate 5α-dione pathway, but both first need to be converted to A4 (16).

It is also interesting to note that while this study showed that 11KT production is favoured by AKR1C3, with seemingly minimal conversion back to 11KA4 by 17βHSD2, a previous study by our group has shown that 11KT and 11KDHT are metabolized and inactivated by downstream pathways at a significantly lower rate when compared to T and DHT (115). Taken together this data seems to indicate that the production of potent 11-oxygenated androgens is favoured by the upregulation of AKR1C3, and that the resulting 11-oxygenated androgens are inactivated at a low rate, thus suggesting that these steroids could accumulate in CRPC tissue. Indeed, a recent study has shown that 11-oxygenated metabolites are much more abundant in PCa tissue compared to metabolites from the classical pathway. Du Toit *et al*. (161) quantified androgens from PCa tissue samples collected from two patients, one who underwent no prior treatment; and one who underwent treatment with an androgen antagonist. The precursor 11OHA4 was found to be the most prominent steroid in both patients followed by 11KT in the patient who underwent treatment with an androgen antagonist. The potent androgen 11KDHT was found to be 7-fold and 9-fold higher compared to DHT levels in each patient, respectively, thus highlighting that the 11-oxygenated steroids may accumulate.

AKR1C3 as a possible drug target

The increased AKR1C3 expression found in CRPC has made this enzyme a target for the development of a therapeutic drug for the treatment of CRPC. A number of studies collectively

conclude that AKR1C3 plays a central role in intratumoural androgen metabolism leading to the production of potent androgens from adrenal androgen precursors which drives AR-regulated gene expression and cell growth despite castrate levels of T (66, 79, 124, 139, 162, 163). During their research into the alternate 5α-dione pathway Chang *et al.* (111) showed that the conversion of A4 to 5α-dione by SRD5A1 was rapid while the conversion of the latter to DHT was slow, thus leading to the hypothesis that AKR1C3 catalysis the rate-determining step and thus making AKR1C3 a good drug target. Data from this study highlights the importance of AKR1C3 in the 11OHA4 pathway. Inhibiting AKR1C3 could therefore inhibit both pathways, thereby significantly reducing intratumoural androgen levels.

Currently two approved CRPC drugs include abiraterone which inhibits CYP17A1 and enzalutamide which is a synthetic non-steroidal antiandrogen and competitively inhibits androgen binding to androgen receptors and prevents the translocation of the androgen receptor to the nucleus. The inhibition of CYP17A1 by abiraterone prevents the production of all androgens and androgen precursors, but also inhibits the production of other important steroid hormones like the glucocorticoid cortisol. Abiraterone treatments therefore have side effects which need to be countered by glucocorticoid treatment. Conversely, an AKR1C3 inhibitor is predicted to have fewer side effects because it acts further downstream. The use of enzalutamide therapy often leads to acquired resistance against this drug. In a study by Lui *et al.* (164) they developed an enzalutamide-resistant PCa cell line to further investigate this phenomenon. Interestingly they found that AKR1C3 expression is upregulated in the enzalutamide-resistant PCa cells. Furthermore, AKR1C3 was highly expressed in enzalutamide-resistant prostate xenograft tumours. Knockdown or inhibition of AKR1C3 resensitized enzalutamide-resistant PCa cells to enzalutamide treatment both *in vitro* and *in vivo*. These results therefore demonstrate that an AKR1C3 inhibitor may counter the resistance to enzalutamide. The development of an AKR1C3 inhibitor is however a complex task as AKR1C3, AKR1C1, AKR1C2 and AKR1C4 share 84% sequence homology. The drug would therefore need to be highly specific as all these enzymes plays a role in steroid metabolism and off target effects may lead to unwanted side effects.

Future studies

This study has added to the growing body of evidence showing that the 11OHA4 pathway may play an important role in the development and progression of CRPC. Further studies are however required to confirm this. An ongoing project in our laboratory is to characterize all enzymes responsible for metabolism in the 11OHA4 pathway and to build a comprehensive model of intratumoural androgen metabolism. In addition, it is vital that the levels of the 11OHA4 metabolites in PCa and CRPC tissue are determined and compared to that of the classical androgens. This can then be linked to altered enzyme expression also investigated in this tissue. The results from

this study strongly suggest that it would be useful to investigate AKR1C3 inhibitors in the treatment of CRPC.

References

1. Incontinence & Overactive Bladder Health Center (214AD) *WebMD*
2. Thomson, A. A. (2001) Role of androgens and fibroblast growth factors in prostatic development. *Reproduction*. **121**, 187–195
3. Anatomy Of Prostate Gland Zones (2013) *Anat. Hum. BODY Anim.*
4. Aumuller, G., and Seitz, J. (1990) Protein secretion and secretory processes in male accessory sex glands. *Int. Rev. Cytol.* **121**, 127–231
5. Stephan, C., R., Ralla, B., and Jung, K. (2014) Prostate-specific antigen and other serum and urine markers in prostate cancer. *Biochim. Biophys. Acta - Rev. Cancer*. **1846**, 99–112
6. Stenman, U. H. (1997) Prostate-specific antigen, clinical use and staging: an overview. *Br. J. Urol.* **79 Suppl 1**, 53–60
7. Myers, R. P. (2000) Structure of the adult prostate from a clinician's standpoint. *Clin. Anat.* **13**, 214–5
8. Basic Principles: Prostate Anatomy (2010) *Urol. match*
9. Prostate Cancer Information from the Foundation of the Prostate Gland. (2010) *Prostate Cancer Treat. Guid.*
10. Corpechot, C., Baulieu, E. E., and Robel, P. (1981) Testosterone, dihydrotestosterone and androstanediols in plasma, testes and prostates of rats during development. *Acta Endocrinol. (Copenh).* **96**, 127–135
11. Mann, T. (1974) Secretory function of the prostate, seminal vesicle and other male accessory organs of reproduction. *J. Reprod. Fertil.* **37**, 179–188
12. Isaacs, J. T., Furuya, Y., and Berges, R. (1994) The role of androgen in the regulation of programmed cell death/apoptosis in normal and malignant prostatic tissue. *Semin. Cancer Biol.* **5**, 391–400
13. Imperato-McGinley, J., Sanchez, R. S., Spencer, J. R., Yee, B., and Vaughan, E. D. (1992) Comparison of the effects of the 5 alpha-reductase inhibitor finasteride and the antiandrogen flutamide on prostate and genital differentiation: dose-response studies. *Endocrinology*. **131**, 1149–1156
14. Cohen, R. J., Shannon, B. A., Phillips, M., Moorin, R. E., Wheeler, T. M., and Garrett, K. L. (2008) Central Zone Carcinoma of the Prostate Gland : A Distinct Tumor Type With Poor Prognostic Features. *J. Urol.* **179**, 1762–1767
15. Sharifi, N., & Auchus, R. J. (2012) Steroid biosynthesis and prostate cancer. *Steroids*. **77**, 719–725
16. Pretorius, E., Arlt, W., and Storbeck, K.-H. (2016) A new dawn for androgens: Novel lessons from 11-oxygenated C19 steroids. *Mol. Cell. Endocrinol.* 10.1016/j.mce.2016.08.014
17. Deslypere, J. P., Young, M., Wilson, J. D., and McPhaul, M. J. (1992) Testosterone and 5 alpha-dihydrotestosterone interact differently with the androgen receptor to enhance transcription of the MMTV-CAT reporter gene. *Mol. Cell. Endocrinol.* **88**, 15–22
18. Lu, N. Z., Wardell, S. E., Burnstein, K. L., Defranco, D., Fuller, P. J., Giguere, V., Hochberg, R. B., McKay, L., Renoir, J.-M., Weigel, N. L., Wilson, E. M., McDonnell, D. P., and Cidlowski, J. A. (2006) International Union of Pharmacology. LXV. The pharmacology and classification of the nuclear receptor superfamily: glucocorticoid, mineralocorticoid,

progesterone, and androgen receptors. *Pharmacol. Rev.* **58**, 782–797

19. Zhang, L., Johnson, M., Le, K. H., Sato, M., Ilagan, R., Iyer, M., Gambhir, S. S., Wu, L., and Carey, M. (2003) Interrogating Androgen Receptor Function in Recurrent Prostate Cancer. *Cancer Res.* **63**, 4552–4560

20. Mangelsdorf, D. J., Thummel, C., Beato, M., Herrlich, P., Schutz, G., Umesono, K., Blumberg, B., Kastner, P., Mark, M., Chambon, P., and Evans, R. M. (1995) The nuclear receptor superfamily: the second decade. *Cell*. **83**, 835–839

21. Fu, M., Wang, C., Reutens, A. T., Wang, J., Angeletti, R. H., Siconolfi-Baez, L., Ogryzko, V., Avantaggiati, M.-L., and Pestell, R. G. (2000) p300 and p300/cAMP-response Element-binding Protein-associated Factor Acetylate the Androgen Receptor at Sites Governing Hormone-dependent Transactivation. *J. Biol. Chem.* . **275**, 20853–20860

22. Beato, M. Sanchez-Pacheco, A. (1996) Interaction of Steroid Hormone Receptors with the Transcription Initiation Complex. *Endocr. Rev.* **17**, 587–609

23. Aarnisalo, P., Santti, H., Poukka, H., Palvimo, J. J., and Jänne, O. A. (1999) Transcription Activating and Repressing Functions of the Androgen Receptor Are Differentially Influenced by Mutations in the Deoxyribonucleic Acid-Binding Domain. *Endocrinology*. **140**, 3097–3105

24. Lefstin, J. A., and Yamamoto, K. R. (1998) Allosteric effects of DNA on transcriptional regulators. *Nature*. **392**, 885–888

25. Beato, M., Herrlich, P., and Schutz, G. (1995) Steroid hormone receptors: many actors in search of a plot. *Cell*. **83**, 851–857

26. Truss, M., and Beato, M. (1993) Steroid hormone receptors: interaction with deoxyribonucleic acid and transcription factors. *Endocr. Rev.* **14**, 459–479

27. Shafi, A. A., Yen, A. E., and Weigel, N. L. (2013) Androgen receptors in hormone-dependent and castration-resistant prostate cancer. *Pharmacol. Ther.* **140**, 223–38

28. Yuan, X., and Balk, S. P. (2009) Mechanisms Mediating Androgen Receptor Reactivation After Castration. *Urol Oncol*. **27**, 36–41

29. Pascual, G., and Glass, C. K. (2006) Nuclear receptors versus inflammation: mechanisms of transrepression. *Trends Endocrinol. Metab.* **17**, 321–327

30. Palvimo, J. J., Reinikainen, P., Ikonen, T., Kallio, P. J., Moilanen, A., and Jänne, O. A. (1996) Mutual Transcriptional Interference between RelA and Androgen Receptor. *J. Biol. Chem.* . **271**, 24151–24156

31. Sato, N., Sadar, M. D., Bruchovsky, N., Saatcioglu, F., Rennie, P. S., Sato, S., Lange, P. H., and Gleave, M. E. (1997) Androgenic Induction of Prostate-specific Antigen Gene Is Repressed by Protein-Protein Interaction between the Androgen Receptor and AP-1/c-Jun in the Human Prostate Cancer Cell Line LNCaP. *J. Biol. Chem.* . **272**, 17485–17494

32. World health organization Cancer country profiles 2014. *Cancer Ctry. profiles 2014*. [online] http://www.who.int/cancer/country-profiles/en/#S (Accessed February 4, 2015)

33. El Sheikh, S. S., Romanska, H. M., Abel, P., Domin, J., and Lalani, E.-N. (2008) Predictive value of PTEN and AR coexpression of sustained responsiveness to hormonal therapy in prostate cancer--a pilot study. *Neoplasia*. **10**, 949–953

34. Reid, A. H., Attard, G., Ambroisine, L., Fisher, G., Kovacs, G., Brewer, D., Clark, J., Flohr, P., Edwards, S., Berney, D. M., Foster, C. S., Fletcher, A., Gerald, W. L., Møller, H., Reuter, V. E., Scardino, P. T., Cuzick, J., de Bono, J. S., and Cooper, C. S. (2010) Molecular characterisation of ERG, ETV1 and PTEN gene loci identifies patients at low and high risk of death from prostate cancer. *Br. J. Cancer*. **102**, 678–684

35. Taylor, B. S., Schultz, N., Hieronymus, H., Gopalan, A., Xiao, Y., Carver, B. S., Arora, V. K., Kaushik, P., Cerami, E., Reva, B., Antipin, Y., Mitsiades, N., Landers, T., Dolgalev, I., Major,

J. E., Wilson, M., Socci, N. D., Lash, A. E., Heguy, A., Eastham, J. a., Scher, H. I., Reuter, V. E., Scardino, P. T., Sander, C., Sawyers, C. L., and Gerald, W. L. (2010) Integrative Genomic Profiling of Human Prostate Cancer. *Cancer Cell*. **18**, 11–22

36. Helgeson, B. E., Tomlins, S. A., Shah, N., Laxman, B., Cao, Q., Prensner, J. R., Cao, X., Singla, N., Montie, J. E., Varambally, S., Mehra, R., and Chinnaiyan, A. M. (2008) Characterization of TMPRSS2:ETV5 and SLC45A3:ETV5 gene fusions in prostate cancer. *Cancer Res.* **68**, 73–80

37. Tomlins, S. A., Rhodes, D. R., Perner, S., Dhanasekaran, S. M., Mehra, R., Sun, X.-W., Varambally, S., Cao, X., Tchinda, J., Kuefer, R., Lee, C., Montie, J. E., Shah, R. B., Pienta, K. J., Rubin, M. A., and Chinnaiyan, A. M. (2005) Recurrent Fusion of TMPRSS2 and ETS Transcription Factor Genes in Prostate Cancer. *Science (80-.).* **310**, 644–648

38. Tomlins, S. A., Mehra, R., Rhodes, D. R., Smith, L. R., Roulston, D., Helgeson, B. E., Cao, X., Wei, J. T., Rubin, M. A., and Chinnaiyan, A. M. (2006) TMPRSS2 : ETV4 Gene Fusions Define a Third Molecular Subtype of Prostate Cancer. *Cancer Res.* **66**, 3396–3400

39. Tomlins, S. A., Laxman, B., Varambally, S., Cao, X., Yu, J., Helgeson, B. E., Cao, Q., Prensner, J. R., Rubin, M. A., Shah, R. B., Mehra, R., and Chinnaiyan, A. M. (2008) Role of the TMPRSS2-ERG Gene Fusion in Prostate Cancer. *Neoplasia*. **10**, 177–188

40. Cerveira, N., Ribeiro, F. R., Peixoto, A., Costa, V., Henrique, R., and Jero, C. (2006) TMPRSS2 – ERG Gene Fusion Causing ERG Overexpression Precedes Chromosome Copy Number Changes in Prostate Carcinomas and Paired HGPIN Lesions. *Neoplasia*. **8**, 826–832

41. Seth, A., and Watson, D. K. (2005) ETS transcription factors and their emerging roles in human cancer. *Eur. J. Cancer*. **41**, 2462–2478

42. Penning, T. M. (2010) New frontiers in androgen biosynthesis and metabolism. *Curr. Opin. Endocrinol. Diabetes. Obes.* **17**, 233–239

43. Aapro, M. S. (2012) Management of Advanced Prostate Cancer in Senior Adults: The New Landscape. *Oncologist*. **17**, 16–22

44. Robinson, D., Van Allen, E. M., Wu, Y.-M., Schultz, N., Lonigro, R. J., Mosquera, J.-M., Montgomery, B., Taplin, M.-E., Pritchard, C. C., Attard, G., Beltran, H., Abida, W., Bradley, R. K., Vinson, J., Cao, X., Vats, P., Kunju, L. P., Hussain, M., Feng, F. Y., Tomlins, S. A., Cooney, K. A., Smith, D. C., Brennan, C., Siddiqui, J., Mehra, R., Chen, Y., Rathkopf, D. E., Morris, M. J., Solomon, S. B., Durack, J. C., Reuter, V. E., Gopalan, A., Gao, J., Loda, M., Lis, R. T., Bowden, M., Balk, S. P., Gaviola, G., Sougnez, C., Gupta, M., Yu, E. Y., Mostaghel, E. A., Cheng, H. H., Mulcahy, H., True, L. D., Plymate, S. R., Dvinge, H., Ferraldeschi, R., Flohr, P., Miranda, S., Zafeiriou, Z., Tunariu, N., Mateo, J., Perez-Lopez, R., Demichelis, F., Robinson, B. D., Schiffman, M., Nanus, D. M., Tagawa, S. T., Sigaras, A., Eng, K. W., Elemento, O., Sboner, A., Heath, E. I., Scher, H. I., Pienta, K. J., Kantoff, P., de Bono, J. S., Rubin, M. A., Nelson, P. S., Garraway, L. A., Sawyers, C. L., and Chinnaiyan, A. M. (2016) Integrative Clinical Genomics of Advanced Prostate Cancer. *Cell*. **161**, 1215–1228

45. Voeller, H. J., Truica, C. I., and Gelmann, E. P. (1998) Beta-catenin mutations in human prostate cancer. *Cancer Res.* **58**, 2520–2523

46. Komiya, Y., and Habas, R. (2008) Wnt signal transduction pathways. *Organogenesis*. **4**, 68–75

47. Assie, G., Letouze, E., Fassnacht, M., Jouinot, A., Luscap, W., Barreau, O., Omeiri, H., Rodriguez, S., Perlemoine, K., Rene-Corail, F., Elarouci, N., Sbiera, S., Kroiss, M., Allolio, B., Waldmann, J., Quinkler, M., Mannelli, M., Mantero, F., Papathomas, T., De Krijger, R., Tabarin, A., Kerlan, V., Baudin, E., Tissier, F., Dousset, B., Groussin, L., Amar, L., Clauser, E., Bertagna, X., Ragazzon, B., Beuschlein, F., Libe, R., de Reynies, A., and Bertherat, J.

(2014) Integrated genomic characterization of adrenocortical carcinoma. *Nat. Genet.* **46**, 607–612

48. Giannakis, M., Hodis, E., Jasmine Mu, X., Yamauchi, M., Rosenbluh, J., Cibulskis, K., Saksena, G., Lawrence, M. S., Qian, Z. R., Nishihara, R., Van Allen, E. M., Hahn, W. C., Gabriel, S. B., Lander, E. S., Getz, G., Ogino, S., Fuchs, C. S., and Garraway, L. A. (2014) RNF43 is frequently mutated in colorectal and endometrial cancers. *Nat Genet*. **46**, 1264–1266

49. Seshagiri, S., Stawiski, E. W., Durinck, S., Modrusan, Z., Storm, E. E., Conboy, C. B., Chaudhuri, S., Guan, Y., Janakiraman, V., Jaiswal, B. S., Guillory, J., Ha, C., Dijkgraaf, G. J. P., Stinson, J., Gnad, F., Huntley, M. A., Degenhardt, J. D., Haverty, P. M., Bourgon, R., Wang, W., Koeppen, H., Gentleman, R., Starr, T. K., Zhang, Z., Largaespada, D. A., Wu, T. D., and de Sauvage, F. J. (2012) Recurrent R-spondin fusions in colon cancer. *Nature*. **488**, 660–664

50. Finn, R. S., Crown, J. P., Lang, I., Boer, K., Bondarenko, I. M., Kulyk, S. O., Ettl, J., Patel, R., Pinter, T., Schmidt, M., Shparyk, Y., Thummala, A. R., Voytko, N. L., Fowst, C., Huang, X., Kim, S. T., Randolph, S., and Slamon, D. J. (2016) The cyclin-dependent kinase 4/6 inhibitor palbociclib in combination with letrozole versus letrozole alone as first-line treatment of oestrogen receptor-positive, HER2-negative, advanced breast cancer (PALOMA-1/TRIO-18): a randomised phase 2 study. *Lancet Oncol.* **16**, 25–35

51. Pritchard, C. C., Morrissey, C., Kumar, A., Zhang, X., Smith, C., Coleman, I., Salipante, S. J., Milbank, J., Yu, M., Grady, W. M., Tait, J. F., Corey, E., Vessella, R. L., Walsh, T., Shendure, J., and Nelson, P. S. (2014) Complex MSH2 and MSH6 mutations in hypermutated microsatellite unstable advanced prostate cancer. *Nat Commun*

52. Geng, C., He, B., Xu, L., Barbieri, C. E., Eedunuri, V. K., Chew, S. A., Zimmermann, M., Bond, R., Shou, J., Li, C., Blattner, M., Lonard, D. M., Demichelis, F., Coarfa, C., Rubin, M. A., Zhou, P., O'Malley, B. W., and Mitsiades, N. (2013) Prostate cancer-associated mutations in speckle-type POZ protein (SPOP) regulate steroid receptor coactivator 3 protein turnover. *Proc. Natl. Acad. Sci. U. S. A.* **110**, 6997–7002

53. Grasso, C. S., Wu, Y.-M., Robinson, D. R., Cao, X., Dhanasekaran, S. M., Khan, A. P., Quist, M. J., Jing, X., Lonigro, R. J., Brenner, J. C., Asangani, I. A., Ateeq, B., Chun, S. Y., Siddiqui, J., Sam, L., Anstett, M., Mehra, R., Prensner, J. R., Palanisamy, N., Ryslik, G. A., Vandin, F., Raphael, B. J., Kunju, L. P., Rhodes, D. R., Pienta, K. J., Chinnaiyan, A. M., and Tomlins, S. A. (2012) The mutational landscape of lethal castration-resistant prostate cancer. *Nature*. **487**, 239–243

54. Barbieri, C. E., Baca, S. C., Lawrence, M. S., Demichelis, F., Blattner, M., Theurillat, J.-P., White, T. A., Stojanov, P., Van Allen, E., Stransky, N., Nickerson, E., Chae, S.-S., Boysen, G., Auclair, D., Onofrio, R. C., Park, K., Kitabayashi, N., MacDonald, T. Y., Sheikh, K., Vuong, T., Guiducci, C., Cibulskis, K., Sivachenko, A., Carter, S. L., Saksena, G., Voet, D., Hussain, W. M., Ramos, A. H., Winckler, W., Redman, M. C., Ardlie, K., Tewari, A. K., Mosquera, J. M., Rupp, N., Wild, P. J., Moch, H., Morrissey, C., Nelson, P. S., Kantoff, P. W., Gabriel, S. B., Golub, T. R., Meyerson, M., Lander, E. S., Getz, G., Rubin, M. A., and Garraway, L. A. (2012) Exome sequencing identifies recurrent SPOP, FOXA1 and MED12 mutations in prostate cancer. *Nat Genet*. **44**, 685–689

55. Chen, C. D., Welsbie, D. S., Tran, C., Baek, S. H., Chen, R., Vessella, R., Rosenfeld, M. G., and Sawyers, C. L. (2004) Molecular determinants of resistance to antiandrogen therapy. *Nat Med*. **10**, 33–39

56. Feldman, B. J., and Feldman, D. (2001) The development of androgen-independent prostate cancer. *Nat Rev Cancer*. **1**, 34–45

57. Mohler, J. L., Gregory, C. W., Ford, H., Kim, D., Weaver, C. M., Petrusz, P., Wilson, E. M., and French, F. S. (2004) The Androgen Axis in Recurrent Prostate Cancer. *Clin. Cancer*

Res. **10**, 440–448

58. Visakorpi, T., Hyytinen, E., Koivisto, P., Tanner, M., Keinanen, R., Palmberg, C., Palotie, A., Tammela, T., Isola, J., and Kallioniemi, O.-P. (1995) In vivo amplification of the androgen receptor gene and progression of human prostate cancer. *Nat Genet*. **9**, 401–406

59. Takahashi, H., Furusato, M., Allsbrook, W. C., Nishii, H., Wakui, S., Barrett, J. C., and Boyd, J. (1995) Prevalence of androgen receptor gene mutations in latent prostatic carcinomas from Japanese men. *Cancer Res.* **55**, 1621–1624

60. Tilley, W. D., Buchanan, G., Hickey, T. E., and Bentel, J. M. (1996) Mutations in the androgen receptor gene are associated with progression of human prostate cancer to androgen independence. *Clin. Cancer Res.* **2**, 277–285

61. Ruizeveld de Winter, J. A., Janssen, P. J., Sleddens, H. M., Verleun-Mooijman, M. C., Trapman, J., Brinkmann, A. O., Santerse, A. B., Schröder, F. H., and van der Kwast, T. H. (1994) Androgen receptor status in localized and locally progressive hormone refractory human prostate cancer. *Am. J. Pathol.* **144**, 735–746

62. Baretton, G. B., Klenk, U., Diebold, J., Schmeller, N., and Löhrs, U. (1999) Proliferation- and apoptosis-associated factors in advanced prostatic carcinomas before and after androgen deprivation therapy: prognostic significance of p21/WAF1/CIP1 expression. *Br. J. Cancer*. **80**, 546–555

63. Brooke, G. N., and Bevan, C. L. (2009) The role of androgen receptor mutations in prostate cancer progression. *Curr. Genomics*. **10**, 18–25

64. Shi, X.-B., Ma, A.-H., Xia, L., Kung, H.-J., and de Vere White, R. W. (2002) Functional analysis of 44 mutant androgen receptors from human prostate cancer. *Cancer Res.* **62**, 1496–1502

65. Han, G., Buchanan, G., Ittmann, M., Harris, J. M., Yu, X., Demayo, F. J., Tilley, W., and Greenberg, N. M. (2005) Mutation of the androgen receptor causes oncogenic transformation of the prostate. *Proc. Natl. Acad. Sci. U. S. A.* **102**, 1151–1156

66. Montgomery, R. B., Mostaghel, E. A., Vessella, R., Hess, D. L., Kalhorn, T. F., Higano, C. S., True, L. D., and Nelson, P. S. (2008) Maintenance of intratumoral androgens in metastatic prostate cancer: A mechanism for castration-resistant tumor growth. *Cancer Res.* **68**, 4447–4454

67. Gregory, C. W., Johnson, R. T., Mohler, J. L., French, F. S., and Wilson, E. M. (2001) Androgen Receptor Stabilization in Recurrent Prostate Cancer Is Associated with Hypersensitivity to Low Androgen Androgen Receptor Stabilization in Recurrent Prostate Cancer Is Associated with Hypersensitivity to Low Androgen 1. *Cacner Res. Res.* **61**, 2892–2898

68. McCubrey, J. A., Steelman, L. S., Chappell, W. H., Abrams, S. L., Wong, E. W. T., Chang, F., Lehmann, B., Terrian, D. M., Milella, M., Tafuri, A., Stivala, F., Libra, M., Basecke, J., Evangelisti, C., Martelli, A. M., and Franklin, R. A. (2007) Roles of the raf/mek/erk pathway in cell growth, malignant transformation and drug resistance. *Biochim. Biophys. Acta*. **1773**, 1263–1284

69. Liao, R. S., Ma, S., Miao, L., Li, R., Yin, Y., and Raj, G. V (2013) Androgen receptor-mediated non-genomic regulation of prostate cancer cell proliferation. *Transl. Androl. Urol.* **2**, 187–196

70. Sarwar, M., Sandberg, S., Abrahamsson, P.-A., and Persson, J. L. (2014) Protein kinase A (PKA) pathway is functionally linked to androgen receptor (AR) in the progression of prostate cancer. *Urol. Oncol. Semin. Orig. Investig.* **32**, 25.e1–25.e12

71. Merkle, D., and Hoffmann, R. (2011) Roles of cAMP and cAMP-dependent protein kinase in the progression of prostate cancer: cross-talk with the androgen receptor. *Cell. Signal.* **23**,

507–515

72. Sadar, M. D. (1999) Androgen-independent induction of prostate-specific antigen gene expression via cross-talk between the androgen receptor and protein kinase A signal transduction pathways. *J. Biol. Chem.* **274**, 7777–7783

73. Haile, S., and Sadar, M. D. (2011) Androgen receptor and its splice variants in prostate cancer. *Cell. Mol. Life Sci.* **68**, 3971–3981

74. Attard, G., Reid, A. H. M., Yap, T. A., Raynaud, F., Dowsett, M., Settatree, S., Barrett, M., Parker, C., Martins, V., Folkerd, E., Clark, J., Cooper, C. S., Kaye, S. B., Dearnaley, D., Lee, G., and de Bono, J. S. (2008) Phase I clinical trial of a selective inhibitor of CYP17, abiraterone acetate, confirms that castration-resistant prostate cancer commonly remains hormone driven. *J. Clin. Oncol.* **26**, 4563–4571

75. Martine P Roudier, MD, PhDcorrespondence, Lawrence D True, MD, Celestia S Higano, MD, Hubert Vesselle, MD, William Ellis, MD, Paul Lange, MD, Robert L Vessella, P. (2003) Phenotypic heterogeneity of end-stage prostate carcinoma metastatic to bone. *Hum. Pathol.* **34**, 646–653

76. Shah, R. B., Mehra, R., Chinnaiyan, A. M., Shen, R., Ghosh, D., Zhou, M., Macvicar, G. R., Varambally, S., Harwood, J., Bismar, T. A., Kim, R., Rubin, M. A., and Pienta, K. J. (2004) Androgen-Independent Prostate Cancer Is a Heterogeneous Group of Diseases : Lessons from a Rapid Autopsy Program

77. Mostaghel, E. A. (2013) Steroid hormone synthetic pathways in prostate cancer. **2**, 212–227

78. Mostaghel, E. A. (2014) Beyond T and DHT - Novel steroid derivatives capable of wild type androgen receptor activation. *Int. J. Biol. Sci.* **10**, 602–613

79. Mostaghel, E. A., Montgomery, B., and Nelson, P. S. (2009) Castration-resistant prostate cancer: targeting androgen metabolic pathways in recurrent disease. *Urol. Oncol.* **27**, 251–7

80. Sternberg, C. N., de Bono, J. S., Chi, K. N., Fizazi, K., Mulders, P., Cerbone, L., Hirmand, M., Forer, D., and Scher, H. I. (2014) Improved outcomes in elderly patients with metastatic castration-resistant prostate cancer treated with the androgen receptor inhibitor enzalutamide: results from the phase III AFFIRM trial. *Ann. Oncol.* **25**, 429–34

81. Ryan, C. J., Smith, M. R., Fizazi, K., Saad, F., Mulders, P. F. A., Sternberg, C. N., Miller, K., Logothetis, C. J., Shore, N. D., Small, E. J., Carles, J., Flaig, T. W., Taplin, M.-E., Higano, C. S., de Souza, P., de Bono, J. S., Griffin, T. W., De Porre, P., Yu, M. K., Park, Y. C., Li, J., Kheoh, T., Naini, V., Molina, A., and Rathkopf, D. E. (2015) Abiraterone acetate plus prednisone versus placebo plus prednisone in chemotherapy-naive men with metastatic castration-resistant prostate cancer (COU-AA-302): final overall survival analysis of a randomised, double-blind, placebo-controlled phase 3 study. *Lancet. Oncol.* **16**, 152–160

82. Cabot, R. C., Harris, N. L., Rosenberg, E. S., Shepard, J.-A. O., Cort, A. M., Ebeling, S. H., McDonald, E. K., Scher, H. I., Fizazi, K., Saad, F., Taplin, M.-E., Sternberg, C. N., Miller, K., de Wit, R., Mulders, P., Chi, K. N., Shore, N. D., Armstrong, A. J., Flaig, T. W., Fléchon, A., Mainwaring, P., Fleming, M., Hainsworth, J. D., Hirmand, M., Selby, B., Seely, L., and de Bono, J. S. (2012) Increased Survival with Enzalutamide in Prostate Cancer after Chemotherapy. *N. Engl. J. Med.* **367**, 1187–1197

83. Kumagai, J., Hofland, J., Erkens-Schulze, S., Dits, N. F. J., Steenbergen, J., Jenster, G., Homma, Y., de Jong, F. H., and van Weerden, W. M. (2013) Intratumoral conversion of adrenal androgen precursors drives androgen receptor-activated cell growth in prostate cancer more potently than de novo steroidogenesis. *Prostate*. **73**, 1636–50

84. Clarke, C. L., and Sutherland, R. L. (1990) Progestin Regulation of Cellular Proliferation. *Endocr. Rev.* **11**, 266–301

85. Lydon, J. P., DeMayo, F. J., Funk, C. R., Mani, S. K., Hughes, A. R., Montgomery, C. A.,

Shyamala, G., Conneely, O. M., and O'Malley, B. W. (1995) Mice lacking progesterone receptor exhibit pleiotropic reproductive abnormalities. *Genes Dev.* . **9**, 2266–2278

86. Mulac-Jericevic, B., and Conneely, O. M. (2004) Reproductive tissue selective actions of progesterone receptors. *Reprod.* . **128**, 139–146

87. Goodman, L. S., Gilman, A., Brunton, L. L., Lazo, J. S., & Parker, K. L. (2006) *Goodman & Gilman's the pharmacological basis of therapeuticst*, 12th Ed., McGraw-Hill, New York

88. Katzung, B. G. (2004) *Basic & clinical pharmacology.*, 12th Ed., Lange Medical Books/McGraw Hill., New York

89. Verrey F, Schaerer E, Zoerkler P, Paccolat MP, Geering K, K. J. (1987) Regulation by aldosterone of Na+,K+-ATPase mRNAs, protein synthesis, and sodium transport in cultured kidney cells. *J. Cell Biol.* **104**, 1231–1237

90. Kolla, V., Robertson, N. M., and Litwack, G. (1999) Identification of a mineralocorticoid/glucocorticoid response element in the human Na/K ATPase alpha1 gene promoter. *Biochem. Biophys. Res. Commun.* **266**, 5–14

91. Amasheh, S., Epple, H. J., Mankertz, J., Detjen, K., Goltz, M., Schulzke, J. D., and Fromm, M. (2000) Differential regulation of ENaC by aldosterone in rat early and late distal colon. *Ann. N. Y. Acad. Sci.* **915**, 92–94

92. Epple, H. J., Amasheh, S., Mankertz, J., Goltz, M., Schulzke, J. D., and Fromm, M. (2000) Early aldosterone effect in distal colon by transcriptional regulation of ENaC subunits. *Am. J. Physiol. Gastrointest. Liver Physiol.* **278**, G718-24

93. Kolla, V., and Litwack, G. (2000) Transcriptional regulation of the human Na/K ATPase via the human mineralocorticoid receptor. *Mol. Cell. Biochem.* **204**, 35–40

94. Gonzalez, F. J. (1988) The molecular biology of cytochrome P450s. *Pharmacol. Rev.* **40**, 243–288

95. Walter L. Miller and Richard J. Auchus (2011) The Molecular Biology, Biochemistry, and Physiology of Human Steroidogenesis and Its Disorders. *Endocr. Rev.* **32**, 81–151

96. Miller, W. L. (2011) No TitleMinireview: Regulation of Steroidogenesis by Electron Transfer. *Endocrinology*. **146**, 2544–2550

97. Agarwal, A. K., and Auchus, R. J. (2016) Minireview : Cellular Redox State Regulates Hydroxysteroid Dehydrogenase Activity and Intracellular Hormone Potency. **146**, 2531–2538

98. Penning, T. M. (2016) Molecular Endocrinology of Hydroxysteroid Dehydrogenases. **18**, 281–305

99. Abrahams, L., Semjonous, N. M., Guest, P., Zielinska, A., Hughes, B., Lavery, G. G., and Stewart, P. M. (2012) Biomarkers of hypothalamic–pituitary–adrenal axis activity in mice lacking 11β-HSD1 and H6PDH. *J. Endocrinol.* . **214**, 367–372

100. Zhang, Y., Zhong, X., Gjoka, Z., Li, Y., Stochaj, W., Stahl, M., Kriz, R., Tobin, J. F., Erbe, D., and Suri, V. (2009) H6PDH interacts directly with 11β-HSD1: Implications for determining the directionality of glucocorticoid catalysis. *Arch. Biochem. Biophys.* **483**, 45–54

101. Atanasov, A. G., Nashev, L. G., Gelman, L., Legeza, B., Sack, R., Portmann, R., and Odermatt, A. (2008) Direct protein–protein interaction of 11β-hydroxysteroid dehydrogenase type 1 and hexose-6-phosphate dehydrogenase in the endoplasmic reticulum lumen. *Biochim. Biophys. Acta (BBA)-Molecular Cell Res.* **1783**, 1536–1543

102. Auchus RJ1, R. W. (2004) Adrenarche - physiology, biochemistry and human disease. *Clin Endocrinol*. **60**, 288–96.

103. Mulatero, P., Curnow, K. M., Foekling, M., Veglio, F., Jeunemaitre, X., and Corvol, P. (2016)

Recombinant CYP11B Genes Encode Enzymes that Can Catalyze Conversion of 11-Deoxycortisol to Cortisol ,. **83**, 3996–4001

104. Auchus, R. J., Lee, T. C., and Miller, W. L. (1998) Cytochrome b 5 Augments the 17 , 20-Lyase Activity of Human P450c17 without Direct Electron Transfer *. *J Biol Chem*. **273**, 3158–3165

105. Suzuki, T., Sasano, H., Takeyama, J., Kaneko, C., Freije, W. A., Carr, B. R., and Rainey, W. E. (2000) Developmental changes in steroidogenic enzymes in human postnatal adrenal cortex: immunohistochemical studies. *Clin. Endocrinol. (Oxf).* **53**, 739–747

106. Rege, J., Nakamura, Y., Satoh, F., Morimoto, R., Kennedy, M. R., Layman, L. C., Honma, S., Sasano, H., and Rainey, W. E. (2013) Liquid Chromatography–Tandem Mass Spectrometry Analysis of Human Adrenal Vein 19-Carbon Steroids Before and After ACTH Stimulation. *J. Clin. Endocrinol. Metab.* **98**, 1182–1188

107. Pretorius, E. (2016) *An investigation into the androgenic activity of 11-ketotestosterone and 11-ketodihydrotestosterone*. Ph.D. thesis, University of Stellenbosch

108. Storbeck, K.-H., Bloem, L. M., Africander, D., Schloms, L., Swart, P., and Swart, A. C. (2013) 11β-Hydroxydihydrotestosterone and 11-ketodihydrotestosterone, novel C19 steroids with androgenic activity: a putative role in castration resistant prostate cancer. *Mol. Cell. Endocrinol.* **377**, 135–46

109. Heidenreich, A., Bastian, P. J., Bellmunt, J., Bolla, M., Joniau, S., van der Kwast, T., Mason, M., Matveev, V., Wiegel, T., Zattoni, F., and Mottet, N. (2014) EAU guidelines on prostate cancer. Part II: Treatment of advanced, relapsing, and castration-resistant prostate cancer. *Eur. Urol.* **65**, 467–479

110. Zlotta, A., and Debruyne, F. M. J. (2005) Expert Opinion on Optimal Testosterone Control in Prostate Cancer. *Eur. Urol. Suppl.* **4**, 37–41

111. Chang, K.-H., Li, R., Papari-Zareei, M., Watumull, L., Zhao, Y. D., Auchus, R. J., and Sharifi, N. (2011) Dihydrotestosterone synthesis bypasses testosterone to drive castration-resistant prostate cancer. *Proc. Natl. Acad. Sci. U. S. A.* **108**, 13728–13733

112. Fankhauser M, Tan Y, Macintyre G, Haviv I, Hong K.H.M, Nguyen A, Pedersen J.S, Costello A.J, Hovens C.M, and C. N. . (2014) Canonical androstenedione reduction is the predominant source of signaling androgens in hormone-refractory prostate cancer. *Clin. Cancer Res.* **20**, 5547–57

113. Bloem, L. M., Storbeck, K.-H., Schloms, L., and Swart, A. C. (2013) 11β-hydroxyandrostenedione returns to the steroid arena: biosynthesis, metabolism and function. *Molecules*. **18**, 13228–44

114. Imamichi, Y., Yuhki, K.-I., Orisaka, M., Kitano, T., Mukai, K., Ushikubi, F., Taniguchi, T., Umezawa, A., Miyamoto, K., and Yazawa, T. (2016) 11-ketotestosterone is a major androgen produced in human gonads. *J. Clin. Endocrinol. Metab.* **101**, 3582–3591

115. Pretorius, E., Africander, D. J., Vlok, M., Perkins, M. S., Quanson, J., Storbeck, K.-H. (2016) 11-Ketotestosterone and 1-Ketodihydrotestosterone in Castration Resistant Prostate Cancer: Potent Androgens Which Can No Longer Be Ignored. *PLoS One*

116. Deyashiki, Y., Ogasawara, A., Nakayama, T., Nakanishi, M., Miyabe, Y., Sato, K., and Hara, A. (1994) Molecular cloning of two human liver 3 alpha-hydroxysteroid/dihydrodiol dehydrogenase isoenzymes that are identical with chlordecone reductase and bile-acid binder. *Biochem. J.* **299**, 545–552

117. Lin, H. K., Jez, J. M., Schlegel, B. P., Peehl, D. M., Pachter, J. A., and Penning, T. M. (1997) Expression and characterization of recombinant type 2 3 alpha-hydroxysteroid dehydrogenase (HSD) from human prostate: demonstration of bifunctional 3 alpha/17 beta-HSD activity and cellular distribution. *Mol. Endocrinol.* **11**, 1971–1984

118. Penning, T. M., and Drury, J. E. (2007) Human Aldo-Keto Reductases: Function, Gene Regulation, and Single Nucleotide Polymorphisms. *Arch. Biochem. Biophys.* **464**, 241–250

119. Luu-The, V., Bélanger, A., and Labrie, F. (2008) Androgen biosynthetic pathways in the human prostate. *Best Pract. Res. Clin. Endocrinol. Metab.* **22**, 207–221

120. Penning, T. M., Burczynski, M. E., Jez, J. M., Lin, H.-K., Ma, H., Moore, M., Ratnam, K., and Palackal, N. (2001) Structure-function aspects and inhibitor design of type 5 17β-hydroxysteroid dehydrogenase (AKR1C3). *Mol. Cell. Endocrinol.* **171**, 137–149

121. Stanbrough, M., Bubley, G. J., Ross, K., Golub, T. R., Rubin, M. a., Penning, T. M., Febbo, P. G., and Balk, S. P. (2006) Increased expression of genes converting adrenal androgens to testosterone in androgen-independent prostate cancer. *Cancer Res.* **66**, 2815–2825

122. Jernberg E, Thysell E, Bovinder Ylitalo E, Rudolfsson S, Crnalic S, Widmark A, et al. (2013) Characterization of Prostate Cancer Bone Metastases According to Expression Levels of Steroidogenic Enzymes and Androgen Receptor Splice Variants. *PLoS One*. **8**, e77407

123. Pfeiffer MJ, Smit FP, Sedelaar JP, S. J. (2011) Steroidogenic enzymes and stem cell markers are upregulated during androgen deprivation in prostate cancer. *Mol Med*. **17**, 657–664

124. Byrns, M. C., Mindnich, R., Duan, L., and Penning, T. M. (2012) Overexpression of aldo-keto reductase 1C3 (AKR1C3) in LNCaP cells diverts androgen metabolism towards testosterone resulting in resistance to the 5α-reductase inhibitor finasteride. *J. Steroid Biochem. Mol. Biol.* **130**, 7–15

125. Xue-Ying Hea, Ying-Zi Yanga, Donna M. Peehlb, Alexander Lauderdaleb, Horst Schulzc, S.-Y. Y. (2003) Oxidative 3α-hydroxysteroid dehydrogenase activity of human type 10 17β-hydroxysteroid dehydrogenase. *J. Steroid Biochem. Mol. Biol.* **87**, 191–198

126. Ailin Zhang, Jiawei Zhang, Stephen Plymate, E. A. M. (2016) Classical and Non-Classical Roles for Pre-Receptor Control of DHT Metabolism in Prostate Cancer Progression. *Horm. Cancer*. **7**, 104–113

127. Koh, E., Noda, T., Kanaya, J., and Namiki, M. (2002) Differential expression of 17beta-hydroxysteroid dehydrogenase isozyme genes in prostate cancer and noncancer tissues. *Prostate*. **53**, 154–159

128. Ishizaki, F., Nishiyama, T., Kawasaki, T., Miyashiro, Y., Hara, N., Takizawa, I., Naito, M., and Takahashi, K. (2013) intratumoral synthesis of. 10.1038/srep01528

129. Khvostova EP, Otpuschennikov AA, Pustylnyak VO, G. L. (2015) Gene expression of androgen metabolising enzymes in benign and malignant prostatic tissues. *Horm Metab Res*. **47**, 119–124

130. Yun H, Xie J, Olumi AF, Ghosh R, K. A. (2015) Activation of AKR1C1/ERbeta induces apoptosis by downregulation of c-FLIP in prostate cancer cells: a prospective therapeutic opportunity. *Oncotarget*. **6**, 11600–13

131. Ji Q, Chang L, VanDenBerg D, Stanczyk FZ, S. A. (2003) Selective reduction of AKR1C2 in prostate cancer and its role in DHT metabolism. *Prostate*. **54**, 275–289

132. Titus, M. A., Gregory, C. W., Iii, O. H. F., Schell, M. J., Maygarden, S. J., and Mohler, J. L. (2005) Steroid 5 A -Reductase Isozymes I and II in Recurrent Prostate Cancer. **11**, 4365–4372

133. Jun Luo, Thomas A. Dunn, Charles M. Ewing, Patrick C. Walsh, and W. B. I. (2003) Decreased Gene Expression of Steroid 5Alpha-Reductase 2 in Human Prostate Cancer:Implications for FinasterideTherapyof Prostate Carcinoma. *Prostate*. **57**, 134–139

134. Sharma, K. K., Lindqvist, A., Zhou, X. J., Auchus, R. J., Penning, T. M., and Andersson, S. (2006) Deoxycorticosterone inactivation by AKR1C3 in human mineralocorticoid target

tissues. *Mol. Cell. Endocrinol.* **248**, 79–86

135. Byrns, M. C., Jin, Y., and Penning, T. M. (2011) Inhibitors of Type 5 17β-Hydroxysteroid Dehydrogenase (AKR1C3): Overview and Structural Insights. *J. Steroid Biochem. Mol. Biol.* **125**, 95–104

136. Byrns, M. C., Duan, L., Lee, S. H., Blair, I. A., and Penning, T. M. (2010) Aldo-keto reductase 1C3 expression in MCF-7 cells reveals roles in steroid hormone and prostaglandin metabolism that may explain its over-expression in breast cancer. *J. Steroid Biochem. Mol. Biol.* **118**, 177–187

137. Koda, N., Tsutsui, Y., Niwa, H., Ito, S., Woodward, D. F., and Watanabe, K. (2004) Synthesis of prostaglandin F ethanolamide by prostaglandin F synthase and identification of Bimatoprost as a potent inhibitor of the enzyme: new enzyme assay method using LC/ESI/MS. *Arch. Biochem. Biophys.* **424**, 128–136

138. Matsuura, K., Shiraishi, H., Hara, A., Sato, K., Deyashiki, Y., Ninomiya, M., and Sakai, S. (1998) Identification of a principal mRNA species for human 3alpha-hydroxysteroid dehydrogenase isoform (AKR1C3) that exhibits high prostaglandin D2 11-ketoreductase activity. *J. Biochem.* **124**, 940–946

139. Penning, T. M., Steckelbroeck, S., Bauman, D. R., Miller, M. W., Jin, Y., Peehl, D. M., Fung, K.-M., and Lin, H.-K. (2006) Aldo-keto reductase (AKR) 1C3: role in prostate disease and the development of specific inhibitors. *Mol. Cell. Endocrinol.* **248**, 182–91

140. Suzuki-Yamamoto, T., Nishizawa, M., Fukui, M., Okuda-Ashitaka, E., Nakajima, T., Ito, S., and Watanabe, K. (1999) cDNA cloning, expression and characterization of human prostaglandin F synthase. *FEBS Lett.* **462**, 335–340

141. Bauman, D. R., Rudnick, S. I., Szewczuk, L. M., Jin, Y., Gopishetty, S., and Penning, T. M. (2004) Development of Nonsteroidal Anti-Inflammatory Drug Analogs and Steroid Carboxylates Selective for Human Aldo-Keto Reductase Isoforms: Potential Antineoplastic Agents That Work Independently of Cyclooxygenase Isozymes. *Mol. Pharmacol.* **67**, 60–68

142. Byrns, M. C., Steckelbroeck, S., and Penning, T. M. (2008) An indomethacin analogue, N-(4-chlorobenzoyl)-melatonin, is a selective inhibitor of aldo-keto reductase 1C3 (type 2 3alpha-HSD, type 5 17beta-HSD, and prostaglandin F synthase), a potential target for the treatment of hormone dependent and hormone indepe. *Biochem. Pharmacol.* **75**, 484–493

143. Wu, L., Einstein, M., Geissler, W. M., Chan, H. K., Elliston, K. O., and Andersson, S. (1993) Expression cloning and characterization of human 17 beta-hydroxysteroid dehydrogenase type 2, a microsomal enzyme possessing 20 alpha-hydroxysteroid dehydrogenase activity. *J. Biol. Chem.* **268**, 12964–12969

144. Filling, C., Berndt, K. D., Benach, J., Knapp, S., Prozorovski, T., Nordling, E., Ladenstein, R., Jörnvall, H., and Oppermann, U. (2002) Critical residues for structure and catalysis in short-chain dehydrogenases/reductases. *J. Biol. Chem.* **277**, 25677–25684

145. Jornvall, H., Persson, B., Krook, M., Atrian, S., Gonzalez-Duarte, R., Jeffery, J., and Ghosh, D. (1995) Short-chain dehydrogenases/reductases (SDR). *Biochemistry*. **34**, 6003–6013

146. Miettinen, M. M., Mustonen, M. V, Poutanen, M. H., Isomaa, V. V, and Vihko, R. K. (1996) Human 17 beta-hydroxysteroid dehydrogenase type 1 and type 2 isoenzymes have opposite activities in cultured cells and characteristic cell- and tissue-specific expression. *Biochem. J.* **314**, 839–845

147. Casey, M. L., MacDonald, P. C., and Andersson, S. (1994) 17 beta-Hydroxysteroid dehydrogenase type 2: chromosomal assignment and progestin regulation of gene expression in human endometrium. *J. Clin. Invest.* **94**, 2135–2141

148. Peltoketo, H., Luu-The, V., Simard, J., and Adamski, J. (1999) 17beta-hydroxysteroid dehydrogenase (HSD)/17-ketosteroid reductase (KSR) family; nomenclature and main

characteristics of the 17HSD/KSR enzymes. *J. Mol. Endocrinol.* **23**, 1–11

149. Stanbrough, M., Bubley, G. J., Ross, K., Golub, T. R., Rubin, M. A., Penning, T. M., Febbo, P. G., and Balk, S. P. (2006) Increased Expression of Genes Converting Adrenal Androgens to Testosterone in Androgen-Independent Prostate Cancer. *Cancer Res.* **66**, 2815–2826

150. Gunnarsson, C., Hellqvist, E., and Stal, O. (2005) 17[beta]-Hydroxysteroid dehydrogenases involved in local oestrogen synthesis have prognostic significance in breast cancer. *Br J Cancer*. **92**, 547–552

151. Quanson, J. L., Stander, M. A., Pretorius, E., Jenkinson, C., Taylor, A. E., and Storbeck, K.-H. (2016) High-throughput analysis of 19 endogenous androgenic steroids by ultra-performance convergence chromatography tandem mass spectrometry. *J. Chromatogr. B. Analyt. Technol. Biomed. Life Sci.* **1031**, 131–138

152. Koh, E., Noda, T., Kanaya, J., Namiki, M. (2002) Differential Expressionof 17b-Hydroxysteroid Dehydrogenase Isozyme Genes in Prostate Cancer and Noncancer Tissues. *Prostate*. **53**, 154–159

153. Pfaffl, M. W. (2001) A new mathematical model for relative quantification in real-time RT-PCR. *Nucleic Acids Res.* **29**, e45

154. Willems, E., Leyns, L., and Vandesompele, J. (2008) Standardization of real-time PCR gene expression data from independent biological replicates. *Anal. Biochem.* **379**, 127–129

155. Carruba, G., Adamski, J., Calabrò, M., Miceli, M. D., Cataliotti, a, Bellavia, V., Lo Bue, a, Polito, L., and Castagnetta, L. a (1997) Molecular expression of 17 beta hydroxysteroid dehydrogenase types in relation to their activity in intact human prostate cancer cells. *Mol. Cell. Endocrinol.* **131**, 51–57

156. Horoszewicz, J. S., Leong, S. S., Chu, T. M., Wajsman, Z. L., Friedman, M., Papsidero, L., Kim, U., Chai, L. S., Kakati, S., Arya, S. K., and Sandberg, A. A. (1980) The LNCaP cell line--a new model for studies on human prostatic carcinoma. *Prog. Clin. Biol. Res.* **37**, 115–132

157. Spans, L., Helsen, C., Clinckemalie, L., Van den Broeck, T., Prekovic, S., Joniau, S., Lerut, E., and Claessens, F. (2014) Comparative genomic and transcriptomic analyses of LNCaP and C4-2B prostate cancer cell lines. *PLoS One*. **9**, e90002

158. Chandrasekar, T., Yang, J. C., Gao, A. C., and Evans, C. P. (2015) Mechanisms of resistance in castration-resistant prostate cancer (CRPC). *Transl. Androl. Urol.* **4**, 365–380

159. Lu, M.-L., Huang, Y.-W., and Lin, S.-X. (2002) Purification, Reconstitution, and Steady-state Kinetics of the Trans-membrane 17β-Hydroxysteroid Dehydrogenase 2. *J. Biol. Chem.* . **277**, 22123–22130

160. Eisenthal, R., Danson, M. J., and Hough, D. W. (2016) Catalytic efficiency and kcat/Km: a useful comparator? *Trends Biotechnol.* **25**, 247–249

161. Therina du Toit, Liezl M.Bloem, Jonathan L.Quanson, Riaan Ehlers, Anthony Serafin, A. C. S. (2016) Profiling adrenal 11-hydroxyandrostenedione metabolites in prostate cancer cells, tissue and plasma: UPC2 -MS/MS quantification of 11-hydroxytestosterone, 11keto-testosterone and 11keto-dihydrotestosterone. *J. Steroid Biochem. Mol. Biol.*

162. Hamid, A. R. A. H., Pfeiffer, M. J., Verhaegh, G. W., Schaafsma, E., Brandt, A., Sweep, F. C. G. J., Sedelaar, J. P. M., and Schalken, J. A. (2013) Aldo-keto reductase family 1 member C3 (AKR1C3) is a biomarker and therapeutic target for castration-resistant prostate cancer. *Mol. Med.* **18**, 1449–1455

163. Adeniji, A. O., Chen, M., and Penning, T. M. (2013) AKR1C3 as a Target in Castrate Resistant Prostate Cancer. *J. Steroid Biochem. Mol. Biol.* **137**, 136–149

164. Liu, C., Lou, W., Zhu, Y., Yang, J. C., Nadiminty, N., Gaikwad, N. W., Evans, C. P., and Gao, A. C. (2015) Intracrine Androgens and AKR1C3 Activation Confer Resistance to

Enzalutamide in Prostate Cancer. *Cancer Res.* **75**, 1413-1422